Improving Oil Recovery(IOR) with Polymer Flooding in A Heavy-Oil River-Channel Sandstone Reservoir

Von der Fakultät für Geowissenschaften, Geotechnik und Bergbau
der Technischen Universität Bergakademie Freiberg
genehmigte

DISSERTATION

zur Erlangung des akademischen Grades

Doktor Ingenieur

Dr.-Ing.

vorgelegt

von Dipl.-Ing. Hongjiang Lu

geboren am 20.11.1969 in Shandong, VR China

Gutachter.: Prof. Dr. habil. Häfner
Prof. Dr. Köckritz
Dr. -Ing. Voigt
Prof. Dr. Geistlinger

Tag der Verleihung: 23.04.2004

Acknowledgments

At the time of the completion of this dissertation, I would like to express my gratitude to Prof. Dr. F. Häfner of Freiberg University of Mining and Technology, Germany. My appreciation also goes to Prof. Wenguang Feng of Chengdu University of Technology, China. Without their supervision the research could not have been completed successfully. Their attitude to science and persistent pursuit of truth will always be of great inspiration for me forever.

I am grateful for DAAD and Mrs. Schädlich. DAAD has financed me for two and half years, which made it possible for me to continue my research in Freiberg University of Mining and Technology. Mrs. Schädlich has provided much information and help, which made my life easy and comfortable.

Many thanks also go to Prof. Dr. F. Häfner, Mrs. Pötzschke and Mrs. Beyer. They gave me great help not only in my work but also in my daily life. Their warm-hearted help guaranteed me an excellent working environment.

I would also like to take this opportunity to express my gratitude for all those who helped me.

Mrs. Wenbo Sheng in Shengli Oil Limited Company has provided much useful basic information for this work; Dr. N. Hoth, Dr. A. Behr, Dr. H.D. Voigt, Dr. S. Wagner, Dr. H. Strauß and Dr. A. Pohl of the Institute of Drilling Technology and Fluid Mining in Freiberg University have given me good advice about the dissertation. Dr. A. Moulkamanov and Mr. T. Friedel have helped me with using ECLIPSE. Dr. Yuguo Li of FU Berlin has exchanged idea with me about finite element method.

Mrs. Monecke and Prof. Monecke have given me advice and encouragement about how to obtain my doctorate from Freiberg University of Mining and Technology.

Mrs. Sandner and Dr. Sandner in Dresden have offered their kindness from the first day till to the end when I was in Germany, which eased my homesickness.

Mrs. Xiumei Pu carefully did the English proofreading of this dissertation.

I feel also grateful for my Chinese friends in Freiberg, they are Dr. Yonghua Hao, Dr. Fulin Shang, Dr. Guijun Wang, Dr. Dewen Zeng, Dr. Xiaoping Wu, Dr. Tao Wang, Prof. Dr. Chen Yang, Prof. Dr. Yan Jiang, Prof. Yong He, etc.

My parents, my brother and sister have always given me encouragements in the whole course of my study.

Thanks for all.

Summary

Most of the old oil fields in China have reached high water cut stage, in order to meet the booming energy demanding, oil production rate must be kept in the near future with corresponding IOR (Improving Oil Recovery) methods.

Z106 oilfield lies in Shengli Oilfields Area at the Yellow River delta. It was put into development in 1988. Since the oil belongs to heavy oil, the oil-water mobility ratio is so unfavourable that water cut increases very quickly. Especially for reservoir $Ng2^1$, the sand rock is sediment from river channel, the permeability heterogeneity and heavy oil properties together lead to extremely poor water flooding efficiency. In order to improve the oil recovery, IOR methods are needed urgently. Considering all practical situations for this reservoir and present technique level, polymer flooding method has been selected as an IOR test with numerical simulation.

For polymer flooding, since polymer resolution has the capability of enlarging water viscosity, it controls the mobility of water phase and at the same time improves the driving efficiency. During polymer flooding simulation, many factors must be taken into account for the construction of mathematical model, such as inaccessible pore volume, polymer shear thinning effect, polymer adsorption, relative permeability reduction factors, etc. All simulations were done with black oil model with polymer option in ECLIPSE.

Simulation results for a theoretical river channel reservoir with serious permeability heterogeneity and heavy oil, and simulation results for practical reservoir $Ng2^1$, both have shown that polymer flooding is a feasible method for IOR. For reservoir $Ng2^1$, with polymer slug size of 0.235 PV, polymer concentration at 1.5 kg/m^3, the final oil recovery after polymer flooding could reach 12.8%, the enhanced oil recovery is about 5%. If only the developable oil reserve being taken into account, the final oil recovery is about 34%, and enhanced oil recovery from polymer flooding is more than 12%. For such heavy oil river channel reservoir to reach such a final oil recovery, it could be concluded as a great success.

Since there are still many such oil reservoirs in Shengli Oilfields Area, polymer flooding will be of great importance for improving oil recovery in this area in the near future.

Zusammenfassung

Die Durchführbarkeit der Polymerflutung für Schweröllagerstätten wurde durch Simulation einer hypothetischen fluviatilen Lagerstätte und der realen Lagerstätte Z106Ng2^{1} getestet. Die Simulationsresultate zeigen, dass diese IOR Methode zur Erhöhung der Ölgewinnung anwendbar ist. Für die Lagerstätte Ng2^{1} kann bei einem Verbrauch an Polymerlösung von 0,235 PV und einer Polymerkonzentration von 1,5 kg/m^{3} ein maximaler Grad an Ölausbeute von 12,8% erreicht werden, was einem Zuwachs von 5 Prozent entspricht. Wird ausschließlich der vorhandene Ölvorrat zugrunde gelegt, beträgt der maximale Ausbeutegrad 34%, d.h. es tritt eine Verbesserung von ca. 12% ein. Für eine Schweröllagerstätte mit so heterogenen Speichergestein kann diese Ausbeute als großer Erfolg gewertet werden. Die im Rahmen der Untersuchungen erbrachten Erkenntnisse können in Zukunft auf die Vielzahl analoger Lagerstätten im Shengli-Ölfeld angewendet werden und so zu einer Erhöhung des Ausbeutegrades infolge des Einsatzes von Polymerfluten beitragen.

Contents

Acknowledgments
Summary
1 Introduction……(1)
1.1 Oil production situation of China and Shengli Oilfields……(1)
1.2 Researching area - Z106 Oilfied……(2)
1.3 Possible IOR method for Z106 Oilfield – Polymer Flooding……(3)
2 Theoretical basis for reservoir simulation with polymer flooding……(6)
2.1 Reservoir rock – Porous medium……(6)
2.2 Mathematical model for reservoir simulation and its simplification……(8)
2.2.1 Multi-phase multi-component model……(8)
2.2.2 Black oil model……(10)
2.3 Polymer transport in porous media……(13)
2.3.1 Polymer types and their properties……(13)
2.3.2 Viscosity of polymer solution and its shear thinning……(15)
2.3.3 Inaccessible pore volume in polymer flooding……(16)
2.3.4 Polymer retention in porous media and its effects……(17)
2.3.5 Mathematical model of polymer transport in porous media……(22)
3 Numerical treatment of mathematical model……(24)
3.1 Discretization of equations with control-volume finite element method……(25)
3.2 PEBI grid……(27)
4 Polymer flooding model in ECLIPSE 100 and ECLIPSE Office……(29)
4.1 Polymer flooding model of ECLIPSE 100……(29)
4.1.1 The mathematical model of polymer flood option in ECLIPSE……(29)
4.1.2 Treatment of fluid viscosities in ECLIPSE polymer flood model……(31)
4.1.3 Treatment of polymer adsorption……(32)
4.1.4 Treatment of permeability reductions and dead pore volume……(32)
4.1.5 Treatment of shear thinning effect……(33)
4.2 ECLIPSE Office……(34)
5 Reservoir characterization of $Ng2^1$ in Z106 Oilfield……(36)
5.1 Basic geology of Shengli Oilfields Area and Z106 Oilfield……(36)
5.2 The general situation of Z106 Oilfield……(38)
5.3 Detailed reservoir description $Ng2^1$……(39)
5.3.1 Sandstone distribution of $Ng2^1$ and its top surface structural map……(39)
5.3.2 Reservoir rock properties……(41)
5.3.3 Comprehensive interpretation of geological model with production data……(42)
5.3.4 Fluid properties……(43)
5.4 Production history……(44)

6 Simulation model construction and history matching……(46)
6.1 Simulation model construction……(46)
6.1.1 Grid construction……(46)
6.1.2 PVT……(50)
6.1.3 Capillary pressure and relative permeability……(50)
6.1.4 Well specification and time step……(54)
6.1.5 Summary section ……(54)
6.2 History matching……(55)
6.2.1 History Matching Preparation - The appreciation of observed data……(57)
6.2.2 Error Function Definition And its Sensitivity to Different Parameters……(58)
6.2.3 Well production history matching result and analysis……(61)
6.2.4 Well bottom hole pressure matching result and analysis……(64)
6.2.5 Matching result for whole reservoir……(65)
7 Residual oil distribution and production prediction under water flooding……(67)
8 Polymer flooding simulation……(69)
8.1 Polymer flooding simulation with a theoretical river channel reservoir……(70)
8.1.1 Geo-Model definition……(70)
8.1.2 Water flooding simulation result……(72)
8.1.3 Data system specification for polymer flooding……(75)
8.1.3.1 Viscosity of polymer solution……(75)
8.1.3.2 Polymer shear thinning……(76)
8.1.4 Polymer adsorption effect……(77)
8.1.5 Polymer concentration effect……(78)
8.1.6 Polymer slug size……(80)
8.1.7 Comparison between water flooding and polymer flooding……(81)
8.2 Polymer flooding simulation in reservoir $Ng2^1$……(82)
8.2.1 Polymer flooding specification……(82)
8.2.2 Selection of polymer slug size……(84)
8.2.3 Description of polymer flooding process……(87)
8.2.4 Residual oil saturation distribution after polymer flooding……(90)
9 Conclusions and proposals ……(92)
Nomenclature ……(95)
References ……(98)

Figures

1 China's Oil Production, Exportation and Importation……..……(1)
2 Location of Shengli Oilfields ……..…..(1)
3 Oil Production History of Shengli Oilfield……..(2)
4 Oil reserve distribution in Shengli area…….....…….(5)
5 Molecular structure……..……...……..(14)
6 Polymer viscosity versus concentration…….…….……...(15)
7 Shear thinning effect on viscosity.……..…….....…..(15)
8 Polymer breakout curves……..…..…….…(16)
9 Relation between adsorption and concentration…….…..…..(17)
10 Variation of polymer retention with permeability…….…….…...(17)
11 Variation of capillary pressure.…….…….....….....(18)
12 Relative permeability of Elgin sandstone ……..……..…..…(19)
13 Relative permeability of Okesa sandstone ……..……...…..……...…(20)
14 Relative permeability reduction as a function of polymer adsorption in core…...…(21)
15 Control volume in triangular finite element mesh.……(25)
16 PEBI grid……..……..…..……(27)
17 Location of Shengli Oilfield Area and Z106 Oilfield……...……(37)
18 Sequence definition in North China Basin……...…….…....(38)
19 Sandbody definition with Well L7……..……....(39)
20 Reflection horizon definition……..…….……..(40)
21 Reversion profile interpretation……..…….…..….(40)
22 Thickness distribution of $Ng2^1$……..……...…..……(40)
23 Top surface structural map ……..……..(40)
24 Reservoir profile from Well –67 to Well –19-x13…….…....(41)
25 Porosity isogram of $Ng2^1$…….…….…....(41)
26 Permeability isogram of $Ng2^1$……..…….……(41)
27 Reservoir geological model from comprehensive interpretation……..……...…..(42)
28 Distribution area of sandlayer $Ng2^2$……..……...…..(43)
29 Cumulative oil and water production.…….…….…….(45)
30 Topographic contour map……..……..…..(47)
31 Thickness contour map of $Ng2^1$……..…….…….(47)
32 Thickness contour map of $Ng2^2$……..…….…….(48)
33 Porosity contour map of $Ng2^1$……..……...…..(48)
34 Porosity contour map of $Ng2^2$……..……...…..(48)
35 Horizontal permeability of $Ng2^1$…….……...…..(48)
36 Vertical permeability of $Ng2^1$……..……...…..(49)
37 Horizontal permeability of $Ng2^2$……..……...…..(49)

38 Vertical permeability of $Ng2^2$……..……..…..(49)
39 Grid model for reservoir simulation…….……...….(50)
40 Region distribution, A for $Ng2^1$, B for $Ng2^2$……...……...(51)
41 Capillary pressure for 5 regions.…….……(52)
42 Relative permeability for 5 regions…….……(52)
43 Original oil saturation in 8 cell layers…….……(53)
44 Sketch diagram of error calculation…….……...(59)
45 Pressure matching with different permeability distribution.…….…..(60)
46 Relative permeability comparison.…….……...….(60)
47 Water cut matching with different relative permeability…….…….…..(61)
48 History matching of production rate for well –8-8……..……...(62)
49 History matching result of production rate for well -54…….……....(62)
50 History matching of production rate for well –11-12……..……..……..(63)
51 History matching result of production rate for well –12-12…….……..…....(63)
52 Bottom hole pressure matching result of well -54.…….……..…....(64)
53 Bottom hole pressure matching result of well -67.…….....(64)
54 Production rate matching result for whole reservoir.……..……(65)
55 Water cut matching result for whole reservoir ……(65)
56 Matching result of cumulative production of water and oil……..…….…….....(66)
57 Residual oil distribution till to April 2000 with water flooding.……..……..…..….(67)
58 Production rate and water cut prediction under water flooding.……..……(68)
59 3D Grid Model..…….…….....(70)
60 Porosity distribution…….……..…....(71)
61 Permeability distribution.…….……..…..(71)
62 Region Number.……..…….……(71)
63 Original oil saturation distribution profile……..(72)
64 Water and oil production rate…….…….……...…..(73)
65 Water cut with water flooding…….…….……...…(73)
66 Oil recovery with water flooding…….……...(73)
67 Residual oil saturation distribution after water flooding……..……..(74)
68 Relation between viscosity of polymer solution and temperature.…….……(75)
69 Relation between viscosity and concentration……..…….…….....(75)
70 Polymer solution viscosity function fro polymer flooding simulation.……...(76)
71 Shear thinning factor for polymer solution……..…….……..(76)
72 Polymer adsorption functions …….……...…….....(77)
73 Oil and water production rate with different polymer adsorption function…….....(77)
74 Oil recovery under polymer flooding with
different polymer adsorption function……(78)
75 Oil and water production rate with different polymer concentration.…..……(79)
76 Oil recovery with different polymer concentration…….…….....(79)

77 Oil and water production rate with different polymer injection slug size.....(80)
78 Oil recovery with different polymer slug size.....(80)
79 Residual oil saturation distribution after polymer flooding.....(81)
80 Field oil and water production rate with different polymer slug size.....(84)
81 Field water cut with different polymer slug size.....(84)
82 Reservoir oil recovery with different polymer slug size.....(85)
83 Enhanced oil per ton polymer consumption.....(86)
84 Polymer flooding process for whole reservoir.....(87)
85 Oil, water and polymer production rate of well -54.....(88)
86 Oil, water and polymer production rate of well -60.....(89)
87 Oil, water and polymer production rate of well -67.....(89)
88 Residual oil saturation distribution.....(91)

Tables

Table 1 IOR Methods.....(3)
Table 2 Criteria for Polymer flooding[6] .....(4)
Table 3 Oil properties.....(43)
Table 4 Water properties.....(44)
Table 5 Well List.....(44)
Table 6 Well match result.....(62)
Table 7 Oil recoveries with different polymer concentration.....(79)
Table 8 Oil Recoveries with different polymer slug size.....(81)
Table 9 Well specification.....(83)
Table 10 Simulation result with different polymer slug size.....(86)

1. Introduction

1.1 Oil Production Situation in China and Shengli Oilfields

Currently, China is the world's third largest oil consumer, next to the United States and Japan. During the past two decades, China has changed from an oil-exporting country to a net oil-importing country [1]. Fig. 1 (The data are from statistics of Chinese government.) To backup the economic growth, China is expected to surpass Japan in the oil consumption as the second largest world oil consumer within the next decade, and to reach a petroleum production consumption level of 8.8 million bbl/day by 2020 [2]. Surely more and more oil is to be imported, but in order to avoid energy crisis, China's own production rate must be maintained on an appropriate level; which brings a great challenge to China's Petroleum industry.

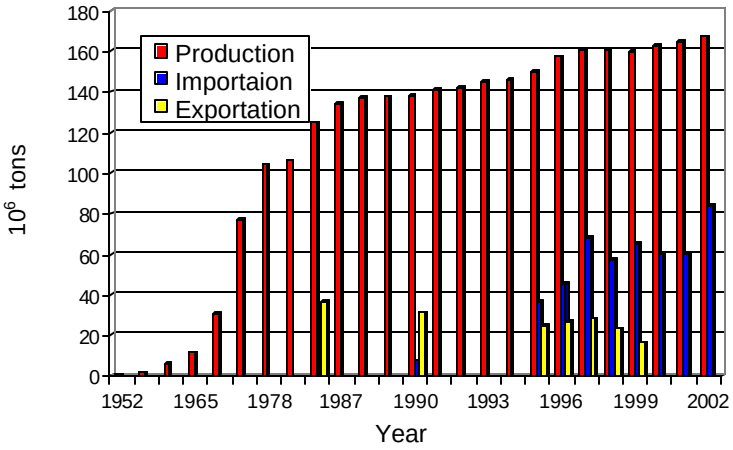

Fig.1 China's Oil Production, Exportation and Importation

Fig. 2 Location of Shengli Oil Field

The increase in China's oil production since 1990's mainly come from offshore oil field. In the near future, great production rate promotion seems impossible, and it is not likely to find great reserves either. As most of the oilfields onshore have reached their high water cut stage, methods of improving oil recovery must be found to meet the increasing demands of oil consumption.

Note: In Fig. 1 the data about the amount of oil importation and exportation in some years are not found.

Shengli Oilfields area is the second largest oil producing base in China, lies in the Yellow River Delta (Fig. 2), covering some 44 thousand sq. KM. Its oil deposits are dispersed over 8 cities or prefectures of Dongying, Binzhou, Dezhou, Jinan, Weifang, Zibo, Liaocheng, and Yantai, including 28 counties.

Till the end of 2000, 69 oil and gas fields of different kinds have been found, including 6 oilfields in beach area, one oilfield offshore. Totally 4.045 billion tons of oil geological reserve and 35.659 billion cubic meter of natural gas geological reserve were proved. 0.366 billion tons of oil geological reserve in the offshore area was proved.

65 oil and gas fields were developed, with 3.333 billion tons of geological reserve available. The production rate has been decreasing since 1991 and now with oil production capability of 26.25 million tons (Fig. 3) . It has produced totally 0.719 billion tons of crude oil. At present, the average comprehensive water cut in the whole area is 89.9%, decline rate is 13.92%, comprehensive decline rate is 6.3%, and the production velocity of the available reserve is 10.02% [3].

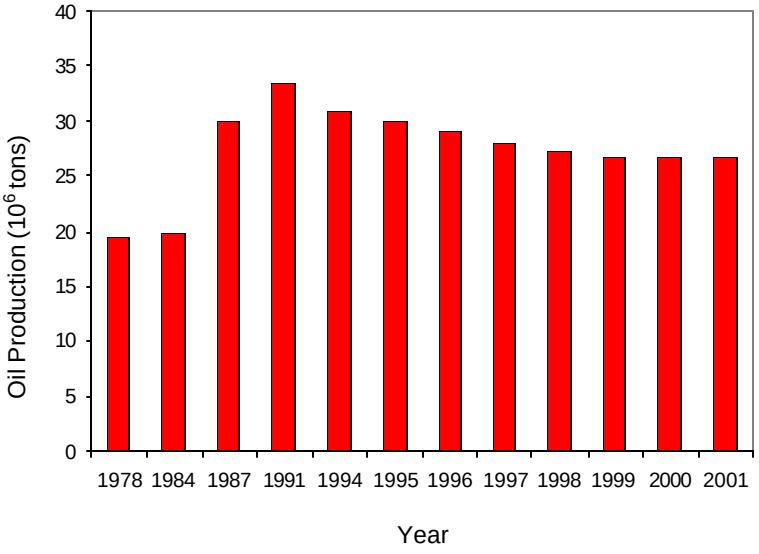

Fig.3 Oil Production History of Shengli Oil Field

Shengli Oilfields plays an enormous role in keeping stable oil production in China. In the past decade many detailed reservoir description projects, aiming at infill-drilling, producing pattern and layers adjustment, have been done in most of the oil fields. The average recovery of total Shengli Oilfields till now is only about 21.57%. In order to improve oil recovery and maintain the production rate, different IOR methods should be applied to different reservoirs in the coming decade.

1.2 Researching Area - Z106 Oilfield

Z106 oil field lies in the northern part of Shengli Oilfields area. It was found through well Z106 in 1986, and has been developed from 1988 (Fig.17). The Reservoir's depth is between 1300-1450 meters under sea level. The viscosity of its oil under reservoir condition with resolved gas is 95.9 cp, under surface condition it is between 305- 673 cp; its density is

0.9441 g/cm^3 (18.38 °API). According to the definition by Okandan [4] the oil of **Z106** oilfield belongs to heavy oil.

During the reservoir's development the water cut increased very quickly. At the end of 2000 water cut reached 93.4%, but the oil recovery was only about 20.5%.

Due to the extremely high oil-water viscosity ratio and permeability heterogeneity of river-channel sandstone etc., the oil production velocity is very low, the predicted final recovery will be also very low. Method of improving the water flooding efficiency and getting a higher oil recovery is needed urgently.

1.3 Possible IOR Method for Z106 Oilfield – Polymer Flooding

Improving Oil Recovery (**IOR**) is an researching area aiming to obtain more oil from existing oil reservoirs. Because reservoir rock is a multi-porous media, when more than two phases exist in the pore volume, there must be capillary pressure; it is because of the capillary pressure , immiscibility of water and oil and their different mobility, we can not obtain all the oil in place, but we want to get more oil by using IOR methods to change these factors respectively.

Table 1 IOR Methods

Chemical	1. Microemulsion or micellar emulsion flooding **2. Polymer-Augmented water flooding** 3. Alkaline flooding
Thermal	1. Steamdrive Injection 2. In-Situ combustion 3. Cyclic steam injection
Miscible	1. Miscible fluid displacement 2. CO_2 augmented water flooding 3. Immiscible CO_2 displacement

Based on the elementary mechanisms of oil recovery, IOR methods can be classified into three categories: **Chemical**, **Thermal** and **Miscible** methods [5] (Table 1).

Different IOR methods are suitable for different oil reservoirs, and for different IOR methods some preconditions must be satisfied.

Miscible methods are only suitable for light oil reservoir [6]. The oil viscosity should be lower than 10 cp and density more than 20 °API. The average value for current worldwide field projects is more than 35°API.

For heavy oil reservoir only thermal EOR methods and Polymer flooding (one chemical IOR method) are feasible [7].

With steam injection methods the reservoir depth is limited under 4500 ft (1370 meter) owing to the limitation of technique at present. The commercial risk becomes much more higher when reservoir depth increases. In-Situ combustion method is specially applied to reservoir with moderately heavy oil containing asphalt and naphtha compounds.

Considering the preconditions of IOR methods, polymer flooding seems the most favourable method for Z106 oilfield. Seen in Table 2 [6].

Table 2 Criteria for Polymer flooding [6]

EOR Method	Oil Properties				Reservoir Characteristics				
	°API	Viscosity (cp)	Composition	Oil Saturation (%PV)	Formation Type	Net Thickness (ft)	Average Permeability (mD)	Depth (ft)	T emperature (°F)
Polymer flooding	>15 till to 40	<150, >10	N.C.	>70	Sandstone preferred	N.C.	>1000	<9000	<200

N.C.: not critical.

Polymer flooding - a technique using polymer solutions to increase oil recovery- was first introduced in secondary or tertiary oil-recovery operations in the early 1960´s [8]. Since then, this chemical IOR method has attained wide-spread commercial application and enormous publications could be found for different reservoir cases.

In polymer flooding, a water-soluble polymer is added into the flood water. This increases the viscosity of water. There are three potential ways in which a polymer flooding makes the oil recovery process more efficient: (1) through the effects of polymers on fractional flow, (2) by decreasing the water/oil mobility ratio, and (3) by diverting injected water from zones that have been swept [9].

The most important preconditions for polymer flooding are reservoir temperature and the chemical properties of reservoir water. At high temperature or with high salinity in reservoir water, polymer can not be kept stabile and polymer concentration will lose most of its viscosity. In Z106 oil field these preconditions can all be satisfied, since the reservoir temperature is only about 65°C and the total salinity is between 2434 – 4566 mg/l.

But the sandstone in Z106 oil field is mainly of river channel facies; permeability heterogeneity is very serious; because of the narrow-banded distribution of sandstone, wells can not be drilled in regular pattern; some reservoirs even have bottom water. At present, water cut has already reached 93.4%. When all these situations being taken into consideration, whether polymer flooding is still really practical, it should be further

investigated before putting it into practice. Unfortunately, in the existing literature there is still no systematic discussion about polymer flooding in such heavy oil reservoir.

Since 1980's reservoir simulation has become more and more important in reservoir development or in an IOR project, because it provides quantitative prediction about feasibility and effect of the IOR method.

This dissertation is aimed at studying the feasibility of polymer flooding in Z106 Oilfield, taking reservoir $Z106Ng2^1$ as an example, and by means of simulation with simulator: **ECLIPSE**.

Such reservoir as $Z106Ng2^1$ is widespread in Shengli Oilfields area. Fig. 4 is the oil reserve distribution in depth in Shengli Oilfields area [10]. The strata at this depth belong to Miocene of Neogene. In the north-China basin the strata are mainly of river facies. From this view, this research is of great value for improving oil recovery not only in Z106 oil field but also in the whole Shengli Oilfields area, as a result, also of enormous significance to keep oil production stable for the coming decades.

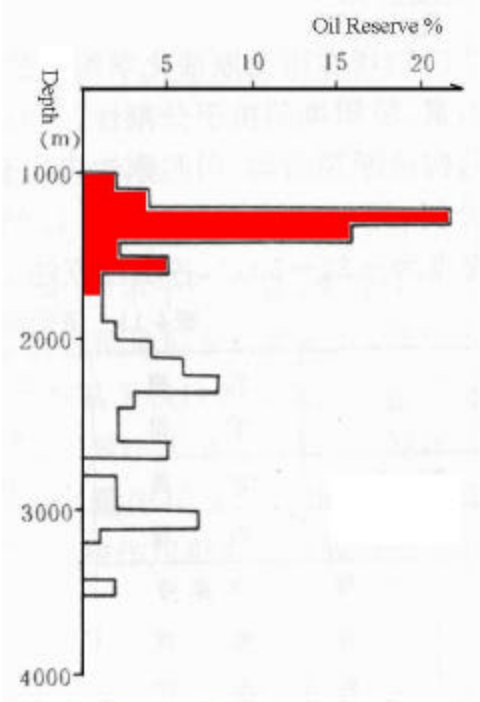

Fig. 4 Oil Reserve Distribution in Shengli Area
(from Wang Binghai and Qian Kai)

2 Theoretical Basis for Reservoir Simulation with Polymer Flooding

Simulation is the only way to quantitatively describe the flow process of multi-phases in a heterogeneous reservoir; owing to the development of computer and computing techniques reservoir simulation has gained great progress in the past decades, from the simplest single-phase model to multi-phase multi-component models, and got wide usage throughout the world. Many commercial software companies have provided their simulators, and thus have gained great commercial profits. Some research institutes or universities also have their own simulators aiming at theoretical research or education.

Though softwares have been upgraded version by version so quickly, the theoretical basis of most of those softwares still is multi-phase multi-component flow model or its simplified models. This chapter introduces the basic dynamics of fluids and mathematical model of fluid and polymer transport process in porous media.

2.1 Reservoir Rock - Porous Medium

Reservoir rock is characterized by presence of solid matrix and a void space. The void space is usually occupied by fluids- water and oil (and/or gas). As a porous medium it has two important properties: **porosity** f and **permeability** K.

The porosity of a rock is a measurement of the storage capacity (pore volume) that is capable of holding fluids. Quantitatively, the porosity is the ratio of the pore volume (V_p) to the total volume (bulk volume V_b). This important rock property is determined mathematically by the following generalized relationship:

$$f = \frac{V_p}{V_b} \qquad (2\text{-}1)$$

As for geologists there are different concepts of porosity: absolute porosity and effective porosity. Here we mean the **effective porosity,** and assume that all pores are interconnected and effective for fluid flow.

Permeability, K, is a property of the porous medium that measures the capacity and ability of reservoir rock to transmit fluids. Henry Darcy first defined this characterization mathematically in 1856. The equation that defines permeability in terms of measurable quantities is called **Darcy's Law**.

$$v = -\frac{K}{m}\frac{dp}{dL} \qquad (2\text{-}2)$$

Where v = apparent fluid flowing velocity, cm/sec
K = permeability, Darcys
m = viscosity of flowing fluid, cp
dp/dL= pressure gradient, atm/cm

Natural reservoir rock is usually not isotropic but anisotropic. Permeability is a directional tensor with 3 principle directions in 3D space [11].

$$K = \begin{pmatrix} K_{xx} & K_{xy} & K_{xz} \\ K_{yx} & K_{yy} & K_{yz} \\ K_{zx} & K_{zy} & K_{zz} \end{pmatrix} \qquad (2\text{-}3)$$

This is a symmetrical tensor, with coordinate system rotation we get a diagonal matrix as follows:

$$K = \begin{pmatrix} K_{xx} & 0 & 0 \\ 0 & K_{yy} & 0 \\ 0 & 0 & K_{zz} \end{pmatrix} \qquad (2\text{-}4)$$

For sandstone, between the horizontal permeability K_{xx} and K_{yy}, there is not so great difference as that from vertical permeability K_{zz}, in this study they are assumed equal.

$$K_{xx} = K_{yy} > K_{zz} \qquad (2\text{-}5)$$

Owing to the different original sedimentary environments and later diagenesis in geological history, reservoir rock is not only anisotropic but also heterogeneous in micro-scaling and macro-scaling. The properties mentioned above are all discussed on Representative Elementary Volume (REV) [11]. The variation of these properties is assumed to be continuous in space and not variable in time dimension.

2.2 Mathematical Model for Reservoir Simulation and Its Simplification

Mathematical model can be complicated as multi-phase multi-component model for some condensate reservoir simulation, or simplified as black-oil model for some normal oil reservoir simulation. For some oil reservoir it can even be simplified as a two-phase (oil and water) flow model, and gas resolution can be neglected. Which kind of model is needed is determined by the precision demand of the research. For all these models the principles are the same: conservation of **mass**, of **energy** and (/or) of **momentum**. In this dissertation only the principle of conservation of mass is considered, because the temperature variation in the aimed reservoir can be neglected. We consider it an isothermal process.

2.2.1 Multi-phase Multi-component Model [12-13]

In a 3 phases (oil, gas and water) N components model, the mass conservation principle does not fit for any phase, because there is always mass transformation between any two phases during the flow process. The conservation equation can be only constructed by component.

Based on mass conservation principle and Darcy's Law, N continuity equations are constructed for N components:

$$\nabla \cdot (\sum_{j} (Z_{i,j} r_j \frac{k k_{rj}}{m_j} (\nabla p_j - r_j g \nabla H))) - \sum_{j} Z_{i,j} q_{m,j} = \sum_{j} \frac{\partial}{\partial t} (f r_j s_j Z_{i,j}) \qquad (2\text{-}6)$$

$i = 1,2,\ldots,N;\ j = o,g,w$

$Z_{i,j}$ = mass fraction of i component in j phase, unitless

r_j = density of j phase, kg/m^3

k = permeability, MDarcy

k_{rj} = relative permeability of j phase, unitless

p_j = pressure of j phase, bar

g = acceleration of gravity, constant, m/s^2

H = depth, m

$q_{m,j}$ = mass flow rate per unit of volume of rock through well, kg/m3day

s_j = saturation of j phase, fraction, unitless

Equilibrium equations between phases:

$$K_{i,go} = \frac{Z_{i,g}}{Z_{i,o}} = K_{i,go}(P_g, P_o, T, Z_{1,o}, Z_{2,o} \cdots, Z_{N,o}, Z_{1,g}, Z_{2,g} \cdots, Z_{N,g}) \qquad (2\text{-}7)$$

$$K_{i,gw} = \frac{Z_{i,g}}{Z_{i,w}} = K_{i,gw}(P_g, P_w, T, Z_{1,w}, Z_{2,w} \cdots, Z_{N,w}, Z_{1,g}, Z_{2,g} \cdots, Z_{N,g}) \qquad (2\text{-}8)$$

State equations of three phases:

$$r_j = r_j(P_j, Z_{1,j}, Z_{2,j}, \cdots, Z_{N,j}) \qquad \text{j = o,g,w.} \qquad (2\text{-}9)$$

Viscosities of three phases:

$$m_j = m_j(P_j, Z_{1,j}, Z_{2,j}, \cdots, Z_{N,j}) \qquad \text{j = o,g,w.} \qquad (2\text{-}10)$$

Other equations for component model:

$$S_o + S_g + S_w = 1 \qquad (2\text{-}11)$$

$$P_{c,ow} = P_o - P_w \qquad (2\text{-}12)$$

$$P_{c,go} = P_g - P_o \qquad (2\text{-}13)$$

$$k_{ro} = f(S_o) \qquad (2\text{-}14)$$

$$k_{rw} = f(S_w) \qquad (2\text{-}15)$$

$$k_{rg} = f(S_o, S_g) \qquad (2\text{-}16)$$

$$\sum_{i=1}^{N} Z_{i,j} = 1 \qquad \text{j = o, g, w} \qquad (2\text{-}17)$$

Theoretically, this 3N+15 equations group together with a set of initial and boundary conditions is already a fully closed system and could be solved.

2.2.2 Black-oil Model [12-14]

Since the component model has so many variables that it is very complicated to solve it especially with large grid density. In practice, black-oil model is more widely used for most of the reservoirs, because it provides simulation results with enough precision.

Black-oil model was got from simplification of component model with the following assumptions:

(1) only three components: oil, gas and water,
(2) three phases: oil, gas and water,
(3) gas component could be resolved in oil phase,
(4) the equilibrium between oil and gas phases could be got simultaneously,
(5) no condensate oil in gas phase,
(6) in water phase there is only water component.

The equations group could be simplified as follows:

For oil component: $$\nabla \cdot (\frac{kk_{ro}}{m_o B_o}(\nabla P_o - r_o g \nabla H)) - \tilde{q}_{v,o} = \frac{\partial}{\partial t}(\frac{fS_o}{B_o}) \quad (2\text{-}18a)$$

For gas component: $$\nabla \cdot (\frac{kk_{rg}}{m_g B_g}(\nabla P_g - r_g g \nabla H)) + \nabla \cdot (\frac{kk_{ro}R_s}{m_o B_o}(\nabla P_o - r_o g \nabla H)) - (\tilde{q}_{v,g})_{tot} = \frac{\partial}{\partial t}(f(\frac{S_g}{B_g} + \frac{R_s S_o}{B_o})) \quad (2\text{-}18b)$$

For water component: $$\nabla \cdot (\frac{kk_{rw}}{m_w B_w}(\nabla P_w - r_w g \nabla H)) - \tilde{q}_{v,w} = \frac{\partial}{\partial t}(\frac{fS_w}{B_w}) \quad (2\text{-}18c)$$

Where: $r_o = \frac{r_{o,sc} + r_{g,sc}R_s}{B_o}$, oil density, kg/m^3

$r_w = \frac{r_{w,sc}}{B_w}$, water density, kg/m^3

$r_g = \frac{r_{g,sc}}{B_g}$, gas density, kg/m^3

$\tilde{q}_{v,o} = \frac{\tilde{q}_{m,o}}{r_{o,sc} + r_{g,sc}R_s}$, oil flow rate per unit volume of rock through well, m^3/day m^3

$(\tilde{q}_{v,g})_{tot} = \frac{\tilde{q}_{m,g}}{r_{g,sc}} + q_{o,sc}R_s$, gas flow rate per unit volume of rock through well, m^3/day m^3

$\tilde{q}_{v,w} = \frac{q_{m,v}}{r_{w,sc}}$, water flow rate per unit volume of rock through well, m^3/day m^3

$r_{o,sc}, r_{g,sc}, r_{w,sc}$ are densities of oil, gas and water under standard conditions.

For reservoir $Z106N_g2$[1], gas resolution in oil is only 16.35 m^3/m^3, and bubble point pressure is 6.87 MPa, average reservoir pressure is 13.27 MPa. Since water had been injected before the reservoir was put into production, it is believed that there is no free gas in reservoir condition during oil production. To simplify the problem, the gas component can also be neglected in the mathematical model.

Equations simplified as follows:

$$\nabla \cdot (\frac{kk_{ro}}{m_o B_o}(\nabla P_o - r_o g \nabla H)) - \tilde{q}_o = \frac{\partial}{\partial t}(\frac{fS_o}{B_o}) \qquad (2\text{-}19a)$$

$$\nabla \cdot (\frac{kk_{rw}}{m_w B_w}(\nabla P_w - r_w g \nabla H)) - \tilde{q}_w = \frac{\partial}{\partial t}(\frac{fS_w}{B_w}) \qquad (2\text{-}19b)$$

Where:

$$r_o = \frac{r_{o,sc}}{B_o}, \qquad \tilde{q}_o = \frac{\tilde{q}_{m,o}}{r_{o,sc}}$$

Other two additional equations:

$$S_o + S_w = 1 \qquad P_w = P_o - P_{c,ow}$$

The derivatives of $P_{c,ow}$, and r or B in space are much less than derivatives of pressure and saturation. In the equations they can be neglected, too. And the equations mentioned above can be derived as follows:

$$\nabla \cdot ((\frac{kk_{ro}}{m_o} + \frac{kk_{rw}}{m_w})\nabla P_o - g\nabla \cdot ((\frac{r_o kk_{ro}}{m_o} + \frac{r_w kk_{rw}}{m_w})\nabla H) - \tilde{q}_{o+w} = fC_f \frac{\partial P_o}{\partial t} \qquad (2\text{-}20a)$$

$$\nabla \cdot (\frac{kk_{rw}}{m_w}\nabla P_w) - g\nabla \cdot (\frac{r_w kk_{rw}}{m_w}\nabla H) - \tilde{q}_w = fS_w C_{fw}\frac{\partial P_o}{\partial t} + f\frac{\partial S_w}{\partial t} \qquad (2\text{-}20b)$$

Where: $C_f = \frac{f^0}{f} C_r + S_o C_o + S_w C_w$,

$$C_{fw} = \frac{f^0}{f} C_r + C_w$$

C_r, C_o, C_w are compressibilities of rock, oil and water.

In the left part of water equation in (2-20b), $fS_w C_{fw} \frac{\partial P_o}{\partial t} << f \frac{\partial S_w}{\partial t}$, in practice, it is usually neglected, too. As a result, the first equation of (2-20) is for pressure, and the second for saturation. With corresponding boundary conditions, original condition and a few functions to define parameters in the equations, the equations group is solvable.

For most of the water-flooded oil field with medium or heavy oil, this mathematical model can meet the precision demands of reservoir simulation. But with polymer flooding, considering the changes of fluids' properties, the mathematical model should be rectified and another equation is needed for description of the flow process of polymer concentration. This will be introduced in the coming corresponding sections.

2.3 Transport of Hydrolysed Polymer in Porous Media

The main objective of polymer injection during water flooding of oil reservoir is to decrease the mobility of the injected water by increasing its viscosity and decreasing rock permeability to water with adding polymer – a water soluble high molecule organic compound – into injected water. Different polymer has different properties. Polymer's transportation in porous media is also affected by many other factors.

2.3.1 Polymer Types and Their Properties [15]

Polymers can be categorized into two types: polyacrylamides and polysaccharides (biopolymer) as seen in Fig. 5.

Polyacrylamides (HPAM)

These polymers' monomeric unit is the acrylamide molecule (Fig.5 (a)). When used in polymer flooding, polyacrylamides have undergone partial hydrolysis, which causes anionic (negatively charged) carboxyl groups ($-COO^-$) to be scattered along the backbone chain. For this reason these polymers are called partially hydrolysed polyacrylamides (HPAM). Typical degrees of hydrolysis are 30-35% of the acrylamides monomers; hence the HPAM molecule is negatively charged, which accounts for many of its physical properties. This degree of hydrolysis has been selected to optimise certain properties such as water solubility, viscosity, and retention. If hydrolysis is too small, the polymer will not be water-soluble. If it is too large, the polymer will be too sensitive to salinity and hardness [16].

The viscosity-increasing feature of HAPM lies in its large molecular weight. This feature is accentuated by the anionic repulsion between polymer molecules and between segments in the same molecule. The repulsion causes the molecule in solution to elongate and snag on those similarly elongated, an effect that accentuates the mobility reduction at higher concentrations.

If the brine salinity or hardness is high, this repulsion is greatly decreased through ionic shielding since the freely rotating carbon-carbon bonds allow the molecule to coil up.

The shielding causes a corresponding decrease in the effectiveness of the polymer since snagging is greatly reduced. Almost all HPAM properties show a large sensitivity to salinity and hardness, which is an obstacle to use HPAM in many reservoirs; on the other hand, HPAM is inexpensive and relatively resistant to bacterial attack, and it exhibits permanent permeability reduction.

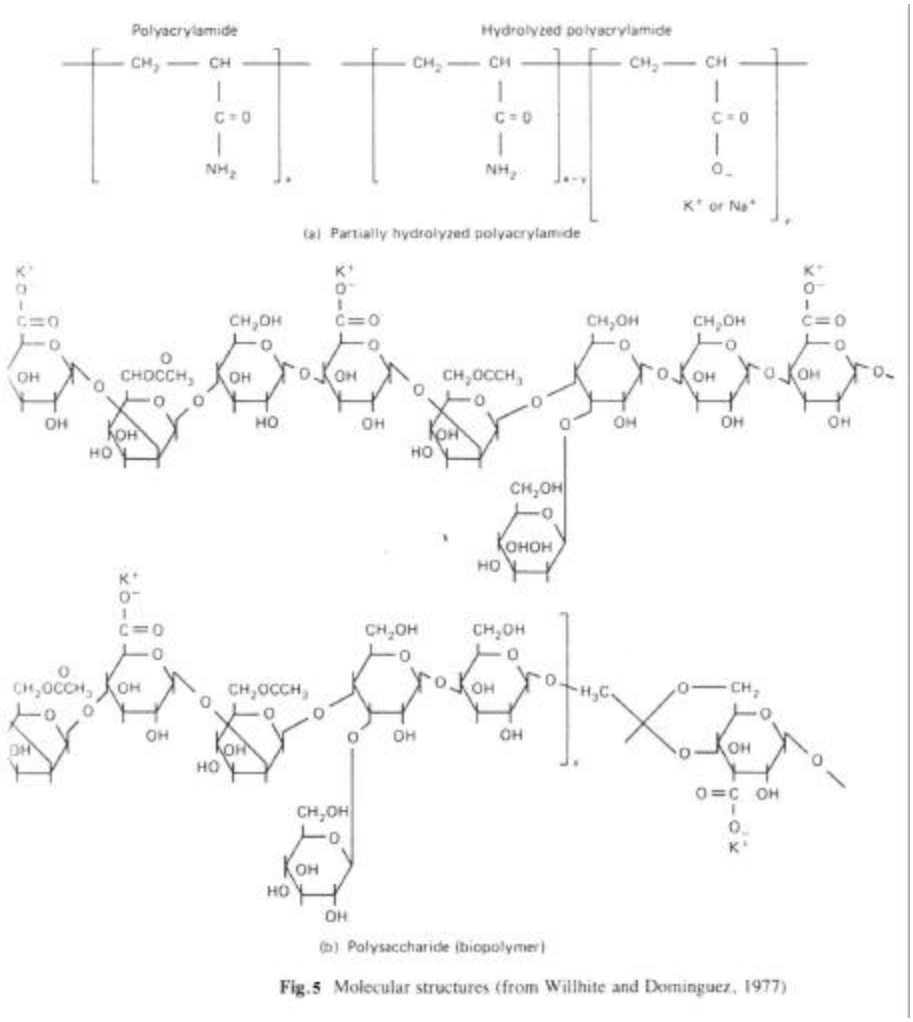

Fig.5 Molecular structures (from Willhite and Dominguez, 1977)

Polysaccharides

This kind of polymer is formed from the polymerisation of saccharide molecules (Fig.5 (b)), a bacterial fermentation process. This process leaves substantial debris in the polymer product that must be removed before the polymer is injected. The polymer is also susceptible to bacterial attack after it has been introduced into the reservoir. The disadvantages are also offset by the insensitivity of polysaccharide properties to brine salinity and hardness.

The polysaccharide molecule is relatively non-ionic and, therefore, free of the ionic shielding effects of HPAM. Polysaccharides are more branched than HPAM, and the oxygen-ringed carbon bond does not rotate fully; hence the molecule increases brine viscosity by snagging and adding a more rigid structure to the solution. Polysaccharides do not exhibit permeability reduction. Molecule weights of polysaccharides are generally around 2 million.

HPAM is much cheaper than Polysaccharides so it was used in most of the polymer flooding projects. In this research HPAM is also adopted since the water brine salinity in oil Z106 is only 2434- 4566 mg/l.

2.3.2 Viscosity of Polymer Solution and Its Shear Thinning

Flory [17] provided the following function to describe the relation of polymer solution viscosity via polymer concentration.

$$m_c^1 = m_1(1 + a_1 C_p + a_2 C_p{}^2 + a_3 C_p{}^3 + \cdots) \qquad (2\text{-}21)$$

Where: m_c^1 is viscosity of polymer solution,

$a_1, a_2, a_3, \cdots$ are constants,

C_p is polymer concentration.

With polymer concentration increasing, viscosity of polymer solution increases quickly. Fig. 6 is the data of one HPAM-Polymer under reservoir condition and their regression line. The correlation coefficient is even equal to 1.

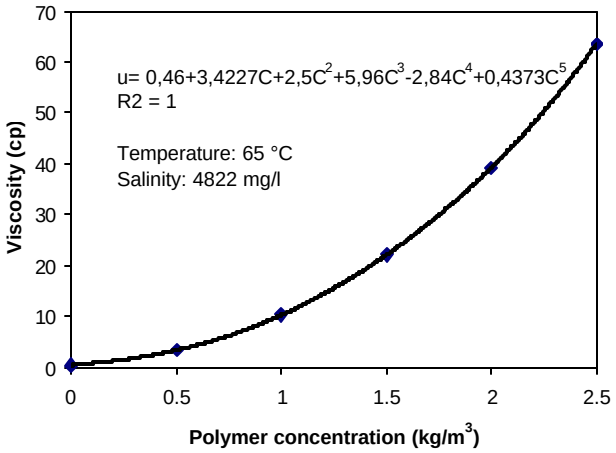

Fig.6 Polymer viscosity via concentration

All polymers have shear thinning; their viscosity decreases with shear rate $\dot{g}$ increasing (Fig.7 from [15]). The shear thinning behaviour of the polymer solution is caused by the uncoiling and unsnagging of the polymer chains when they are elongated in the shear flow [15]. It can be described by a power-law model:

$$m_c^{''} = m_c^1 (\dot{g})^{n_{pl}-1} \qquad (2\text{-}22)$$

Where: $m_c^{''}$ polymer solution viscosity under shear rate $\dot{g}$,

n_{pl} $0 < n_{pl} < 1$.

For different polymer, it is different. It is also a parameter to evaluate the quality of polymer.

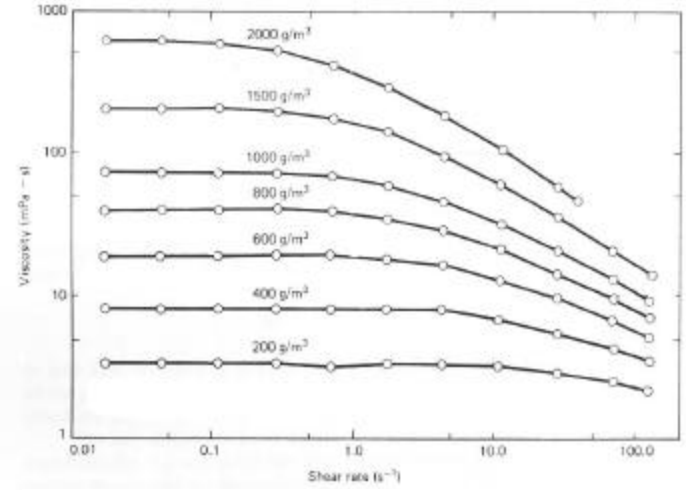

Fig. 7 Shear thinning effect on viscosity (from [15])

For any polymer product it has a critical shear rate, at this rate polymer chain can be broken and lose its properties forever. Below the critical shear rate, the behaviour is partly reversible. With reasonable injection rate the shear rate near wellbore should be controlled under the critical shear rate, so as to avoid polymer molecule's breaking down.

In this research this property has been taken into account in simulation process. Because shear rate can be controlled by injection rate, it is assumed that the shear thinning is reversible.

2.3.3 Inaccessible Pore Volume in Polymer Flooding

Rapier Dawson and Ronald B. Lantz [18] found that during the solution of typical polymers flowing through the porous media, it could not occupy all of the effective pore volume in this porous media. The remainder of the pore volume is inaccessible to polymer solution. This inaccessible pore volume is occupied by water that contains no polymer. This allows changes in polymer concentration to be propagated through porous media more rapidly than similar changes in salt concentration. Seen in Fig.8 (from [18]).

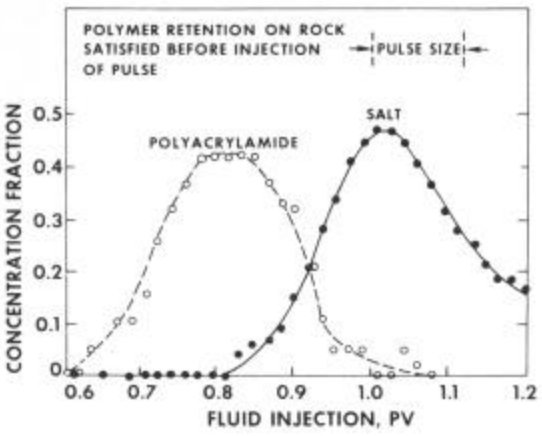

FIG. 8 POLYMER BREAKOUT CURVES.

As a result, in porous media the saturation of polymer solution is not equal to the saturation of aqueous phase.

$$S_w^* = S_w - S_{IPV} \qquad (2\text{-}23)$$

Where: S_w saturation of the whole aqueous phase

S_{IPV} percentage of inaccessible pore volume in whole effective pore space

S_w^* saturation of polymer solution

S_{IPV} depends on polymer molecular weight, rock permeability, porosity, and pore size distribution [15]. In Eclipse it is assumed that it does not exceed the corresponding connate water saturation [19].

But the effect of inaccessible pore volume could be covered by the effect of polymer adsorption. Polymer adsorption leads to polymer bank to be postponed. It will be discussed in next section.

2.3.4 Polymer Retention in Porous Media and Its Effects

When polymer solution flows through porous media, polymer molecule can be adsorbed onto solid surface or trapped within small pores. Polymer retentions vary with polymer type, molecular weight, polymer concentration, rock composition, permeability, brine salinity, brine hardness, flow rate, and temperature.

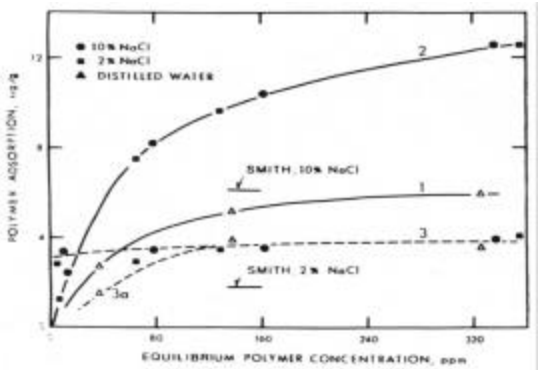

Fig.9 Relation between adsorption and concentration

Szabo [20-21] has done a set of experiments to study the adsorption of hydrolysed polyacrylamides in porous media. His experiment results clearly show that higher polymer concentration leads to higher adsorption. (Fig.9 from Szabo) Dominguez and Willhite have also this conclusion. [22]

Hirasaki and Pope [23] assume that polymer molecules are adsorbed onto solid surface in monolayer, and then conclude that the adsorption amount is in direct proportion to surface area of pore space of the rock. This can better explain the reason of an up-convex adsorption isotherm.

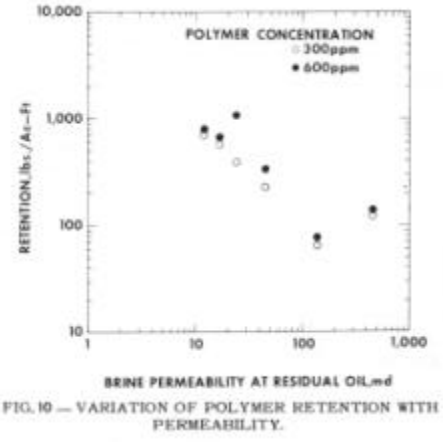

FIG. 10 — VARIATION OF POLYMER RETENTION WITH PERMEABILITY.

Zaitoun and Kohler [24] conclude that an increase in clay both decrease permeability and increase the polymer adsorption. This result is parallel to the results from Saul Vela, Peaceman and Sandvik [25]. They have found that adsorption amount of polymer per gram rock decreases as permeability increases (Fig.10 from [25]). It is also parallel with the result of Hirasaki and Pope, since the clay in rock also increases the surface area of pore space.

For a given rock, the adsorption function can be described by a **Langmuir-type** isotherm [15]:

$$C_a = \frac{a_4 C_p}{1 + b_4 C_p} \qquad \text{or} \qquad C_a = C_{a,\max} \cdot \frac{b_4 C_p}{1 + b_4 C_p} \tag{2-24}$$

Where: C_a polymer adsorption, kg/kg

C_p polymer concentration in solution, kg/m^3

$C_{a,\max}$ maximum amount of polymer adsorption, kg/kg

a_4, b_4 constants, unitless.

Polymer adsorption can be harmful for polymer flooding; due to adsorption, the polymer solution gradually loses its viscosity during propagation. But it has also advantages; lots of literature have talked about the effects of adsorbed polymer [26-35]:

(1) Since of polymer's resolvability in water, adsorbed polymer layer increases water wettability and correspondingly increases the irreducible water saturation. As a result, it induces the decrease of water relative permeability. For oil-wet rock, this polymer layer may change the rock to water-wet and induce a dramatic drop of residual of saturation.

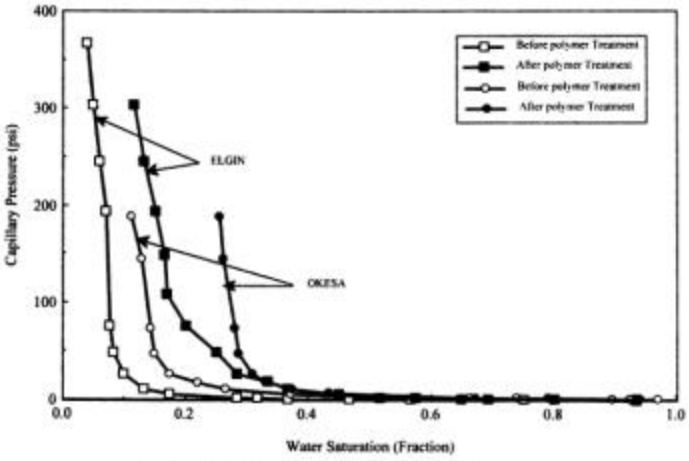

Fig. 11 Variation of capillary pressure (from Ali and Barrufet [35])

(2) Although polymer has little effect on inter facial tension between phases, because the adsorbed polymer layer changes the irreducible water saturation and decreases the radius of pore throats of the rock, it leads to increase of capillary pressure [24]. From Fig. 11, it can be concluded that the increase in capillary pressure mainly comes from the increasing of irreducible wetting phase saturation, when at high water saturation, capillary pressures before and after polymer adsorption have almost no difference.

For oil-wet reservoir rock capillary pressure has great change, even ranging from negative to positive [31].

(3) all experiment results from literature have shown that adsorbed polymer induces a marked reduction in wetting phase relative permeability, degree of these reductions depends

on the amount of adsorption of polymer; it also depends on the rock permeability. Saul Vela et al. [25] have found that the higher the permeability is, the less effect it has.

For no-wetting phase (oil) the effect of polymer adsorption is not so marked as that for the wetting phase (water). Till now there is still no agreement on this phenomenon. The earlier literature [26] has concluded that polymer adsorption has no effect on oil relative permeability.

Later A. Zaitoun and N. Kohler [28] have concluded: the oil relative permeability is shown to be little affected by adsorbed polymer; this phenomenon is interpreted as the result of the competition between the reduction of flow cross section and the enhancement of the water-wettability of the rock, since these two effects reciprocally offset their influence.

Recently, Ali and Barrufet [35] have published their experiment results, which show that the effect of adsorbed polymer on no-wetting phase's (oil's) relative permeability is different in different rocks. A decrease has been observed in Elgin sandstone (Elgin SS), whereas an increase has been observed in Okesa sandstone (Okesa SS) at the same polymer concentration. Seen in Fig.12 and Fig.13.

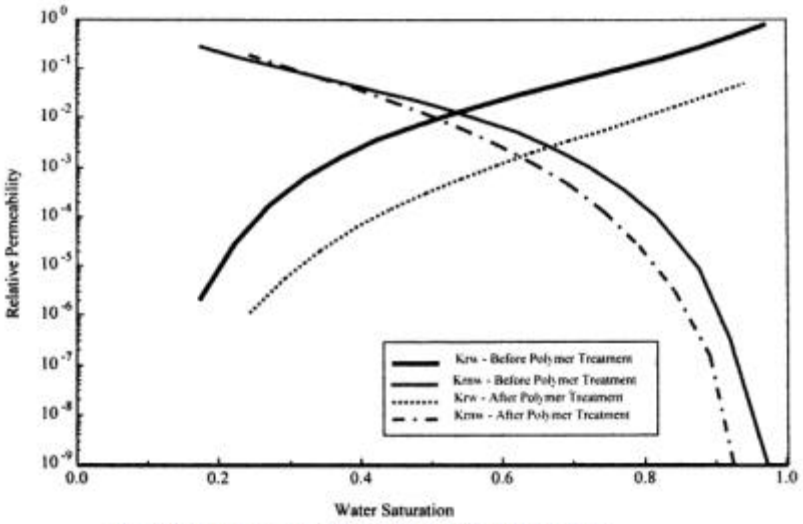

Fig. 12 Relative Permeablity of Elgin sandstone (from [35])

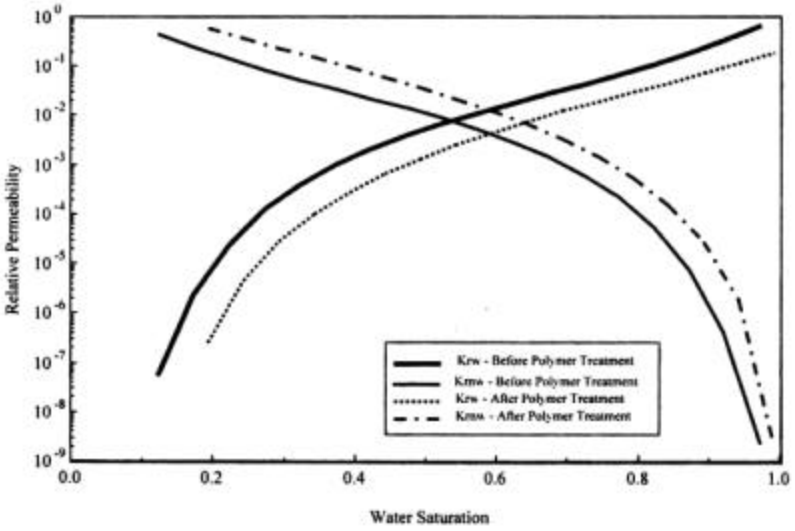

Fig. 13 Relative Permeability of Okesa sandstone (from [35])

They suspect that these differences might be due to the distribution of clays in the pores and to their interaction with the adsorbed polymer. This phenomenon needs to be paid more attention to in the future.

For reservoir simulation of polymer flooding, the effects of polymer adsorption can be taken into account with a permeability reduction or increasing factor for different phases.
They can be defined by:

$$R_{k,j} = \frac{k_j}{k_j^{'}} = \frac{k_{rj}}{k_{rj}^{'}} \qquad (2\text{-}25)$$

Where: $R_{k,j}$ the permeability reduction or increasing factor for j phase,

k_{rj} relative permeability for j phase without polymer adsorption

$k_{rj}^{'}$ relative permeability for j phase with polymer adsorption

j oil or aqueous phase

For a given core, this factor is a function of amount of adsorbed polymer. How to describe this function mathematically, is still a task for researcher in this area, since till now there is no systematic laboratory data, although someone has provided some function type to try to better describe it. For example, C.G. Zheng et al. [33] gave a function based on his experiment data as seen in Fig. 14.

$$R_{k,j} = R_{\max,j} - \frac{R_{\max,j} - 1}{1 + \left(\frac{C_a}{C_{\frac{1}{2}}} \right)^n} \qquad (2\text{-}26)$$

Where: $R_{\max,j}$ the maximum reduction factor for j phase,

$C_{\frac{1}{2}}$ the amount of adsorbed polymer per gram of rock when $R_{k,j} = \frac{1}{2} R_{\max,j}$,

n constant

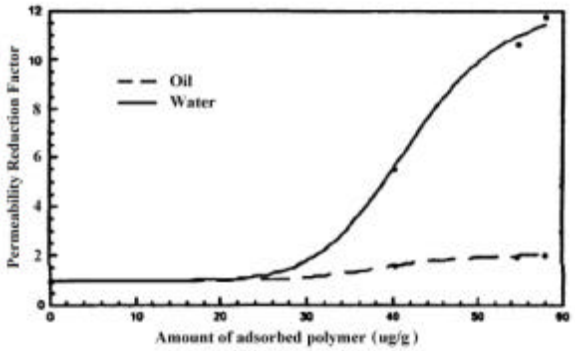

Fig. 14 relative permeability reduction as a function of polymer adsorption in Core (from Zheng [33])

Though this function has such shape as in Fig.14 it is not correct, since when $C_a = C_{\frac{1}{2}}$, $R_{k,j}$ is not $\frac{1}{2} R_{\max,j}$ as he has defined.

At present most of the simulators still use a lineal function to deal with this problem, the equation is as follow [36]:

$$R_k = 1.0 + (R_{\max} - 1.0) \frac{C_a}{C_{a,\max}} \qquad (2\text{-}27)$$

In this dissertation it is accepted as the function of permeability reduction factors.

The variation of capillary pressure has not been taken into account, because: (1) it changes only when the wetting phase's saturation is close to the irreducible water saturation; (2) this reservoir has already been flooded with water, thus the water saturation is much higher than the irreducible water saturation.

2.3.5 Mathematical Model of Polymer Transport in Porous Media

Polymer can be taken as one component of multi-component model, and be assumed not to be resolved in oil phase. Based on mass balance principle the transport equation can be constructed as follows [11,15,37]:

$$\frac{\partial}{\partial t}\left(fS_w^* C_p + r_r(1-f)C_a\right) = div\left(\hat{D}gradC_p - C_p\vec{V}_w\right) - q_w \cdot C_{pi} \qquad (2\text{-}28)$$

Where: C_p polymer concentration in solution, kg/m^3

r_r rock density, kg/m^3

$\hat{D}$ dispersion coefficient, m^2/day

$\vec{V}_w$ Darcy velocity of aqueous phase, m/Day

q_w water flow rate per unit volume of rock through well, m^3/day m^3

C_{pi} polymer concentration of produced water or injected water, kg/m^3

Other symbols are defined as before.

Due to the polymer adsorption, the variation of permeability and relative permeability could be comprehensively justified with factor R_{kw}, as a result, $\vec{V}_w$ can defined as follows:

$$\vec{V}_w = -\frac{k \cdot k_{rw}}{m_{p,eff} R_{kw}}(\nabla P - r_w g \nabla H) \qquad (2\text{-}29)$$

R_{kw} as defined in last section.

$m_{p,eff}$ effective viscosity of polymer solution.

For polymer flooding the dispersion can be neglected, as it has little effect on the oil recovery [36,38]. (2-28) can be simplified as:

$$\frac{\partial}{\partial t}\left(fS_w^* C_p + r_r(1-f)C_a\right) = -div(C_p \cdot \vec{V}_w) - q_w C_{pi} \qquad (2\text{-}30)$$

As polymer also has effect on water and oil, the equations for water and oil should be also adjusted. Their relative permeabilities are adjusted respectively with R_{kw} and R_{ko}. And the viscosity of water phase is taken as $m_{w,eff}$.

$$\nabla\cdot((\frac{kk_{ro}}{m_o R_{ko}}+\frac{kk_{rw}}{m_{w,eff}R_{kw}})\nabla P_o - g\nabla\cdot((\frac{r_o kk_{ro}}{m_o R_{ko}}+\frac{r_w kk_{rw}}{m_{w,eff}R_{kw}})\nabla H)-\tilde{q}_{o+w}=fC_f\frac{\partial P_o}{\partial t} \quad (2\text{-}31)$$

$$\nabla\cdot(\frac{kk_{rw}}{m_{w,eff}R_{kw}}\nabla P_w)-g\nabla\cdot(\frac{r_w kk_{rw}}{m_{w,eff}R_{kw}}\nabla H)-\tilde{q}_w=f\frac{\partial S_w}{\partial t} \quad (2\text{-}32)$$

Where: R_{ko} relative permeability reduction or increasing factor for oil phase,

$m_{w,eff}$ effective water viscosity.

Since R_{ko} is much smaller than R_{kw} and about it there is now still no common idea, in this research it is set equal to 1.

Treatment of the effective viscosity of water and polymer solution [36]:

$$m_{w,eff}=m_w^{(1-w)}m_c^{\,w} \quad (2\text{-}33)$$

$$m_{p,eff}=m_c^{\,w}m_{p,\max}^{(1-w)} \quad (2\text{-}34)$$

w is the Todd-Longstaff mixing parameter. This parameter is to describe the degree of mixing between water and the injected polymer solution. If $w=1$, then the polymer solution and water are fully mixed; if $w=0$, the polymer solution is completely separated from the existing water. In this work it is assumed that water and polymer solution are completely mixed simultaneously, w is set equal to 1. As a result, $m_{p,eff}=m_{w,eff}=\tilde{m}_c''(C_p)$. $m_c''(C_p)$ is the effective viscosity after shear thinning effect. The shear thinning effect has been assumed reversible.

After injection of polymer solution, water is usually injected again. During this process some of the adsorbed polymer on solid surface would surely be desorbed, and again into polymer solution. But about this process there is no believable mathematical model in literature. From the experiment results of Szabo [20], desorption is not so obvious as adsorption. In this work desorption was neglected. In equation (2-30) C_a is set not to decrease when $\frac{dC_p}{dt}<0$.

With proper initial conditions and boundary conditions, Equations (2-30), (2-31) and (2-32) construct a complete model for polymer flooding.

3 Numerical Treatment of Mathematical Model

For a mathematical model as described in last chapter it is impossible to get an analytical solution. Only an approximate solution can be got with numerical method by dividing the reservoir into a number of small blocks and applying the fundamental equations for flow in porous media to each block – differential equation **discretization**, and then solving algebraic equations system.

In order to get the approximate solution, approximation is necessary for equation discretization. This approximation should be consistent with the differential equation, when the time and space steps diminish to zero, the truncation errors tend to zero. Solutions from the discretized equations should also be stable and convergent to analytical solutions.

According to the discretization process the numerical methods of solving partial differential equations can be classified into two types: finite difference method (FDM) and finite element method (FEM). Their difference is mainly from the method to construct the algebraic equations. With FDM it constructs the algebraic equations by displacing the derivatives in the partial differential equation with finite difference quotients or by using integral method to derive the difference equations. FEM is in fact the Ritz-Galerkin method based on variational principle; the only difference is that FEM uses a class of specially selected orthogonal functions.

FEM has been already widely used for solution of Laplace equation. Though it is also introduced into solving hyperbolic and parabolic equations, most of the simulators for reservoir simulation now are still of FDM.

Recently new discretization methods based on unstructured grid have got wide usage in reservoir simulation. With unstructured grid the main advantage is that individual grid points can be specified anywhere inside the domain, regardless of the positions of any other points, as a result, not only the complex reservoir geometries can be easily represented, but also it significantly reduces the orientation effects. At the same time it can take account of the irregular well-points distribution.

Flow simulations on grids based on triangles have been used by various authors inside and outside the petroleum industry. This technique has benn applied to reservoir simulation by Forsyth [39], and is commonly known as the control volume finite element (CVFE) method, the discretization equations are derived from variational principle. Heinemann et al. [40] have applied it as PEBI (Perpendicular Bisection grid) method or the Voronoi Method, in its derivation of discretization the pressure gradient are displaced with finite difference

quotients, since of that, it is in fact a method of control volume finite difference (CVFD) method with irregular orthogonal grid system. Further works on the CVFE method have been presented by Fung [41] and on the PEBI method by Palagi [42].

The general character of these two methods is keeping mass balance in control volume. When with same grid system (and for CVFE with linear element function), their corresponding coefficient matrixes of discretized equations are with same structure, since the structure of coefficient matrix depends on points' order.

The difference of these two methods is that their transmissibilities are calculated differently. With CVFE method, when the arbitrary point is selected at the circumcenter for every triangular element, and for both methods it is assumed that the permeability of each grid point is equal, the calculate d transmissibility will be also the same.

Since the simulation results have been calculated with ECLIPSE, it is mainly based on CVFD, only description CVFD method is introduced in the following section in 2D as an example.

3.1 Discretization of Equations for Orthogonal Grid System with Control-Volume Finite Difference Method

For numerical simulation reservoir should be separated into a number of arbitrary cells. As in everyone of these control volume, mass balance for anyone component should be kept, the conservative equation can be integrated on each of these control volumes. For the control volume i in Fig.15:

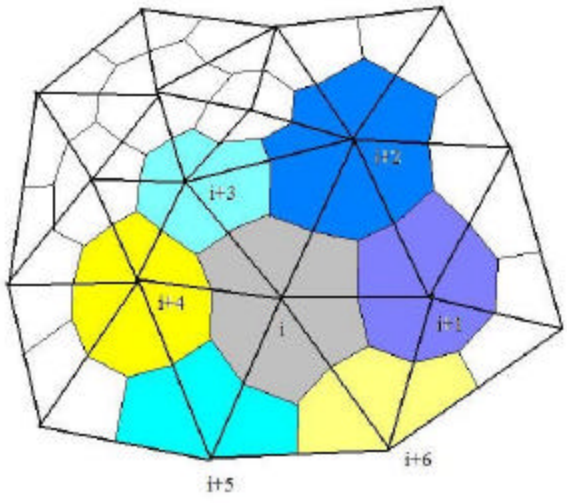

Fig. 15 Control volume in triangular finite element mesh

$$\int_{V_i} \frac{\partial}{\partial t}(f r_w S_w)dv = \int_{V_i} \nabla \cdot (\frac{k k_{rw} r_w}{m_{w,eff} R_{kw}} \nabla \Phi)dv - \int_{V_i} q_w dv \qquad (3\text{-}1)$$

By applying the Gauss divergenc e theorem with a lump mass approach to the accumulation terms, the following equations can be achieved:

$$V_i \frac{(f r_w S_w)^{n+1} - (f r_w S_w)^n}{\Delta t} = \int_s \frac{k k_{rw} r_w}{m_{w,eff} R_{kw}} \nabla\Phi \cdot \vec{n} ds - Q_{wi} \qquad (3\text{-}2a)$$

for explicitness or

$$V_i \frac{(f r_w S_w)^n - (f r_w S_w)^{n-1}}{\Delta t} = \int_s \frac{k k_{rw} r_w}{m_{w,eff} R_{kw}} \nabla\Phi \cdot \vec{n} ds - Q_{wi} \qquad (3\text{-}2b)$$

for implicitness. Where:

$\Phi = p + r_w gH$ is the potential;

V_i the bulk volume of the i control volume;

$\vec{n}$ the outward direction vector of surface of i control volume;

Q_{wi} water production rate or injecting rate through well(s) in control volume i, when there is no well, it is zero;

n-1, n, n+1 time steps.

The integral in the equation (3-2) is a surface integral over all the edges of the control volume.

It can be discretized as sum of integrals over every edge between element i and its neighbouring elements. The discretized equation is as follows:

$$V_i \frac{(f r_w S_w)^n - (f r_w S_w)^{n-1}}{\Delta t} = \sum_{j=1}^{N_i} \left[\frac{T_{ij} r_w k_{rw}}{m_{w,eff} R_{kw}} (P_i^n - P_j^n - r_w g dH_{ij}) \right] - Q_{wi} \qquad (3\text{-}3)$$

Where: N_i the number of neighbouring elements around element i,

T_{ij} Transmissibility between element i and its neighbouring j elements

dH_{ij} Depth deference between element i and its neighbouring j elements

n-1, n superscript means time step

One could refer to references [39-44] for details on the calculation of T_{ij}. $\frac{k_{rw}}{m_{w,eff} R_{kw}}$ should be evaluated using upstream weighting [14].

For the oil equation the discretisation is almost the same as for water equation. For polymer equation integral the equation over V_i:

$$\int_{V_i}\left(\frac{\partial}{\partial t}\left(fS_w^* C_p + r_r(1-f)C_a\right)\right)dv = \int_{V_i} div\left(\frac{k\cdot k_{rw}}{m_{p,eff}R_{kw}} C_p \cdot grad\Phi\right)dv - \int_{V_i} q_w C_{pi}\,dv \qquad (3\text{-}4)$$

Using Gauss divergence theorem on the first term at the right side of (3-4):

$$\int_{V_i} div\left(\frac{k\cdot k_{rw}}{m_{p,eff}R_{kw}} C_p \cdot grad\,\Phi\right)dv = \int_{S_i} \frac{k\cdot k_{rw}}{m_{p,eff}R_{kw}} C_p \cdot grad\,\Phi \cdot \vec{n}\,ds \qquad (3\text{-}5)$$

The right term in the equation can be discretized the same as for water equation.

$$V_i \frac{(fS_w^* C_p + r_r(1-f)C_a)^n - (fS_w^* C_p + r_r(1-f)C_a)^{n-1}}{\Delta t} = \sum_{j=1}^{N_i}\left[\frac{T_{ij}k_{rw}C_p}{m_{p,eff}R_{kw}}(P_i^n - P_j^n - r_w g dH_{ij})\right] - Q_{wi}C_{pi}$$

(3-6)

In the discretized equation, C_p should be evaluated with upstream weighting.

Since it has been assumed that there is no desorption, when $\frac{\partial C_p}{\partial t} < 0$, C_a should be set equal to the maximum as it has reached.

3.2 PEBI Grid

When we construct the control volume around each grid point, if circumcenters as A, B, C, D, E and F of the triangles around i are selected, then we get an special case of control volume finite difference method – **PEBI** grid. [42, 45]

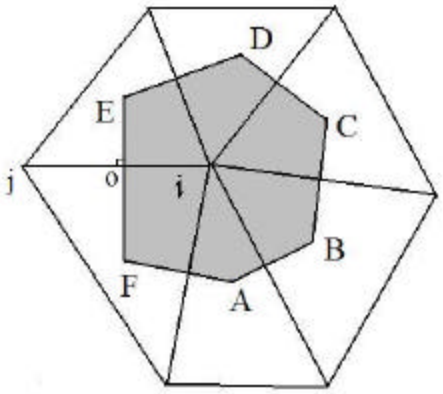

Fig. 16 PEBI Grid

As seen in Fig. 16, the edges of control volume i are separately perpendicular to the lines, which connect two adjacent grid points, and the lines are also bisected.

The discretisation of equations under PEBI grid is the same as under common control volume finite elements grid. And it is simpler to calculate the transmissibility between adjacent grid blocks.

During PEBI grid construction, wells can be taken into account and be set at centres of some of the control volume elements, as a result, the off-centre effect can be avoided.

As PEBI grid has also the advantage of normal irregular grid, it can suit for reservoir with irregular shape. K. Aziz [66], based on his experience, has pointed out that grids should be as close to be orthogonal as possible and PEBI grid is usually more reliable than block-centred grid.

In this research the reservoir has been simulated with PEBI grid, and all discretizations are with implicitness to keep the difference equations always stable.

4 Polymer Flooding Model in ECLIPSE 100 and ECLIPSE Office **[19]**

ECLIPSE is one of the most popular reservoir simulators in the oil industry worldwide. Since of its multi-capabilities and its suitability for polymer flooding research it is selected as the simulator for this project.

ECLIPSE Office is used as simulation project manager for inputting data and displaying simulation results.

4.1 Polymer Flooding Model of ECLIPSE 100

The simulator suite – **ECLIPSE -** consists of two separate simulators: ECLIPSE 100, specializing in black oil modelling, and ECLIPSE 300, specializing in compositional modelling. We introduce here only one special option of the ECLIPSE 100: **Polymer flood model**. All parameters and functions it needs are input through keywords.

4.1.1 The Mathematical Model of Polymer Flood Option in ECLIPSE

The Polymer Flood option uses a fully implicit five-component model (oil/ water/ gas/ polymer/ brine) to allow the detailed mechanisms involved in polymer displacement process to be studied. The flow of the polymer solution through the porous medium is assumed to have no influence on the flow of the hydrocarbon phases. The standard black-oil equations are therefore used to describe the hydrocarbon phases in the model. The equations are as follows:

For oil: $$\frac{d}{dt}\left(\frac{VS_o}{B_r B_o}\right) = \sum\left[\frac{Tk_{rw}}{B_o m_o}(dP_o - r_o g D_z)\right] - Q_o \qquad (4\text{-}1)$$

For water: $$\frac{d}{dt}\left(\frac{VS_w}{B_r B_w}\right) = \sum\left[\frac{Tk_{rw}}{B_w m_{w,eff} R_{kw}}(dP_w - r_w g D_z)\right] + Q_w \qquad (4\text{-}2)$$

For polymer: $$\frac{d}{dt}\left(\frac{VS_w^* C_p}{B_r B_w}\right) + \frac{d}{dt}\left(Vr_r C_a \frac{1-f}{f}\right) = \sum\left[\frac{Tk_{rw} C_p}{B_w m_{p,eff} R_{kw}}(dP_w - r_w g D_z)\right] + Q_w C_{pi} \qquad (4\text{-}3)$$

For brine: $$\frac{d}{dt}\left(\frac{VS_w C_n}{B_r B_w}\right) = \sum\left[\frac{Tk_{rw} C_n}{B_w m_{s,eff} R_{kw}}(dP_w - r_w g D_z)\right] + Q_w C_{ni} \qquad (4\text{-}4)$$

$$S_w^* = S_w - S_{dpv} \qquad (4\text{-}5)$$

Where: S_{dpv} denotes the dead pore space within each grid cell

C_a denotes the adsorption isotherm which is a function of the local polymer solution concentration

r_r denotes the mass density of the rock formation

f denotes the porosity

r_w denotes the water density

r_o denotes the oil density

Σ denotes the sum over neighbouring cells

R_{kw} denotes the relative permeability reduction factor for the aqueous phase due to polymer retention

C_p, C_n denote the local concentration of polymer and sodium chloride in the aqueous phase

m_{eff} denotes the effective viscosity of the water, polymer and salt components.

B denotes the formation volume factor of rock, oil and water.

V denotes the pore volume in the grid sell

T Transmissibility

D_z Depth difference

The model makes the assumption that the density and formation volume factor of the aqueous phase are independent of the local polymer and sodium chloride concentrations. The polymer solution, reservoir brine and the injected water are represented in the model as miscible components of the aqueous phase, where the degree of mixing is specified through the viscosity terms in the conservation equations.

The principal effects of polymer and brine on the flow of the aqueous phase are represented by equations (4-1) to (4-5) above. The fluid viscosities ($m_{w,eff}, m_{p,eff}, m_{s,eff}$) are dependent on the local concentrations of salt and polymer in the solution. Polymer adsorption is represented by the additional mass accumulation term on the left hand side of the equation (4-3). The adsorption term requires the user to specify the adsorption isotherm C_a as a function of the local polymer concentration for each rock species. The effect of pore blocking and adsorption on the aqueous phase relative permeability is treated through the term R_{kw} requires the input of a residual resistance factor for each rock type.

The equations solved by the ECLIPSE polymer model are a discretized form of the differential equations (4-1) - (4-5). In order to avoid numerical stability problems which could be triggered by strong changes in the aqueous phase properties over a timestep (resulting from large changes in the local polymer/sodium chloride concentrations) a fully implicit time discretization is used. The ECLIPSE polymer flood model is therefore free from this type of instability.

4.1.2 Treatment of Fluid Viscosities in ECLIPSE Polymer Flood Model

The viscosity terms used in the fluid flow equations contain the effects of a change in the viscosity of the aqueous phase due to the presence of polymer and salt in the solution. However, to incorporate the effects of physical dispersion at the leading edge of the slug and also the fingering effects at the rear edge of the slug, the fluid components are allocated effective viscosity values which are calculated by using the Todd-Longstaff technique.

To get the effective polymer viscosity, it is required to enter the viscosity of a fully mixed polymer solution as an increasing function of the polymer concentration in solution ($m_m(C_p)$). The viscosity of the solution at the maximum polymer concentration also needs to be specified and denotes the injected polymer concentration in solution (m_p). The effective polymer viscosity is calculated as follows:

$$m_{p,eff} = m_m(C_p)^w \, m_p^{(1-w)} \qquad (4\text{-}6)$$

Where: w is the Todd-Longstaff mixing parameter.

The mixing parameter is useful in modelling the degree of segregation between the water and the injected polymer solution. If w = 1, then the polymer solution and water are fully mixed in each block. If w = 0, the polymer solution is completely segregated from the water.

The partially mixed water viscosity is calculated in an analogous manner by using the fully mixed polymer viscosity and the pure water viscosity (m_w),

$$m_{w,e} = m_w^{(1-w)} m_m(C_p)^w \qquad (4\text{-}7)$$

In order to calculate the effective water viscosity to be inserted into (4-7), the total water equation is written as the sum of contributions from the polymer solution and the pure water. The following expression then gives the effective water viscosity to be inserted into (4-7):

$$\frac{1}{\mu_{w,eff}} = \frac{1-\overline{C}}{\mu_{w,e}} + \frac{\overline{C}}{\mu_{p,eff}} \qquad (4\text{-}8)$$

$$\overline{C} = \frac{C_p}{C_{p,\max}} \qquad (4\text{-}9)$$

Where: $\overline{C}$ is the effective saturation for the injected polymer solution within the total aqueous phase in the cell.

If the salt-sensitive option is active, the above expressions are still suitable for the effective polymer and water viscosity terms. The injected salt concentration needs to be specified in order to evaluate the maximum polymer solution viscosity, μ_p. The effective salt component viscosity to be used in (4-4) is set equal to the effective water viscosity.

4.1.3 Treatment of Polymer Adsorption

Adsorption is treated as an instantaneous effect in the model. The effect of polymer adsorption is to create a stripped water bank at the leading edge of the slug. Desorption effects may occur as the slug passes.

The adsorption model can handle both stripping and desorption effects. The user specifies an adsorption isotherm, which tabulates the saturated rock adsorbed concentration versus the local polymer concentration in solution.

There are currently two adsorption models, which can be selected. The first model ensures that each grid cell retraces the adsorption isotherm as the polymer concentration rises and falls in the cell. The second model assumes that the adsorbed polymer concentration on the rock may not decrease with time, and hence does not allow for any desorption. More complex models of the desorption process can be implemented if required.

4.1.4 Treatment of Permeability Reductions and Dead Pore Volume

The adsorption process causes a reduction in the permeability of the rock to the passage of the aqueous phase and is directly correlated with the adsorbed polymer concentration. In order to compute the reduction in rock permeability, the user is required to specify the residual resistance factor (RRF) for each rock type. The actual resistance factor can then be calculated:

$$R_{kw} = 1.0 + (RRF - 1.0)\frac{C_a}{C_{a,\max}} \qquad (4\text{-}10)$$

The value of the maximum adsorbed concentration, $C_{a,\max}$, depends on the rock type and needs to be specified by the user. Alternative expressions for the resistance factor can also be implemented if required.

The dead pore space is specified by the user for each rock type. It represents the amount of total pore space in each grid cell which is inaccessible to the polymer solution. The effect of the dead pore space within each cell is to cause the polymer solution to travel at a greater velocity than inactive tracers embedded in the water. The ECLIPSE model assumes that the dead pore space for each rock type does not exceed the corresponding irreducible water saturation.

4.1.5 Treatment of the Shear Thinning Effect

The shear thinning of polymer has the effect of reducing the polymer viscosity at higher flow rates. ECLIPSE assumes that shear rate is proportional to the flow velocity. This assumption is not valid in general, for example, a given flow in a low permeability rock will have to pass through smaller pore throats than the same flow in a high permeability rock, and consequently the shear rate will be higher in the low permeability rock. For a single reservoir, however, this assumption is probably reasonable.

The flow velocity is calculated as:

$$v = B_w \cdot \frac{F_w}{fA} \qquad (4\text{-}11)$$

Where: F_w is the water flow rate in surface units

B_w is the water formation volume factor

f is the average porosity of the two cells

A is the flow area between two cells.

The reduction in the polymer viscosity is assumed to be reversible, and is given by:

$$m = m_w[(P-1)M + 1] \qquad (4\text{-}12)$$

Where: m_w is the viscosity of water with no polymer present

P is the viscosity multiplier assuming no shear effect (entered using the PLYVISC or PLYVISCS keywords)

M is the shear thinning multiplier supplied in the PLYSHEAR keyword.

The well inflows are treated in a manner analogous to the treatment of block to block flows. The viscosity of the polymer solution flowing into the well is calculated, assuming a velocity at a representative radius from the well. The representative radius is:

$$R_r = e^{(\ln(R_w)+\ln(R_a))/2} \qquad (4\text{-}13)$$

Where

R_w well bore radius (taken from diameter input in COMPDAT)

R_a area equivalent radius of the grid block in which the well is completed.

In the present version of ECLIPSE, the radial inflow equation is not integrated over distance from the well to account for the local viscosity reduction due the local velocity.

4.2 ECLIPSE Office

ECLIPSE Office provides an interactive environment for the creation and modification of the simulation project, the submission and control of runs, the analysis of results and report generation. Data sets may be created by using a PEBI gridding module, correlations for PVT and SCAL data, keyword panels, or input from other pre-processors. It functions to manage the simulation process more efficiently and to display simulation result more systematically.

ECLIPSE Office consists of five managers: Case Manager, Data Manager, Run Manager, Result Viewer and Report Generator.

Case manager

The Case Manager helps to capture the relationship between runs and graphically display them. Runs are shown as children to Cases from which they were derived by simply modifying some data.

Data manager

The Data Manager provides user-friendly access to the keywords for all the simulators and to some basic features of FloGrid, Schedule, SCAL and PVTi.

In this management module there is an Unstructured Gridde r where a PEBI grid can be generated. It is allowed to quickly construct a grid from a series of contour maps, well positions and boundary.

Run manager

The Run Manager offers an environment to launch, monitor and control simulation runs. Runs may be started locally or over the network on a server. Multiple realizations generated for well control options and multiple cases may be run simultaneously. With the Run Manager, it is possible to monitor the progress of runs on line plots and solution displays, and if they are not delivering the required results, the runs can be stopped.

Results Viewer

The Results Viewer can display simulation results in both two and three dimensions. It can also be used to create and view solution displays and line plots of production data as a replacement for GRAF. Results from multiple runs can also be displayed simultaneously for comparative purposes and as an aid to quick decision-making.

Report Generator

The Report Generator is used to create reports from the extraction of relevant information from the SUMMARY files or from the .PRT file, and to put them in a form required for the creation of written reports.

5. Reservoir Characterization of $Ng2^1$ in Z106 Oilfield

Reservoir characterization provides the basic geological model for reservoir simulation. In the coming sections reservoir $Ng2^1$ is systematically introduced in details aiming at providing a complete geological concept for model construction in the next chapter.

5.1 Basic Geology of Shengli Oilfields Area and Z106 Oilfield

North China Basin can be separated into a few Depression areas according to their different tectonic region. **Shengli** Oilfields area lies in the southwest part of the North China basin (Fig.17), mainly in **Jiyang** Depression. To the north-east is the **Bozhong** Depression, between them is the Chengbei Low lift; to the north is Huanghua Depression, between them is the Chengning Uplift area. The sedimentary fill of the basin consists of three tectonostratigraphic sequences (Fig.18).

The **Lower Sequence** contains very thick Late Proterozoic, Paleozoic and Mesozoic sedimentary rocks. These have been deposited over long geological periods on a relative stable cratonic platform. This sequence plays no important role in Shengli Oilfields area.

The **Middle Sequence** is synchronous to the Paleogene rifting period. Ongoing extension, tilting and downfaulting have resulted in complex patterns of erosion and deposition. These Early Tertiary clastics are mainly developed in the structural deeper parts of the basin. Areas, which have these sedimentary sequence, are defined as Depression in China; otherwise are Uplift. In Shengli Oilfields area, this sequence contains three formations: Kongdian, Shahejie and Dongying (from old to young). Shahejie Formation provides the source rock in North China Basin. In the southern part of Shengli Area, great percent of oil reserve exists in Shahejie and Dongying Formations. It is shown by the second peak in Fig. 4.

The **Upper Sequence** consists of Late Tertiary and Quaternary clastics of thickness, in Shengli Area, about 1500 m; including three formations: Guantao, Minhuazhen and Pingyuan (from old to young), mainly of shale of alluvial facies, among them there is some sandwiched sandstone of river channel or point bar. In the northern part of Shengli Oilfields area, most of the oil reserve is contained in these sandstones of Guantao Formation, as shown by the first reserve peak in Fig. 4. The objective reservoir rock of Z106 Oilfield also belongs to this formation.

Jiyang Depression consists of six subdepressions: Chengbei, Chezhen, Zhanhua, Huimin, Dongying and Qingdong. **Z106 Oilfield** lies at the southern slope between **Chengbei** subdepression and **Chengzikou** uplift.

The oilfield was found through the first well Z106 in 1986. Reservoir sandstones, with depths from 1300 m to 1450 m under sea level, belong to **Guantao** formation.

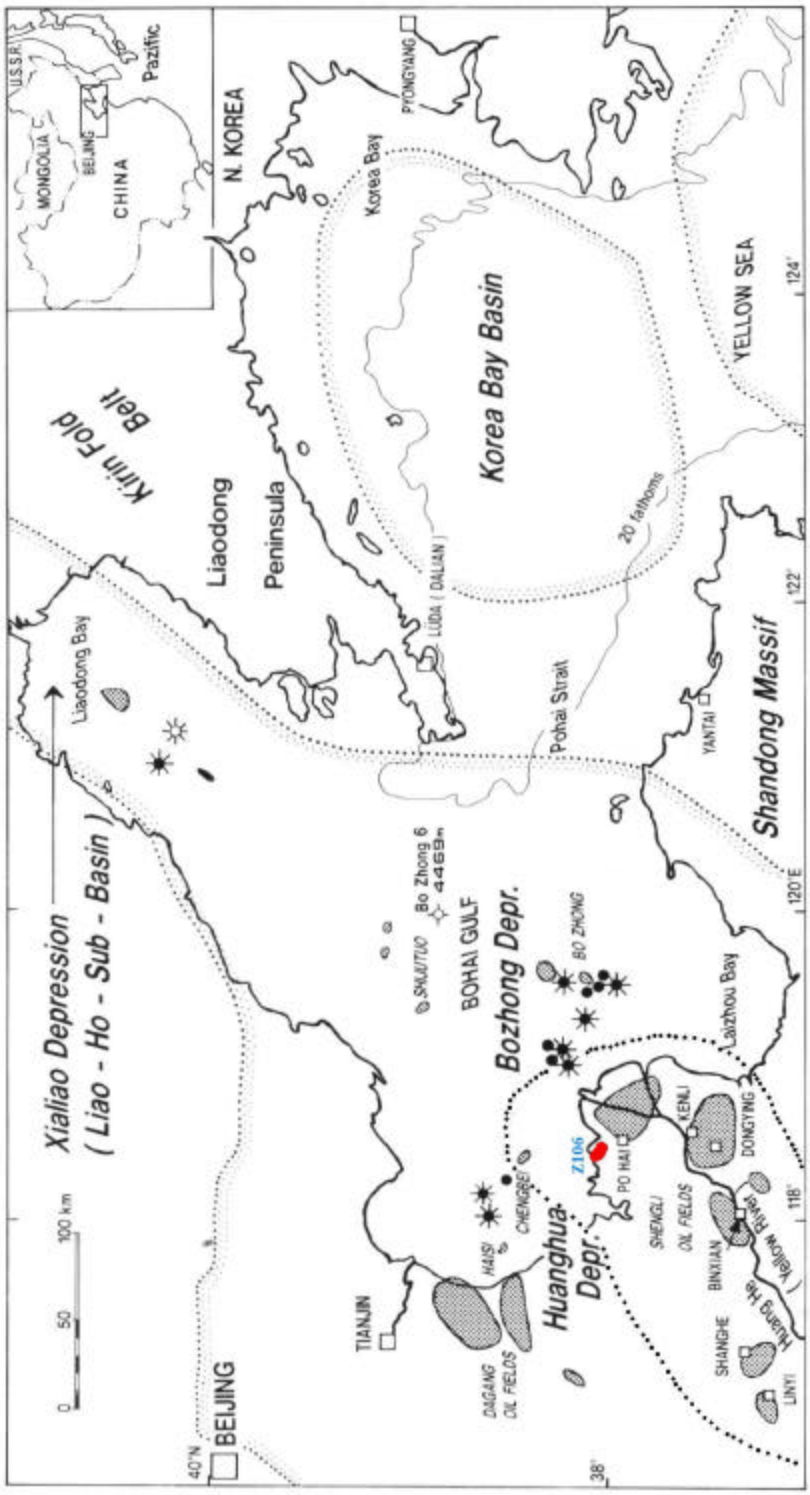

Fig. 17 Location of Shengli Oilfield Area and Z106 Oilfield
(edited after figure from Holger Kulke [47])

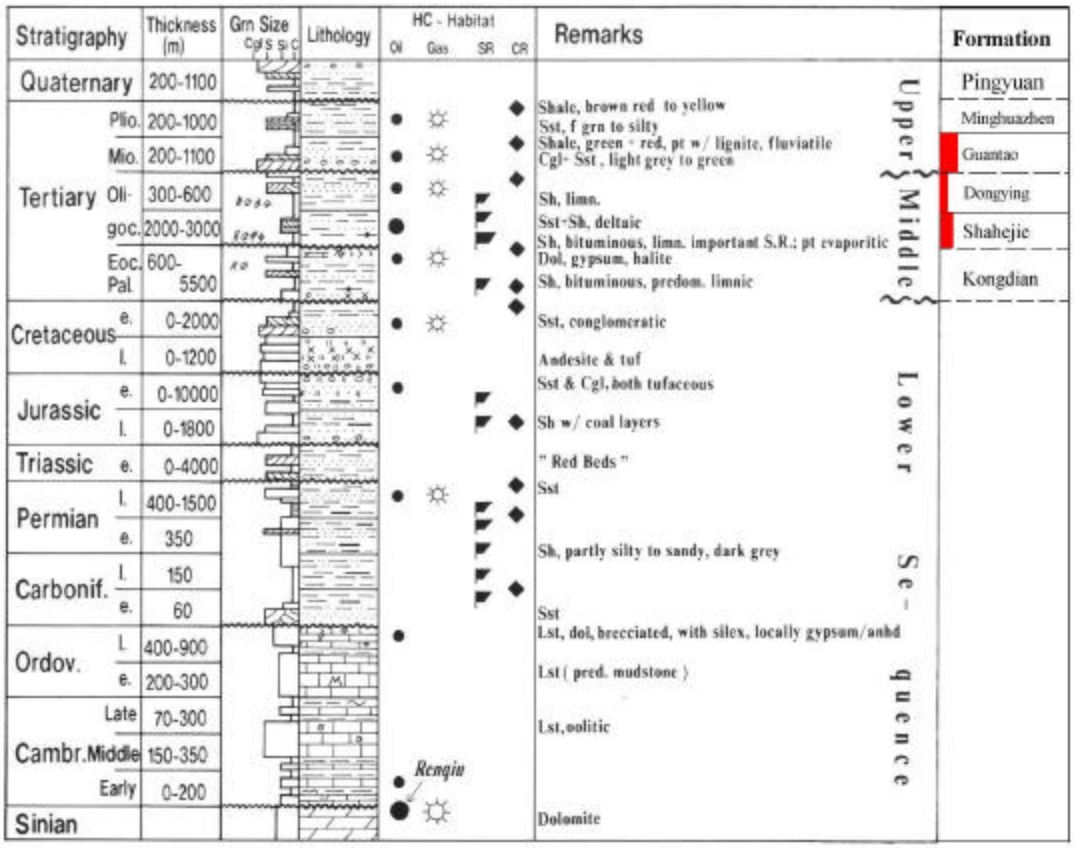

Fig. 18 Sequence defination in North China Basin
(edited after figures from Holger Kulke [47])

5.2 The General Situation of Z106 Oilfield

In Z106 Oilfield the objective interval is upper Guantao Formation, mainly of brown red, light grey fluvial shale, and occasionally fine sand and very fine sand in between from meander river sediment. From up to down the sand layers are divided into 5 groups, in which there are 14 sandstone layers, among them 4 contain oil valuable for production. Oil reserve has been evaluated about $1178*10^4$ tons. For the convenience to describe every reservoir, every reservoir or sandlayer is given a number as follows: **$Ng2^1$**, **$Ng2^3$**, **$Ng3^2$**, **$Ng3^3$**, as seen in Fig. 19. (Note: **N** means Neogene or Upper Tertiary, **g** means Guantao Formation, **2** and **3** mean sandlayers group, superscripts mean sand body ordinal number in the group.)

Till the end of August 1998, 143 wells have been drilled in Z106 Oilfield, of which 103 are for oil production. Cumulative oil production has amounted to $105.2*10^4$ tons, water $338.5*10^4$ m^3. The average water cut has reached 81.5%.

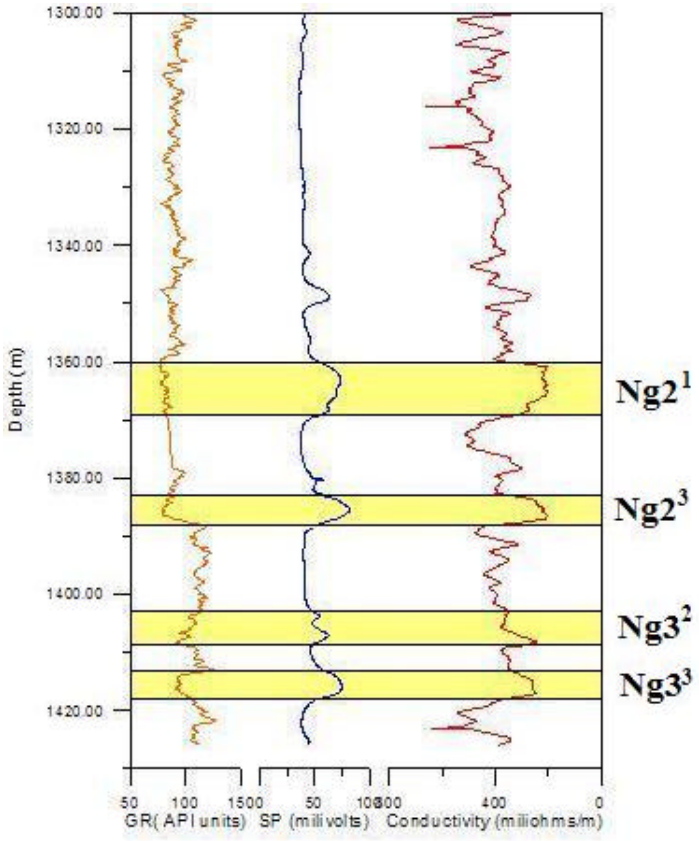

Fig. 19 Sandbody definition with Well L7

5.3 Detailed Reservoir Description of $Ng2^1$

Aiming at researching on the feasibility of polymer flooding in Z106 Oilfield, reservoir $Ng2^1$ is taken as an example for simulation, it will be described in detail in this section.

5.3.1 Sandstone Distribution of $Ng2^1$ and Its Top Surface Structural Map

By using synthetic seismogram from well logging data, the reflection horizon of top surface of $Ng2^1$ has been exactly defined in seismic profile, the reversion profile from 3D seismic data are interpreted comprehensively with well logging data by software STRATA (Fig.20 and Fig.21). From the interpretation results, sandstone thickness distribution and the structural map of the top or bottom surface can be got as seen in Fig.22 and Fig.23.

Because of the sediment from river channel, the sandstone distributes in narrow band, as seen in Fig.22. Along the river channel, its thickness varies very slightly, but in the vertical direction it thins out very quickly. The areal average thickness is about 5 m. In the middle of the river channel, it even reaches 20 m in some area.

The top surface of $Ng2^1$ declines to NW in general (Fig.23), the dip angel is about 0.5-2°; in some area there are regional high points because of different compactibilities between sandstone and its surrounding shale.

$Ng2^1$ can be generally defined as a lithologic reservoir, it is also affected by the structural factor, since in the northwest part there is bottom water. Fig.24 is the reservoir profile along the South to North river channel.

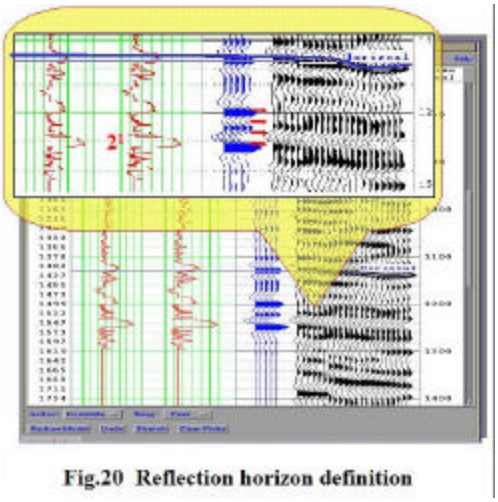

Fig.20 Reflection horizon definition

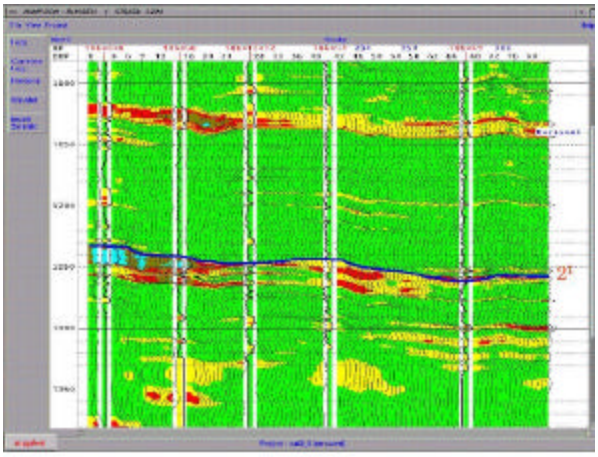

Fig.21 Reversion profile interpretation

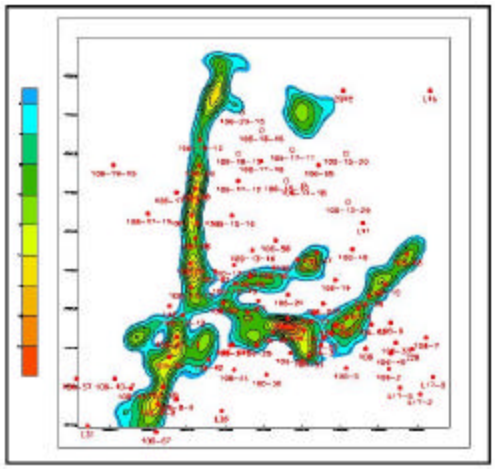

Fig.22 Thickness distribution of $Ng2^1$

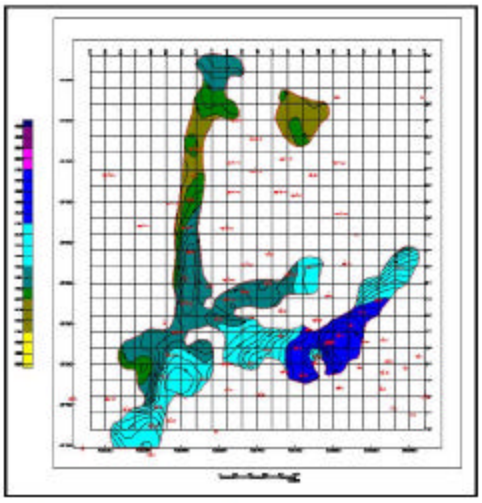

Fig.23 Top surface structural map

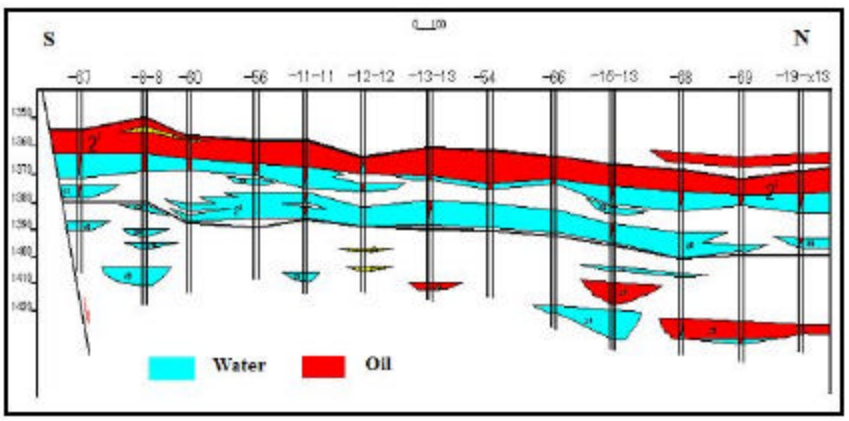

Fig.24 Reservoir profile from Well -67 to Well -9-x13

5.3.2 Reservoir Rock Properties

Reservoir rock varies from very fine sand stone to fine sand stone, grain size 0.05 – 0.25 mm (Quartz 39.5%, Feldspar 35.2%, Rock debris 24.8%), consisting of about 14.9% shale content. The grain size decreases from the middle of the river channel to the edge, and shale contents will be increased.

According to core analysis result from well –69 and –8-8, porosity is between 32-37%, average 35.9%; permeability is between 2000 – 8000 md, average 4392.4 md. Since wells have been always drilled in position with thick sandlayer, the porosity and permeability from core of these wells are higher than those in other area. The thicker the sandlayer is, the higher are their porosity and permeability. Their distribution can be seen in Fig.25 and Fig.26.

Fig.25 Porosity isogram of $Ng2^1$

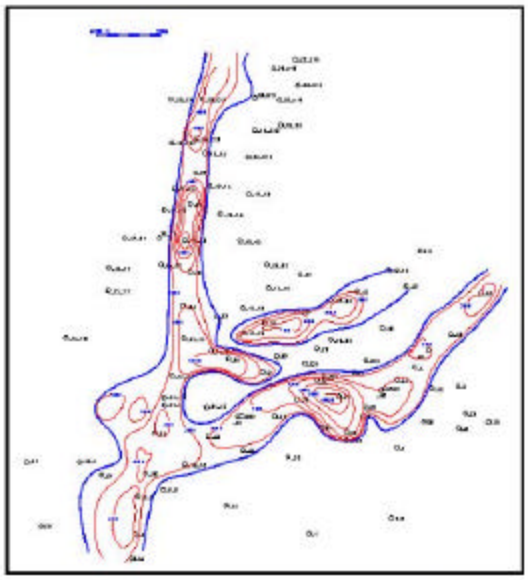

Fig.26 Permeability isogram of $Ng2^1$

5.3.3 Comprehensive Interpretation of Geological Model with Production Data

From the last two sections we see that the geologist and the geophysicist hold different opinion towards the geological model. Due to the limited distinguishability of seismic data and logging data, the interpretation results from them should be proofed and corrected according to the production data.

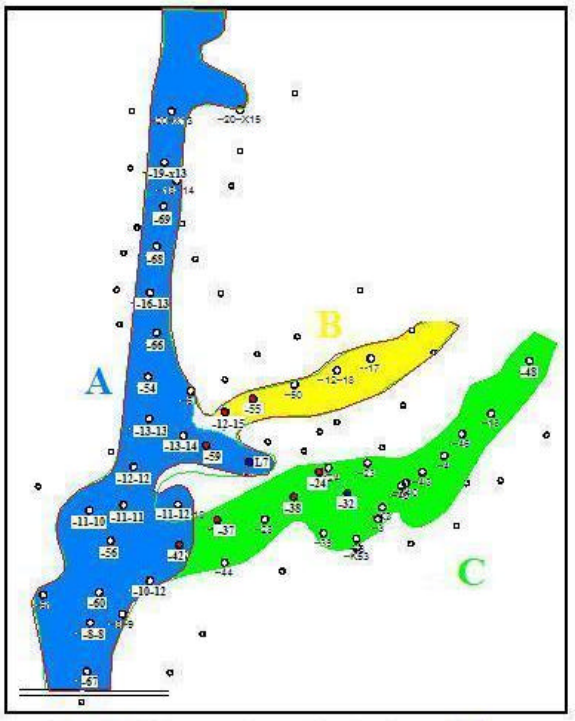

Fig. 27 Reservoir geological model from comprehensice interpretation

As described by the geologist, the property of logging data of wells in the yellow area B in Fig.27 is different from that in other two areas. They are not connected together. The production data from Well –12-15 and Well -59 have proved that this assumption is correct.

Well L7 has been used as injection well from April 1989, injecting water into $Ng2^1$ and $Ng3^2$ at the same time. Well –59 was drilled in June 1995. Before production, the static pressure was about 19.5 MPA. The production rate was very high and water cut at the beginning was already more than 98%. But with Well –12-15 the situation was quite different. The production rate was much lower than that from Well –59.

Another difference lies between well L7 and well –38, -24. As mentioned above, well L7 has been injecting water since April 1989, but the pressure at Well –38 was measured only 7.1 MPa in 1992; and the production situation in well –24 was also not clearly affected. As a result, it was concluded that they were not connected together in one reservoir.

The geologist believe that sandlayer between Well –42 and –37 is continuous, but in seismic profile it is clearly discontinuous. Even though they were connected together the sandlayer thickness must be very thin. Since the liquid rate of well –37 from sandlayer $Ng2^1$ is only about 6 m^3/day.

Based on the above-mentioned analysis, the reservoir can be divided into three discontinuous areas as in Fig.27. In the following polymer flooding simulation, the reservoir $Ng2^1$ always refers to the blue area A.

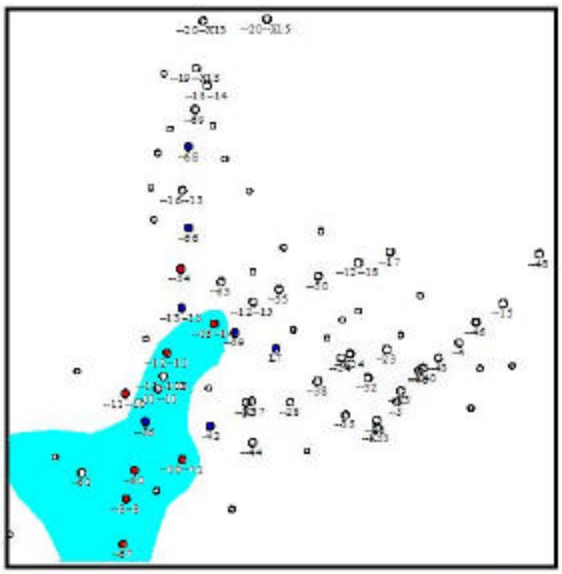

Fig.28 Distribution area of Sandlayer $Ng2^2$

As seen in Fig.24, in the south area there is another sandlayer $Ng2^2$ under $Ng2^1$, its distribution area can be seen in Fig.28. It has been sedimented earlier than $Ng2^1$, and along the river channel they are overlapped together.

Due to the higher capillary pressure, it mainly contains water; the water cut of wells in these area increases very quickly; shortly after the beginning of production, it reaches more than 90%. In simulation it has also been taken into account.

Oil water contact surface is determined at 1378 m from production data of wells in northern area and their logging data. Capillary pressure and the oil-water surface have been checked and adjusted when matching the simulation results with production history.

5.3.4 Fluid Properties

Properties of oil and water as seen in Table 3 and Table 4.

Table 3 Oil properties

Properties	Value	Unit
Density (at surface condition)	0.9301-0.9576,average 0.9441	g/cm^3
Density (at reservoir condition with resolved gas)	0.91	g/cm^3
Gas resolution	16.35	m^3/m^3
Bubble point pressure	6.87	MPa
Viscosity (at surface condition)	309 - 673	mPa.s
Viscosity (underground with Resolved gas)	95.9	mPa.s
Formation volume factor	1.0493	
compressibility	8.0×10^{-4}	1/MPa

Table 4 Water properties

Properties	Value	Unit
Salinity	2334 - 4566	mg/cm^3
Density	1.007	g/cm^3
Viscosity	0.46	mPa.s
Formation volume factor	1.0088	
Compressibility	$4.59.0\times 10^{-4}$	1/MPa

Oil belongs to normal heavy oil according to the standard from [4].

Since water salinity is not high, and reservoir temperature is about 65°C, it is advantageous to polymer flooding.

5.4 Production History

From the discussion in 5.3.3, it is concluded that sand layer in area A belongs to one reservoir. The first well that reaches this reservoir is Well L7, which had produced oil since November 1, 1988. After only a few months of oil producing, it was changed as water injection well, since at that time it was believed that it was connected with well –24 and –38 etc. Well L7 has been used as injecting well till now. In fact the water did not flow to well –24 and –38, but to opposite direction.

The reservoir, in fact, has been put into development only from 1995 as seen in Table 5.

Table 5 Well List

Well	Completion Date	Type
L7	11.1988	Injecting since 04. 1989
-42		Injecting since 07. 1992
-56	05.1995	Injecting since 01. 1998
-59	05.1995	Injecting since 10. 1999
-60	06.1995	
-54	07.1995	
-66	09.1995	Injecting since 05. 1998
-67	10.1995	
-8-8	12.1995	
-12-12	01.1996	

Table 5 Well List (continuous)

-11-11	04.1996	
-16-13	04.1996	
-13-13 -69	04.1996 05.1996	Injecting since 01. 1998 (producing oil from other layer)
-68	07.1996	Injecting since 01. 1999 (not into $Ng2^1$)
-19-x13	09.1996	
-11-12	07.1997	
-11-10	07.1997	
-10-12	08. 1998	
-13-14	08. 1998	

Till 03.2002, cumulative oil production from $Ng2^1$ is 148877 m^3, water 1243791 m^3. (Fig.29)

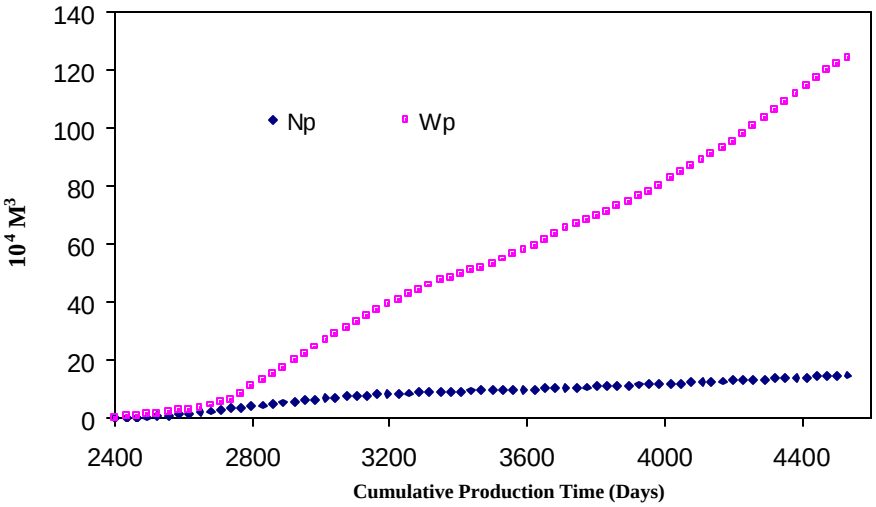

Fig. 29 Cumulative Oil And Water Production of $Ng2^1$

6 Simulation Model Construction And History Matching

For a practical reservoir simulation process, the first step is to construct the simulation model based on all the known information, the second step is, by matching the production data, to validate and (or) verify the simulation model.

6.1 Simulation Model Construction

As needed by numerical method, the reservoir must be divided into grid cells in space dimension. For each cell the following properties must be specified: porosity, permeability, depth, thickness, etc. This section can be done with Grid in Office in Eclipse.

Fluids' PVT properties and rock's property must also be set to describe their variation with pressure. This section can be defined with PVT in Office in Eclipse.

For multi-phases flow, relative permeability should also be respectively defined for each phase with Scal in Eclipse.

Initialisation of pressure of different cell can be calculated by defining a reference pressure at a depth. Water and oil saturations can be initialised by defining water-oil contact depth. Above this contact, water and oil distribute according to the capillary pressure.

In time dimension, the whole process must be divided into time steps, and all production or injection wells should be specified at different timestep with Schedule in Office.

In the Summary section the output data from simulation process are defined.

6.1.1 Grid Construction

In order to adapt to the irregular reservoir shape and irregular well pattern, 2D PEBI grid has been used to construct simulation model. In vertical direction two layers ($Ng2^1$, $Ng2^2$) have been separated into 8 cell layers, $Ng2^1$ into 5 and $Ng2^2$ into 3.

As required by ECLIPSE Office, PEBI grid construction needs boundary (reservoir boundary line), well positions, the topographic contour of top surface, thickness contours, porosity contours and permeability contours for different layers. Seen Fig.30 –Fig.38. It should be declared that all property data have been adjusted for production history matching.

Since there are no vertical permeability data, in this project they are calculated from horizontal permeability with empirical formula from Manseur et al [48] as follows:

$$K_v = 0.5783 K_h^{0.971} \qquad (6\text{-}1)$$

Where, K_v vertical permeability

K_h horizontal permeability.

In model construction it is assumed that horizontal permeability K_x and K_y are the same.

From the property figures it can be seen that thickness, porosity and permeability of sand rock in the middle along the river channel are higher than those of other area.

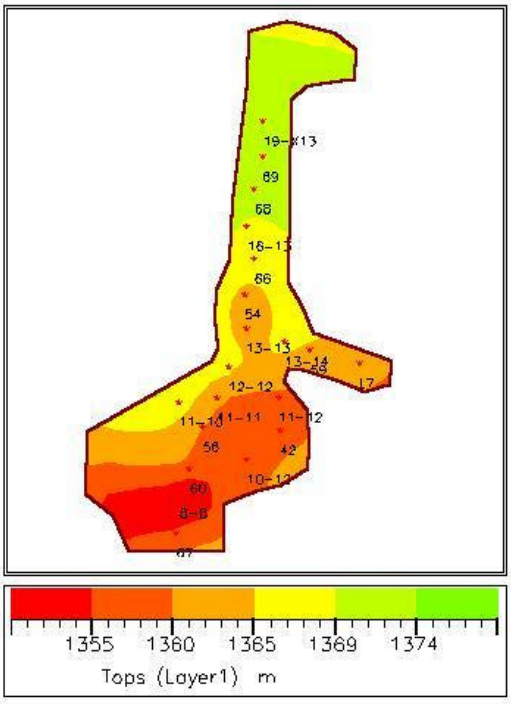

Fig.30 Topographic contour map

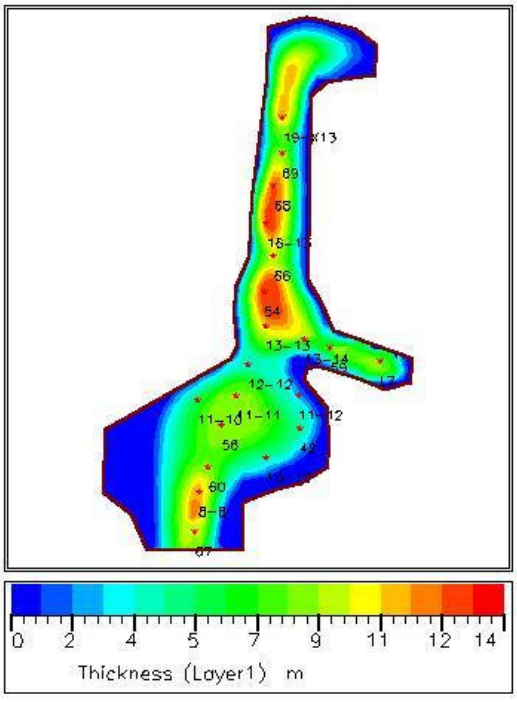

Fig.31 Thickness contour map of $Ng2^1$

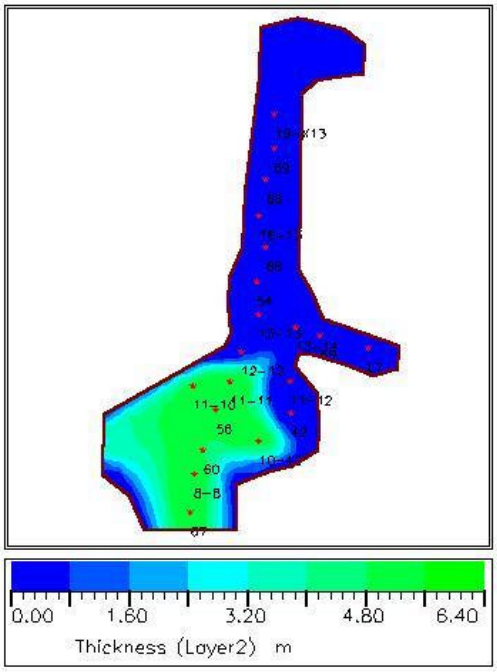

Fig.32 Thickness contour map of $Ng2^2$

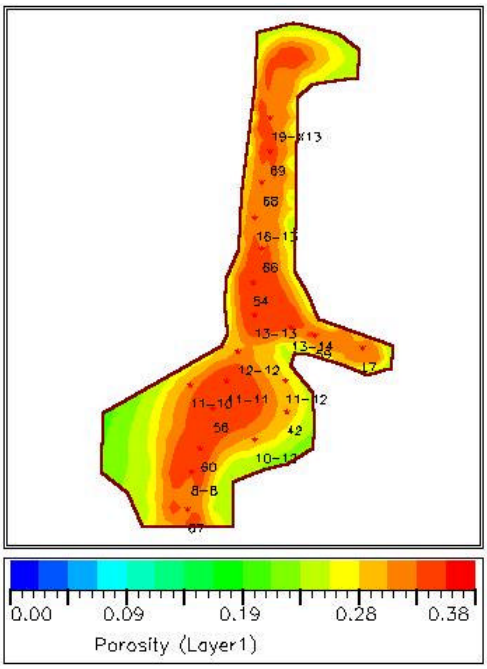

Fig.33 Porosity contour map of $Ng2^1$

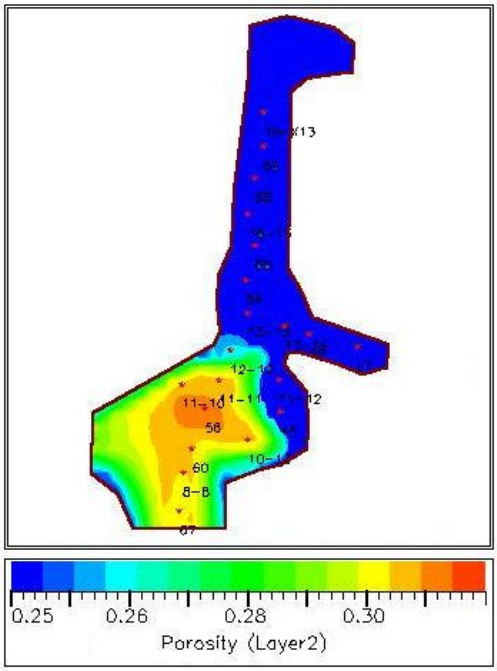

Fig.34 Porosity contour map of $Ng2^2$

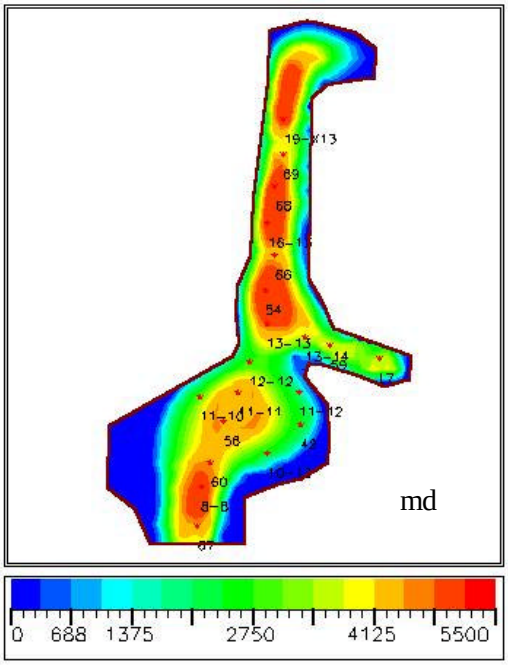

Fig.35 Horizontal permeability of $Ng2^1$

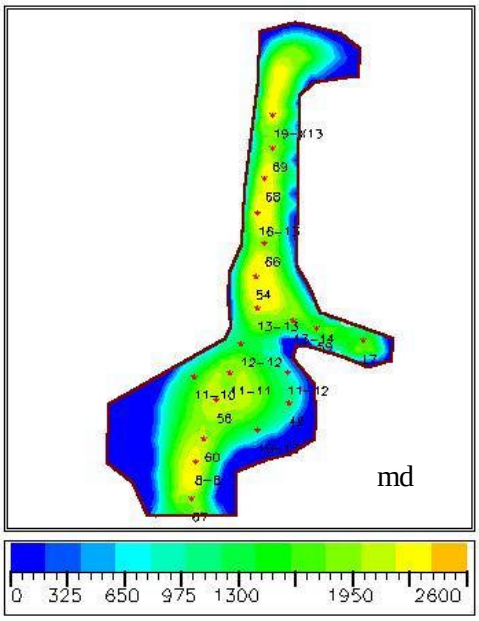

Fig.36 Vertical permeability of Ng2[1]

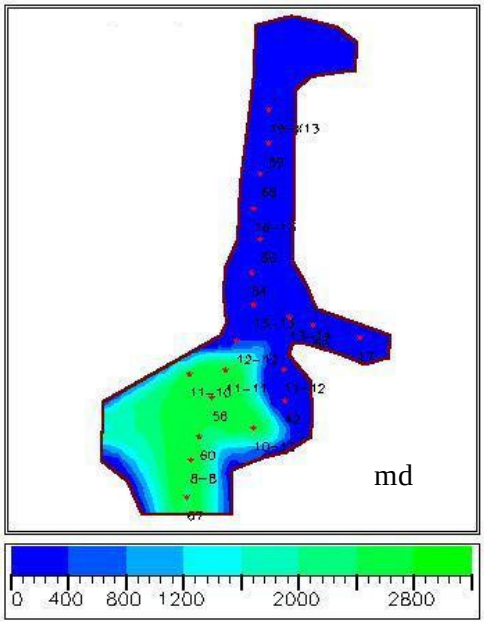

Fig.37 Horizontal permeability of Ng2[2]

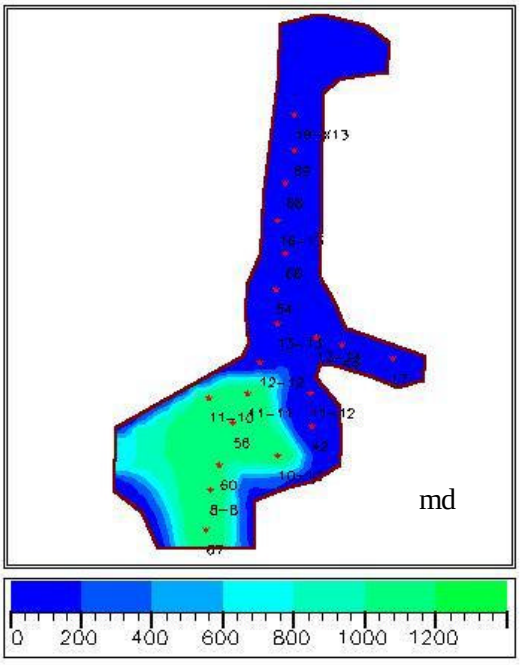

Fig.38 Vertical permeability of Ng2[2]

With the Unstructured Gridder of Office the PEBI grid has been generated as seen in Fig.39. It generates at first the grid then the properties for each cell. The complete producing process can be referred to ECLIPSE manual [19].

Cells, which have well in œntre, have been set as regular hexagons.

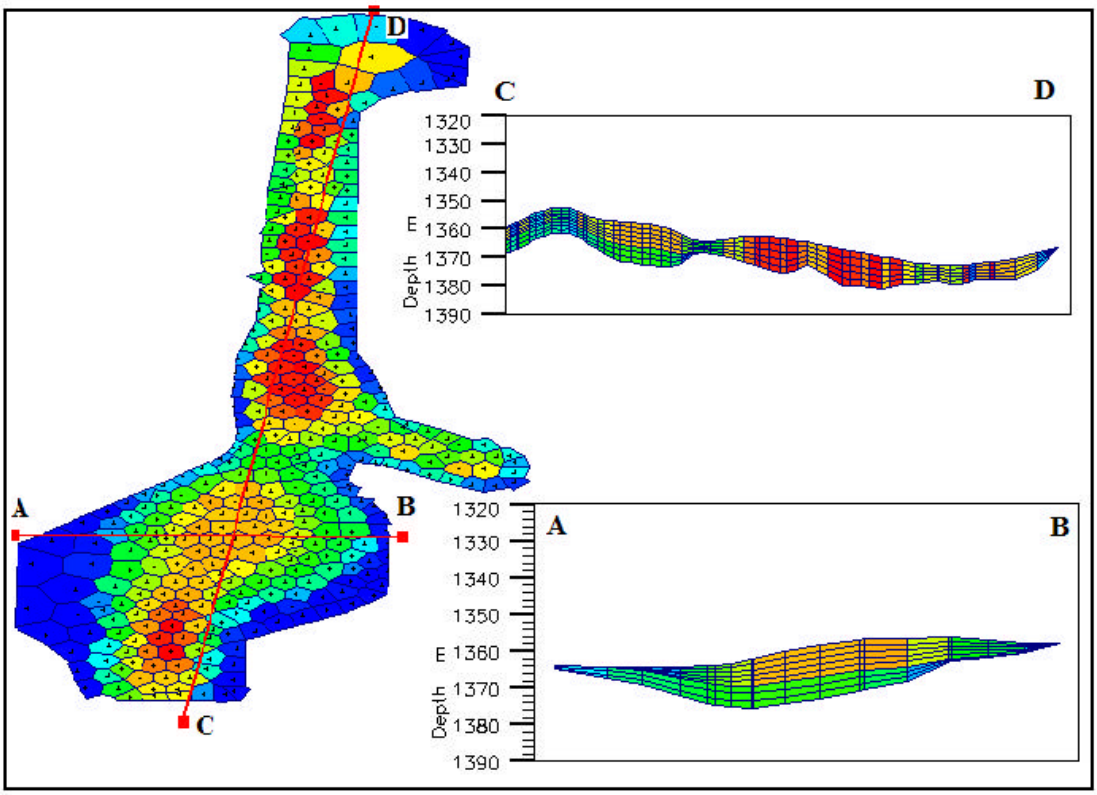

Fig.39 Grid model for reservoir simulation

6.1.2 PVT

Oil and water PVT properties for simulation model as seen in Table 3 and Table 4 in chapter 5.

6.1.3 Capillary Pressure and Relative Permeability

Sand rock originally from different sedimentary facies has different properties, even after the diagenesis during the long geological time. Since of the different aqua-dynamic sedimentary conditions, sand rock sedimented in the middle river channel has usually more coarse corn, as a result, with higher permeability and porosity than rock in other sedimentary facies. Oil is more easily to be accumulated in such area, because the capillary pressure is much lower, and it could be more easily conquered by the buoyancy force from density difference between oil and water. At the original state in reservoir more oil has accumulated in sandstone in the middle of river channel, and less accumulated in the edging area.

In our invested reservoir, there are sandstones from two different sedimentary periods. The underlayer $Ng2^2$ from the earlier period has been sedimented in much weaker dynamic environment than that for $Ng2^1$.

In this project different regions have been used to taken into account for this difference. Layer $Ng2^1$ have been separated into 3 regions, and $Ng2^2$ into 2 regions as seen in Fig. 40.

Theoretically, according to the definition region numbers should increase from edge to the middle along direction vertical to river direction, and be of symmetry. But because the gridder of ECLIPSE Office could not do this job automatically, region number could only be given to each cell manually. In order to simplify the process, Layer $Ng2^1$ have been separated into only three regions: 3, 4 and 5; Layer $Ng2^2$ only into two regions: 1 and 2.

Region 4 and 5 describe the middle area of the river, especially 5, it shows the point bar in the upper layer. Region 2 shows the middle area of layer $Ng2^2$.

For these five different regions different capillary pressure and relative permeability function were given according to their properties (Fig 41 and Fig.42). The source data for these two figures are after history matching.

Since the capillary pressure in region 1 and region 2 are much higher than which in other 3 regions, they are occupied mainly by water, while oil has mainly accumulated in region 5, 4 and 3 (Seen in Fig.43).

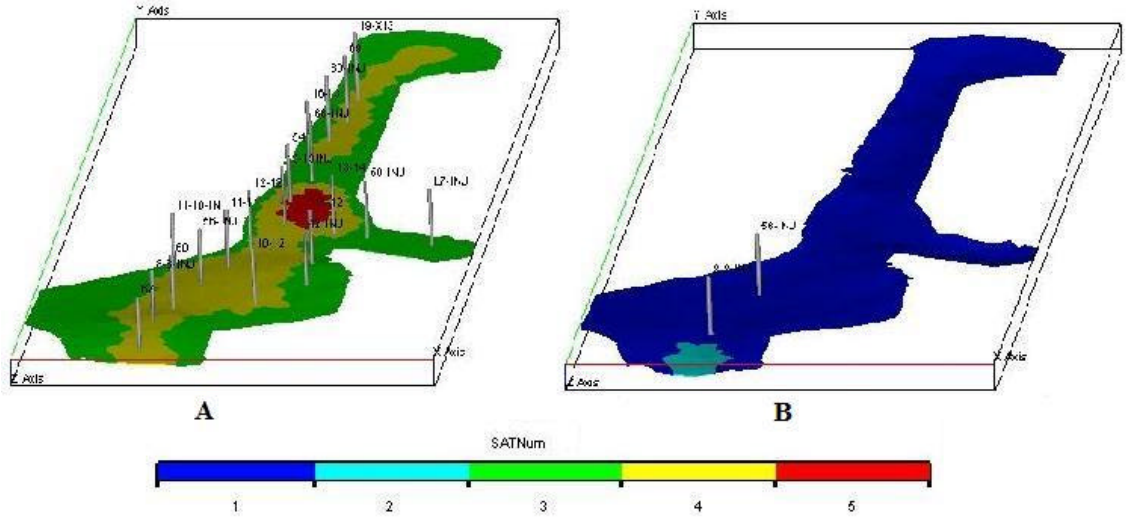

Fig. 40 Region distribution, A for $Ng2^1$, B for $Ng2^2$

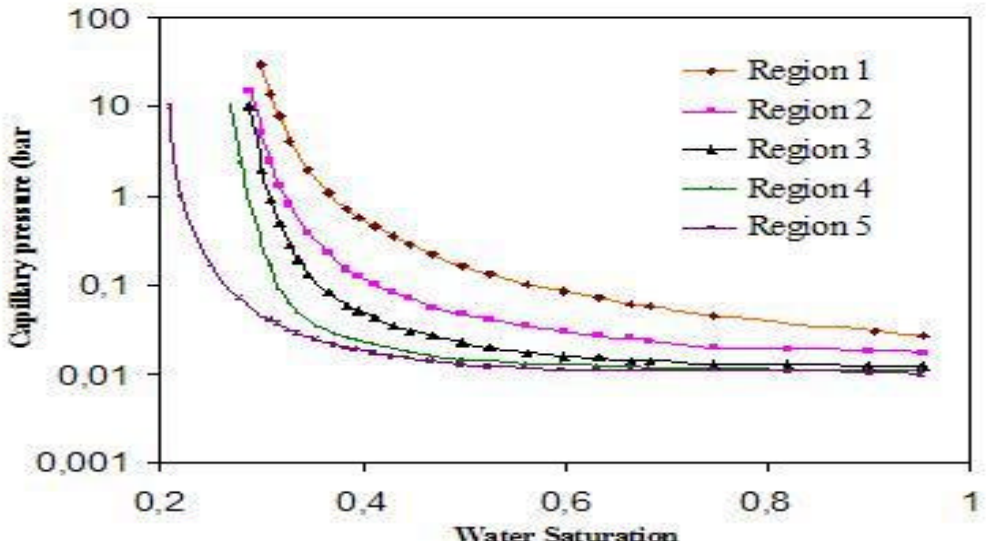

Fig.41 Capillary pressure for 5 Regions

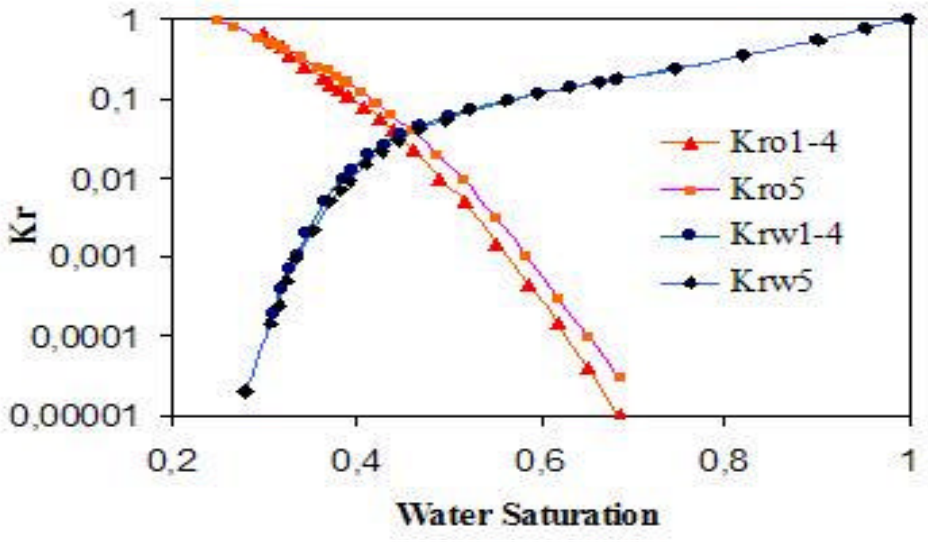

Fig.42 Relative permeability for 5 Regions

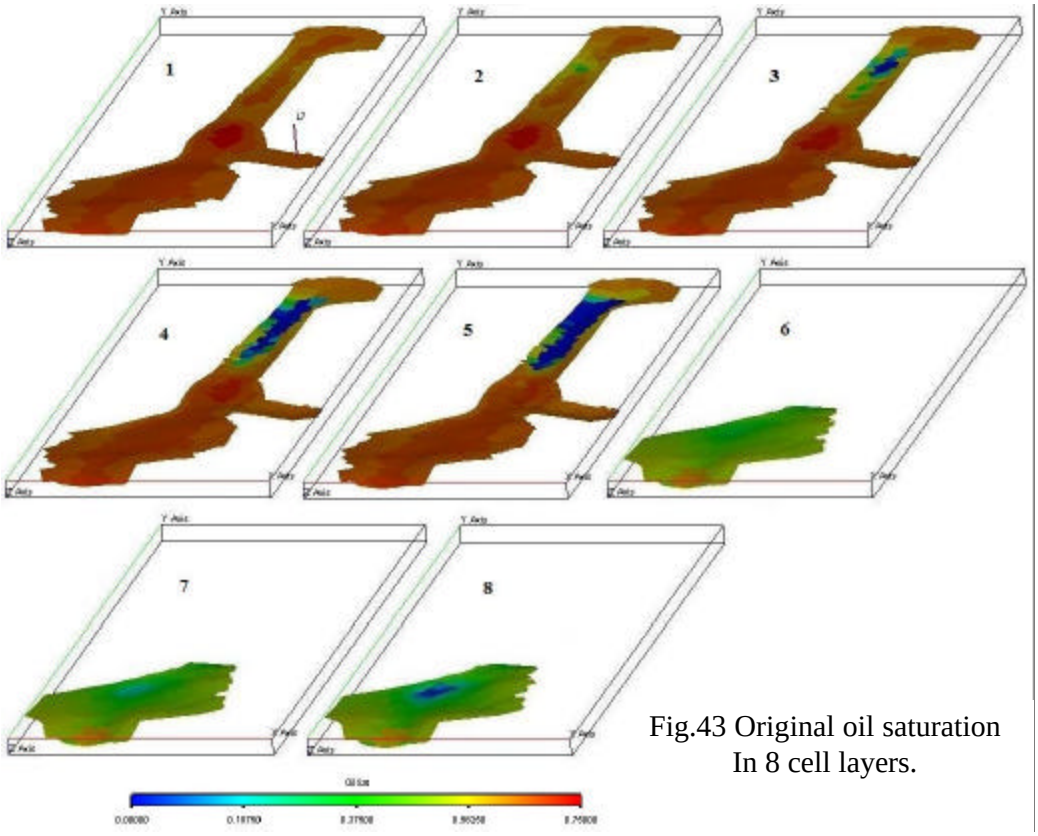

Fig.43 Original oil saturation
In 8 cell layers.

The capillary difference between different regions clearly explains the phenomenon in Fig. 24 in chapter 5, in which there is no horizontal water-oil contact surface.

The depth of zero capillary pressure has been set at 1378 m.

Relative permeability of rock from a same reservoir varies little as they have the same fluid system. The significant difference between regions is permeability and porosity. Many literature listed in [49] have concluded that permeability and porosity have almost no effect on relative permeability. The same water relative permeability has been set for different regions. Oil relative permeability has been set the same for region 1 to region 4. Oil relative permeability for region 5 is a little higher than relative permeability for other regions as needed by history matching.

One common character of relative permeabilities for all regions is that oil relative permeability decreases very quickly with water saturation increasing. This character is normal for heavy oil reservoir. [50]

6.1.4 Well Specification and Time Step

All production wells have been specified with liquid production rate, aiming to matching oil and water production rate, water cut, and bottom hole pressure.

For injection well L7 and −42, bottom hole pressure has been set according to records of injecting pressure, because these wells inject water into different reservoirs at the same time, it is impossible to exactly determine the water injecting rate. For other injection wells injecting rate has been set according to the injection history.

For all wells the well connection has been set according to the well perforation length. Skin factor has all been set as zero, since in this reservoir the permeability is relative very high, the damage from mud during well drilling, damage from well completion and from perforation can be diminished shortly after being putted into production.

The time step was set commonly as 30 days, some steps have been minimized as required by some well's operation, open or shut for some days. Since the fully implicit simulator has been selected for simulation, the simulation process was always stable, no matter how long the time step is.

6.1.5 Summary Section

For most of the production wells, the water cut and bottom hole pressure from simulation have been set as output data for history matching. Water cut and accumulative production of oil and water for the whole reservoir have also been outputted for history matching.

6.2 History Matching [12-13, 51-55]

Reservoir is a Geo-body buried underground as an objective reality; its any existential property should be unique, though some of them may change during exploitation of the reservoir (usually this variation can be neglected in reservoir simulation). Theoretically, if the correct data or functions, which describe the reservoir rock and fluids, were put into the simulation model, its solution would surely match the production history. But unfortunately such occasion will never happen. Since much of the physically measurable information used in the simulator is based on incomplete or inaccurate field measurements, any property data or functions about the reservoir are not absolutely certain, even we have made many efforts: many wells drilled, many logging data, many core analysis data, well production tests, seismic data, etc. We still know only a part about the reservoir, just as we can only see the tip of an iceberg.

Whether a simulation model is reasonably correct or not, there is only one way to test it, that is through changing the property data or functions in the simulation model to let the simulation result match the past production performance of the reservoir - **History matching**. Correspondingly history matching may be taken as an inverse problem [67]. The dependent variable – production data - is known, and the independent variable – reservoir property data and functions - must be determined. As there are so many factors together affecting the solution simultaneously, it is not possible to directly find the real data for simulation model. That is why, since the beginning of the usage of numerical simulation in oil industry, history matching has always been a difficulty puzzling reservoir engineer throughout the world. Though many efforts have been made to look for methods to better the matching result and to reduce the time consumption, even some software companies have offered modular for optimizing history matching, it is and it will still be in the near future a great challenge for numerical reservoir simulation.

For a practical reservoir simulation, history matching can be achieved by manipulating two fundamental processes, which are controllable during history matching: the quantity and distribution of fluid within the system, and the movement of fluid within the system. These processes are manipulated by adjusting input data until a minimal difference remains between the production data and the simulator calculations at the same point in time. One must be noted that these two processes are not independent, but are related to each other. For example, for grid cell with lower permeability, usually its initial oil saturation should also be lower since the capillary pressure is controlled by pore structure, and permeability is also controlled by it. If permeability is lowered, the other data should also be altered correspondingly. As a result, history matching is correspondingly the most time consuming part of a reservoir simulation project.

Fluid property data are usually seldom changed during history matching, since they tend to be more accurately measured than other model input data [68].

Porosity is usually more believable than permeability. Its variation range is relatively much smaller than that for permeability; with core analysis data to calibrate the logging data, then with logging data to calibrate the inversion result from seismic data, combined with the geological situation, the porosity distribution in area can be satisfactorily determined.

Fanchi [55] believed that relative permeability data are typically placed at the top of the hierarchy of uncertainty, because they are modified more often than other data. Some others [13] thought that permeability is more frequently in need of adjustment, because of its unbelievable certainty. Gian Luigi Chierici [12] pointed out that the adjustment of permeability is mainly for matching the pressures and relative permeability for matching water cut.

As described in chapter 2 and chapter 3, permeability and relative permeability all are multipliers of pressure gradient, any change of them will led to variation of pressure. And different combination may lead to same simulation result, this is the main source of uniqueness problem.

During the process of history matching there are **two basic principles** for the adjustment of parameters or functions in the simulation model, which should be kept in mind:

(1) Any changing of property data should be physically reasonable;
(2) It should be also geologically reasonable and possible in certain situation.

In this project both permeability and relative permeability are adjusted to match the history data.

Another problem about history matching is that the set of physical parameters, which result from the history matching, may not be unique. It is possible to find another set of parameters that provide as good a match to the reservoir history as the accepted set. The set of parameters and functions, which is more closely concerned with the geological understanding of reservoir at present, should be selected as the best one for further simulation. From this viewpoint, the geologist's opinion should be admired, and at the same time the history matching proves his opinion.

With the decided simulation model, the simulation result would provide the fluid distribution variation underground in the reservoir during the developing time and residual oil distribution at present, thus corresponding method can be selected to enhance the oil recovery. The residual oil distribution will be discussed in the next chapter.

In this chapter, history matching process and its result analysis will be discussed. As declared in the last section, wells are specified with liquid production rate; oil and water production rate, cumulative production, water cut, and well bottom hole pressures will be matched.

6.2.1 History Matching Preparation - The Appreciation of Observed Data

History matching requires data on the production history of all the wells in the reservoir, with a reasonable estimate of their accuracy. Usually the following well data must be provided:

- Completion history, including:
  - Record of each completion
  - Intervals open to production
  - Well stimulations and their results
  - Squeezes and other cement jobs
- Production history:
  - Oil, [$q_{o,sc}(t)$]
  - Gas, [$q_{g,sc}(t)$]
  - Water, [$q_{w,sc}(t)$]
- Water injection history of injecting wells
- Records of all static and dynamic well bottom-hole pressure measurements.
- Production test reports, including the pressure buildups, productivity indices, and skin factors.
- Production logs, to define the relative contributions from the open intervals in each well.
- Fluid properties at different times.
- Cased hole monitoring logs to track the movement of oil/water contact behind casing.

It does not mean that any reservoir or well has so complete data; some wells have been put into production without any test. Some data may be not correct, their accuracy and reliability must be checked before using.

As conditioned by the common technique level in the company and the reservoir management, it is very difficult to systematically get all needed data for reservoir Z106Ng2[1].

Some injection wells inject water into different layers at the same time, but not separately. It is almost impossible to determine how much water has been injected into one reservoir, and how much into other reservoirs. Even you separate them according to their calculated kh, it is

still not very believable, since k is not surely known. The injecting pressure is also an average in month.

Injection data of wells, which inject water only into the reservoir, can be very reliable, since the water accumulation can be easily measured and errors in them can be neglected.

For producing wells, there have been few static pressure measurement. The only bottom hole pressure data are calculated from the moving liquid surface in well bore. Whether they are a monthly average or only from some day in the month, it can not be proved. As a result, the pressure data are only taken as reference.

The production data are always exactly measured in China. How much oil, how much water and how much gas, usually water and oil data are very exact, for low gas resolvable reservoir, gas is sometimes not taken into account. For this reservoir the production data for oil and water are the most believable information.

As for this situation, during history matching process the production rate and water cut matching have been taken more seriously, the pressure matching has been taken only as reference.

All pressure data and production data have been organized in format as Eclipse requires.

6.2.2 Error Function Definition And Its Sensitivity to Different Parameters

During history matching the errors between observed data and calculated result from simulation model should be quantitatively defined, since SimOpt in ECLIPSE does not support PEBI grid, one objective error function is defined as follows:

$$ERROR = \frac{\int_0^T | f_{Obs} - f_C | dt}{\int_0^T f_{Obs} dt} = \frac{\sum_{n=1}^{N} | f_{Obs} - f_c | \Delta t_n}{\sum_{n=1}^{N} f_{Obs} \Delta t_n}$$

Where f_{Obs}, observed data (Pressure, water cut or production rate of water or oil)

f_c, calculated data (Pressure, water cut or production rate of water or oil)

T, time of production, days

Δt_n, time step, days

ERROR, the relative error of calculated result from simulation model, unitless.

As seen in Fig.44 this function calculates the percentage of area between observed data and calculated data. By changing the parameters and functions in the simulation model this error tends to diminish to zero. For a practical reservoir simulation project, the error upper limit can not be set as zero. It is impossible for the calculated data to totally coincide with the observed data. The accuracy of history matching depends on the demand of simulation project.

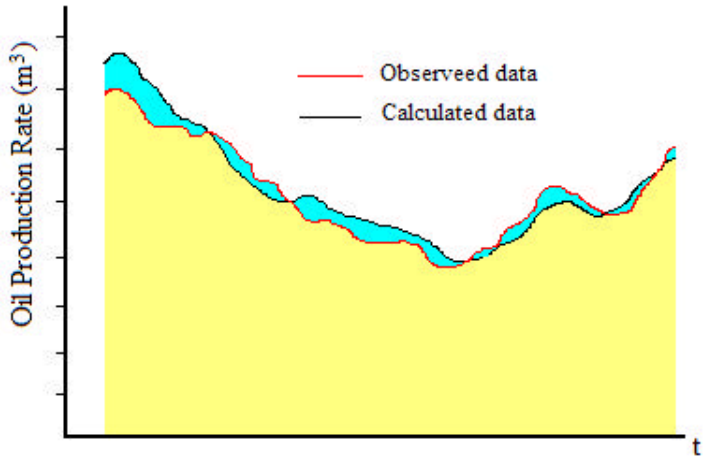

Fig.44 Sketch diagram of error calculation

Sensitivity analysis is to analyse the error value variation with adjusting model parameters or functions. When one parameter or a function is changed, the more sensible the error is to the parameter or function, the more quickly its value varies. Usually the most sensible parameter should be selected at first for adjustment.

From the equations in chapter 2 and chapter 3 it can be seen that for pressure matching the sensible parameter and functions are as follows [13]:

- parameters which are related to fluid's underground volume, such as porosity, fluid's saturation, rock thickness;
- compressibility
- permeability and relative permeability, etc.

In general, permeability is the principal reservoir variable used to obtain a match of pressure behaviour [51]. Because permeability is the most sensible for pressure matching and also the most poorly defined parameters. Fig. 45 shows pressure matching with different permeability distribution. The relative error of well bottom hole pressure for z106-54 from run 7 is 43.40%, from run 8 is 37.23%, and from run 9 is 33.77%. The permeability for run 8 and run 9 have been got by multiplying 2 and 1.7 respectively with the permeability for run 7. For run 9 the permeability distribution can be seen in Fig.35 – Fig.38 in last section.

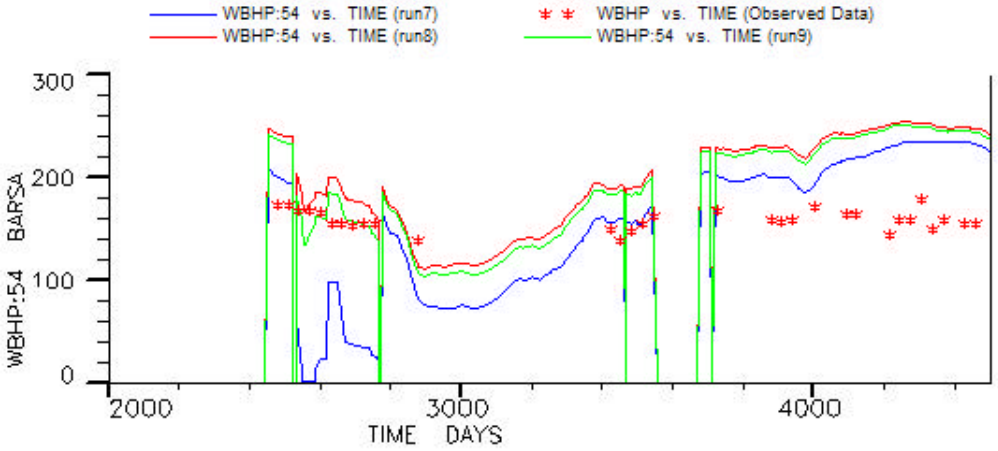

Fig.45 Pressure Matching with Different Permeability Distribution

In order to match history of each well, usually the permeability of some grid sells should also be adjusted. Considering the time limitation, this detailed work has not done.

Water cut is sensible to relative permeability. Different relative permeabilities (seen in Fig.46) have been tried, the water cuts of whole reservoir are compared as seen in Fig.47. Relative permeability data of core from well z106-69 are numbered as No.21, 32 and 46. Because the fluids used in experiment (Water viscosity: 0.582 mPa.s, Oil viscosity: 57.76 mPa.s) are quite different from the fluids in reservoir, the water cut of simulation result with Kro-No32 and Krw-No.32 do not match the observed data so better as which with adjusted relative permeabilities (also seen in Fig 42 in last section). The relative errors are respectively 4.694% and 3.067%. The relative error has been obviously diminished.

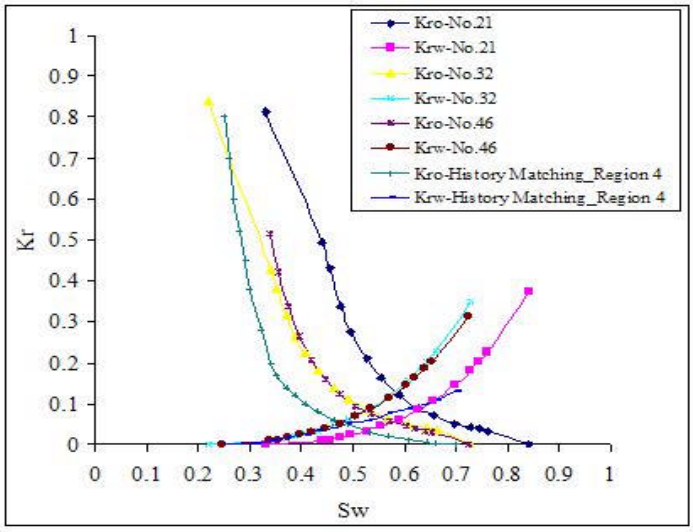

Fig.46 Relative Permeability Comparison

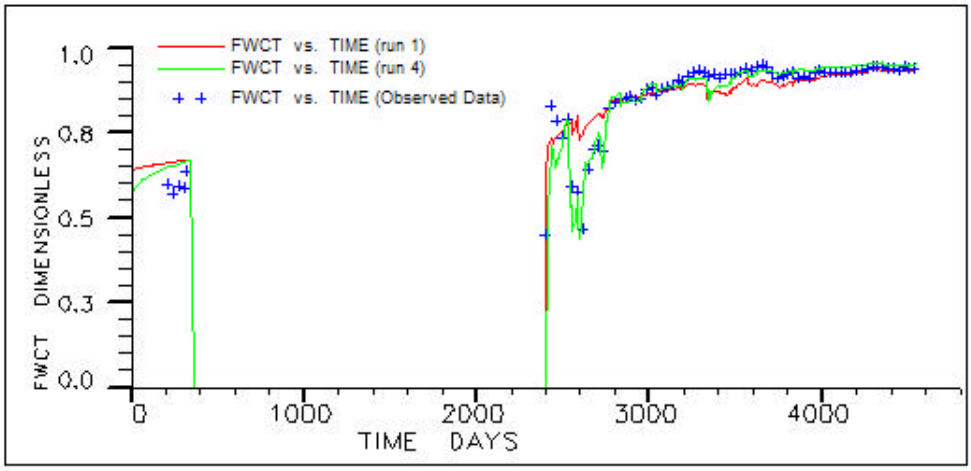

Fig.47 Water Cut Matching with Different Relative Permeabilities

Water cut is also very sensible to initial fluid's saturation. This saturation is controlled by capillary pressure and its distance to water-oil contact. For the run with Kr_No.32, the capillary has already been adjusted; otherweise, the error would be much more high. The capillary pressure has been talked in the last section.

6.2.3 Well Production History Matching Result and Analysis

In the history matching process, permeability and relative permeability are mainly adjusted according to the matching performance. Porosity is not changed since it has little effect on the production performance, it mainly affects the reserve. Fluid properties are mainly from laboratory test, it should be kept unchanged.

Together, there are 17 well, which have produced or are producing oil and water from the reservoir, among which 13 wells has been good matched, the matching results of other 4 wells are not so perfect. Seen in Table 6(* means matched, - means matched not perfectly). One well –42 has been used as an injecting well from the beginning, since it injects water to other layer at the same time, there are no exact data for matching. As examples for matched wells, the history matching results can be seen in Fig. 48 - Fig. 49.

Table 6

Well match result

Well	
L7	*
-56	*
-59	*
-60	*
-54	*
-67	*
-8-8	*
-11-10	*
-11-11	*
-13-13	*
-13-14	*
-16-13	*
-19-x13	*
-10-12	-
-11-12	-
-12-12	-
-66	-

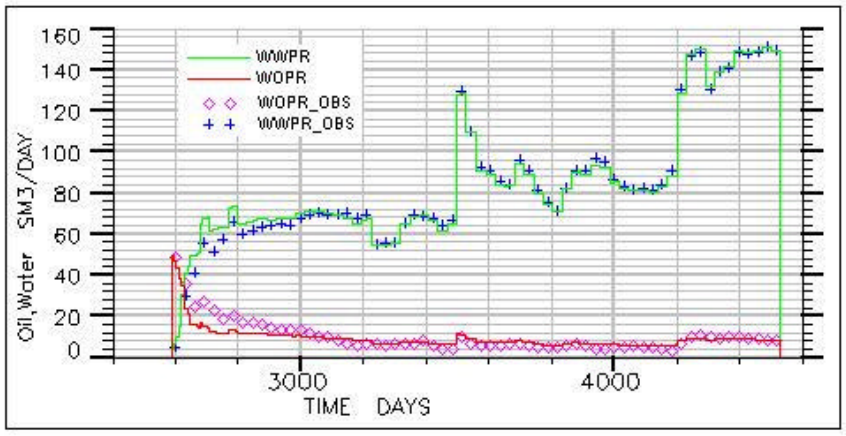

Fig.48 History matching of production rate for well –8-8

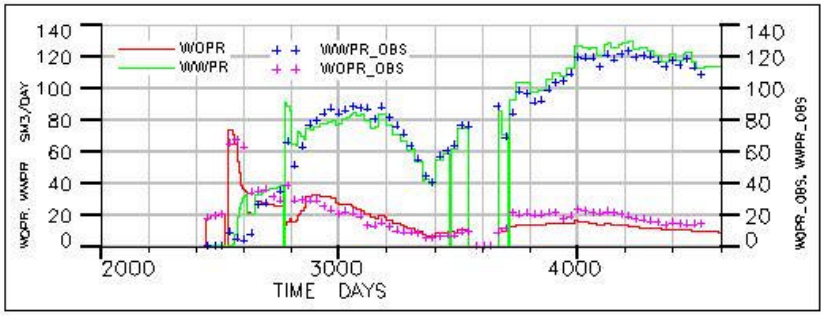

Fig. 49 History matching result of production rate for well -54

Almost all wells, which produce oil from this reservoir, have no pure oil production period, and oil production rate decreased quickly, water cut reached more than 90% shortly after the beginning. Only one well, z106–54, has pure oil production period, but the period is very short, only a few months; and then water cut reached about 90%. The simulation results for all wells have also this phenomenon. Since most of the wells have been matched; it proves that the models for original oil distribution and relative permeability are quite believable.

For well –10-12 and –11-12, the water pr oduction rate have not been fully matched (Fig.50). The main reason is probably of permeability. In the area the permeability has been set lower than that in the other areas, because the reflection in seismic profile in this area is not so strong.

Although the matching result is not so good, the production-changing trend has been simulated out. Due to time limitation for this work, no more efforts could be allowed for detailed permeability adjustment.

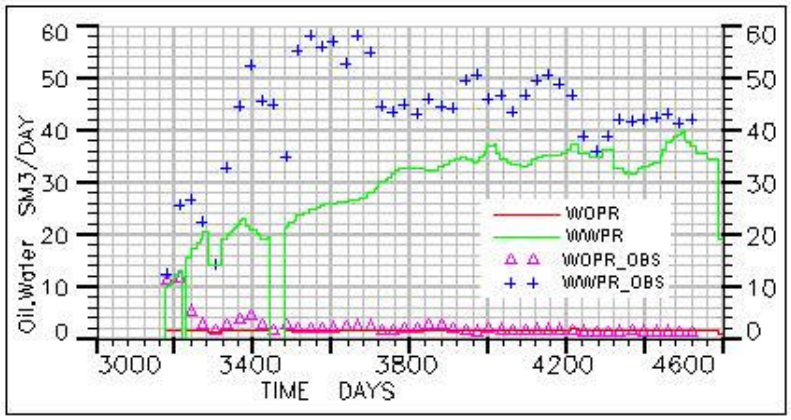

Fig.50 History matching of production rate for well–11-12

For well –12-12 the water and oil rate are also not matched (Fig.51). The error comes from grid generation. From the reservoir profile, it is very clear that layer $Ng2^1$ and $Ng2^2$ are separated by 3 m thick shale. Since they were overlapped together in other area, when constructing geological model, the shale is not taken into account, as a result, the water cut from simulation is higher than the observed data. But the production variation trend is the same as that from observed production data.

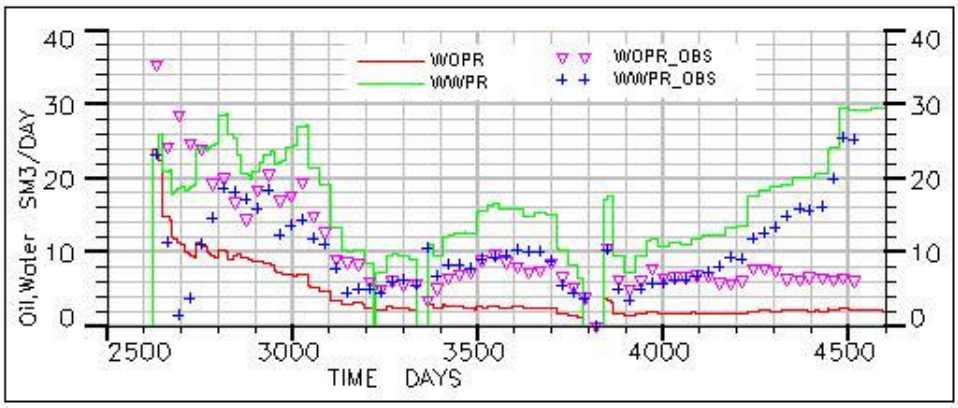

Fig.51 History matching result of production rate for well –12-12

For well –66, the water production rate from simulation is much lower than that in observed data. From logging data interpretation result, the sandlayer $Ng2^1$ is interpreted as oil containing sand layer. And its structure position is also not very low. It seems that the water cut should not be so high as observed data showed. Maybe the underlayered water source in the northern area is more active than it was thought. This well has been changed later into an injecting well. Because the production period is not very long, this error is not considered serious.

6.2.4 Well Bottom Hole Pressure Matching Result and Analysis

Many literatures have listed the strategy of history matching, which pointed out that the first step of history matching is to match pressure, but for this reservoir it is impossible. It is only taken as a reference to appreciate the matching result.

Generally speaking, the pressure matching results are not so good as the water cut (Fig.52 and Fig.53). There are 6 reasons: (1) there are no certain pressure data from this reservoir as reference; (2) gas resolution has not been taken into account; (3) permeability distribution is very difficult to determine exactly; (4) injecting pressures of injecting wells L7 and –42 have great influence on the pressure changing behaviour, but their input data can not be sure for the reason listed in section 6.2.1; (5) the cumulative injected water into $Ng2^1$ from Well L7 and -42 can not be determined quantitatively; (6) the injecting bottom hole pressure of these two wells are not measured exactly.

In general, permeability is the principle reservoir variable used to obtain a match of pressure behaviour. Any variation should be compatible and reasonable according to the geological principle. Because of the limitation of original geological and geophysical data, it is difficult to get the real value distribution of permeability underground in the reservoir. For this simulation process, only the pressure-changing trend has been matched. It can be seen that simulated bottom hole pressure for well –67 and –54 decrease or increase with the same trend for the observed data.

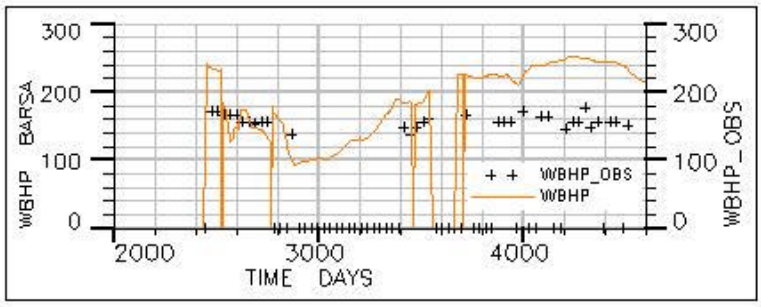

Fig. 52 Bottom hole pressure matching result of well -54

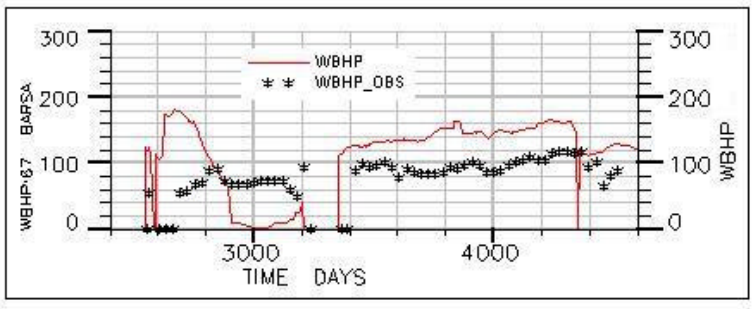

Fig. 53 Bottom hole pressure matching result of well -67

6.2.5 Matching Result for Whole Reservoir

Oil and water production rates for the whole reservoir have also the character that oil is mainly produced with high water cut, no pure oil production period. The comprehensive water cut increases from 44.5% (May 1995) to 90.3% (June 1997); for most of the production time till April 2000, water cut has been more than 90%. The simulation results have perfectly matched this process.

Match for a whole reservoir is usually more easily than a match for individual well performance [56]. The matching results of the researched reservoir are as seen in Fig.54, Fig.55 and Fig. 56. Especially for accumulative production of water and oil, the relative error is less than 1.5%.

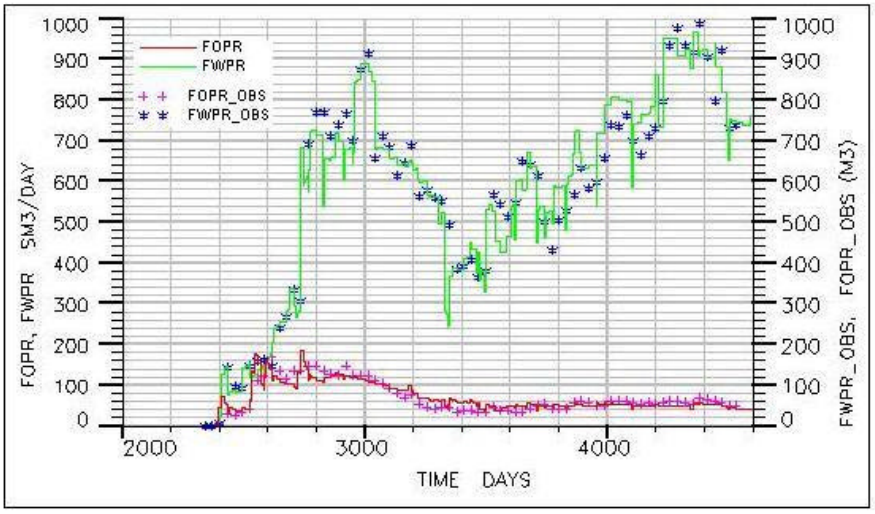

Fig. 54 Production rate matching result for whole reservoir

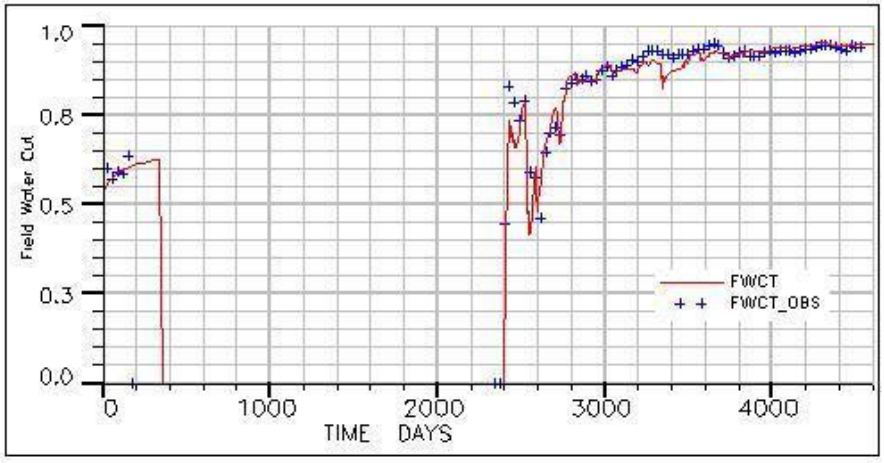

Fig.55 Water cut matching result for whole reservoir

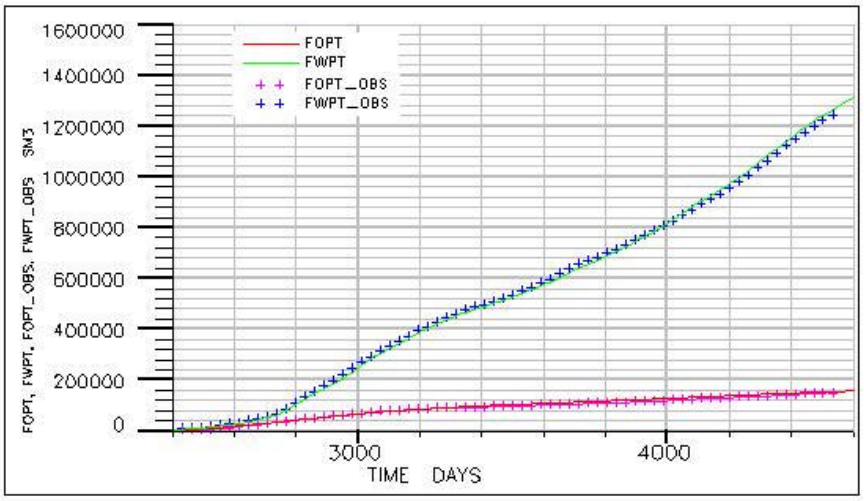

Fig. 56 Matching result of cumulative production of water and oil

Based on the discussion in the last few sections, it can be concluded that the simulation model is already reliable for prediction of further performance of the reservoir and it can be taken as a basis for the later-discussed polymer flooding simulation.

7. Residual Oil Distribution and Production Prediction under Water Flooding

All though the comprehensive water cut has reached 93.6%, for some wells even more than 97%, most of the oil reserve is still residual underground. It can be concluded by comparing the Fig.57 and Fig.43 in the last chapter.

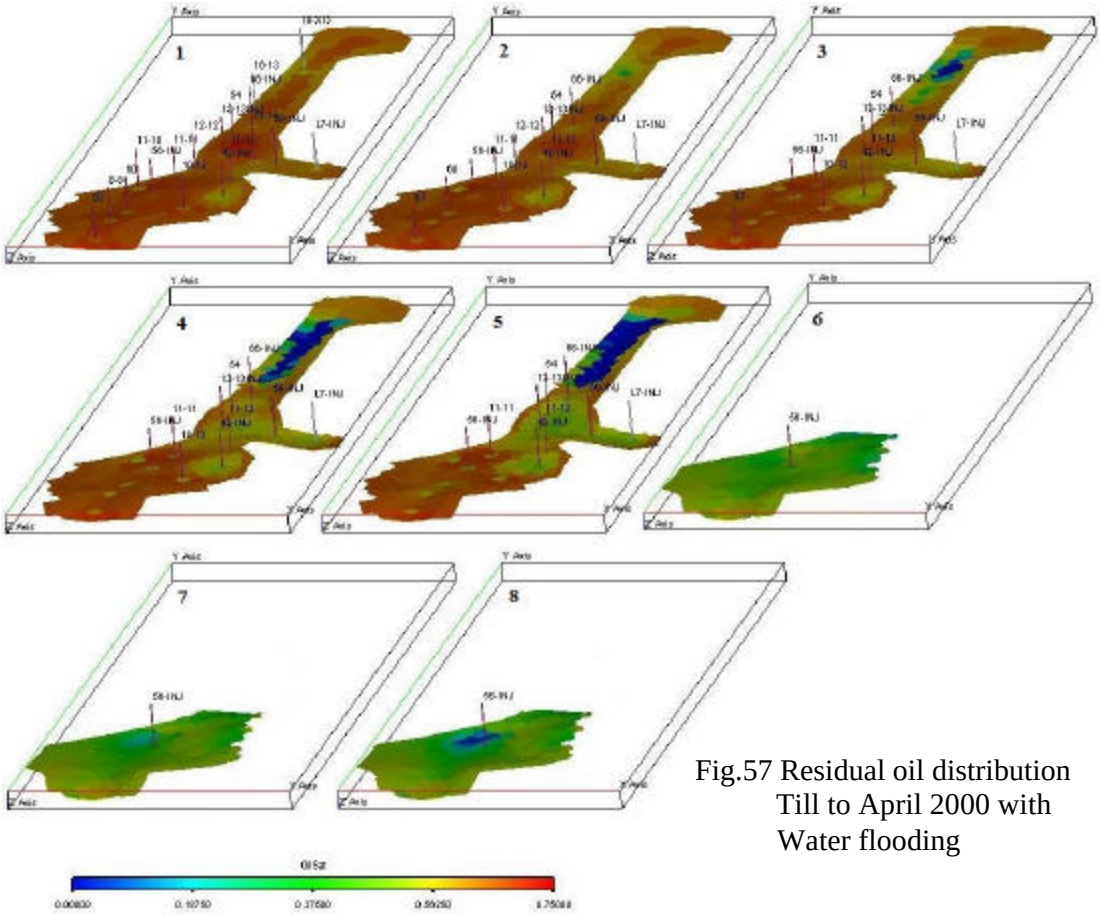

Fig.57 Residual oil distribution Till to April 2000 with Water flooding

In Fig.57, it is seen that oil saturation has obviously decreased only in area near the well; oil saturation, in area between the wells and where there is no well, is still very high in the upper sandlayer.

Due to the capillary pressure the original oil saturation decreases from up to down, saturation of water is higher than irreducible water saturation, especially in region 1, 2 and 3, it is much higher than irreducible water saturation. At the production beginning of well L7 the water cut is already more than 50%. Because oil-water viscosity ratio is so high as 207.826 under reservoir condition, water is much more active than oil. The injected water flows quickly

from injecting wells to producing wells. This is the main cause for high water cut and low oil production velocity.

Based on the matched simulation model, the predicted production is as seen in Fig.58. With water flooding the water cut will be kept very high, and oil production will be so low as near to the economic limitation. In order to improve the oil production velocity and oil recovery ratio, method of enhanced oil recovery must be adopted urgently. As introduced in chapter 1, polymer flooding method will be tried by simulation. It will be systematically discussed in next chapter.

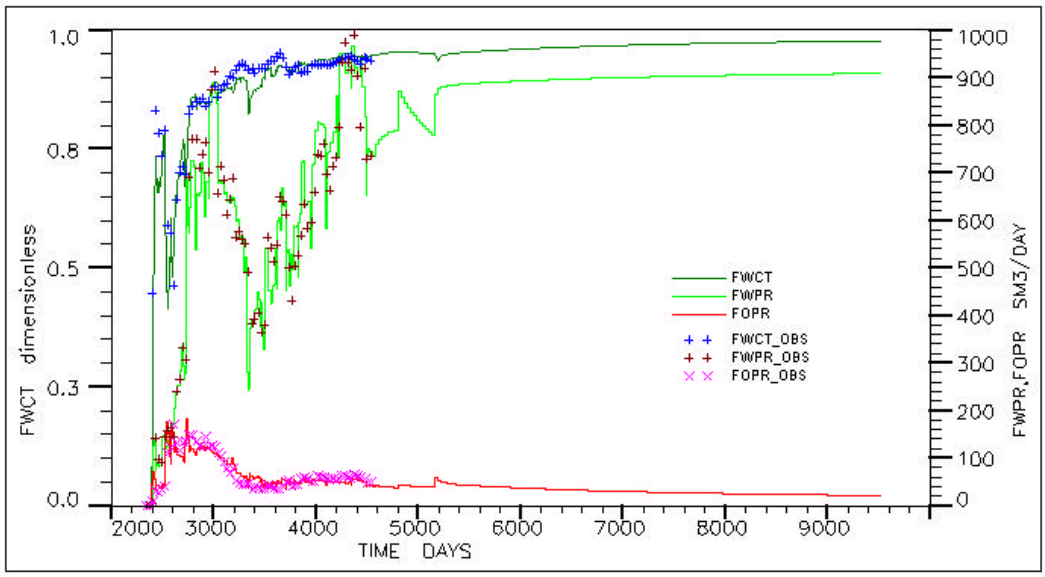

Fig.58 Production rate and water cut prediction under water flooding

8 Polymer Flooding Simulation

History matching result with water flooding has shown that the water sweep efficiency is not ideal due to the unfavourable mobility ratio between water and oil, and serious heterogeneity of permeability in the river channel sandstone reservoir.

Many literatures have reviewed the success of enhanced oil recovery with polymer flooding [56-58]. In most of the projects polymer flooding has been used as secondary recovery method, the average polymer flood recovery is approximately 8% of the original oil in place, and the average amount of polymer injected is around 0.011 kg/m^3 [56]. Water cut before polymer flooding is lower than 90%.

In some projects polymer floods have been used as tertiary applications, and the oil recovery are increased with an average of 1.8% OOIP, the polymer consumption is approximately 0.018 kg/m^3 [56].

Some later literatures have given even much better results. Mahendra Pratap et al. [59] have provided a successful field experiment in India with incremental oil recovery of 9.4% due to polymer flooding; Maitin B.K. [60] has even concluded an incremental oil recovery of 8-22% in a northern German oil field. Polymer flooding as tertiary method has also been proved successful in Daqing Oilfield in northeast China, and Henan Oilfield in middle China [61-62].

Homayoun Hodaie and A.S. Bagci have concluded with their experiment that polymer augmented water flooding shows better oil recovery especially with under-water zone [63].

Ezeddin Shirrif has done a set of experiments to test mobility control by polymers under bottom-water conditions, oil recovery increases significantly when the mobility ratio is reduced when a bottom water zone is present [64].

But a few problems still remain to be solved:

(1) In most of the reservoir projects or laboratory experiments, oil is not so viscous as in our researched reservoir,
(2) The heterogeneity of permeability is not so serious as in river channel sandstone,
(3) For most of the polymer flooding projects in literature, the well pattern is usually regular, but for narrow river channel reservoir, wells can only be drilled in the middle along the river, as a result, they could not construct complete well pattern,
(4) At very high water cut stage.

Though B.L. Knight and J.S. Rhudy [65] have got attractive incremental recovery with heavy oil in laboratory, whether polymer flooding method is economically feasible for a practical river channel reservoir, it still needs further studying. This is the main purpose of this simulation project.

In the following sections a theoretical river channel reservoir has been simulated at first, then for reservoir $Ng2^1$. The polymer flooding mathematical model has been described in chapter 2 and chapter 4. Different factors, which affect polymer flooding efficiency, have been taken into account, and corresponding results are discussed.

8.1 Polymer Flooding Simulation with A Theoretical River Channel Reservoir

Since reservoir $Ng2^1$ is from river channel sediment, it looks like a lens in vertical profile and the permeability is seriously heterogeneous. For convenience of understanding and commenting the polymer flooding efficiency, a theoretical river channel geological model has been designed for simulation.

8.1.1 Geo-Model Definition

A 3D model has been designed for simulation after shape of a normal river channel reservoir, as seen in Fig 59.

Regular Grid: $11 \times 10 \times 5$

Equal Cell Area: $25 \times 30 m$

Cell thickness decreases gradually from the middle to the edge, 3.2m and 0.6m respectively. For 5 cell layers, the sandstone thickness in the middle is 16 m; at the edge it is 3 m.

Porosity and permeability do not change along river channel direction, in its vertical direction they change as seen in Fig.60 and Fig.61.

The areal permeability K_x and K_y are assumed equal, vertical permeability K_z is calculated with equation (6-1) from [48].

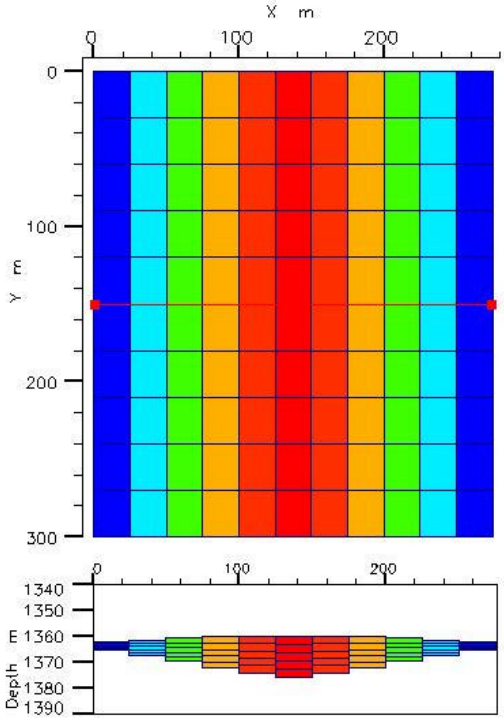

Fig.59 3D Grid Model

In the middle of the channel, permeability is much higher than that in the edging area. This is compatible with the sandstone sedimentary condition. Coarse sand is usually located in the middle, to the edge it turns gradually fine and contains more shale content, as a result, the porosity and permeability decrease correspondingly.

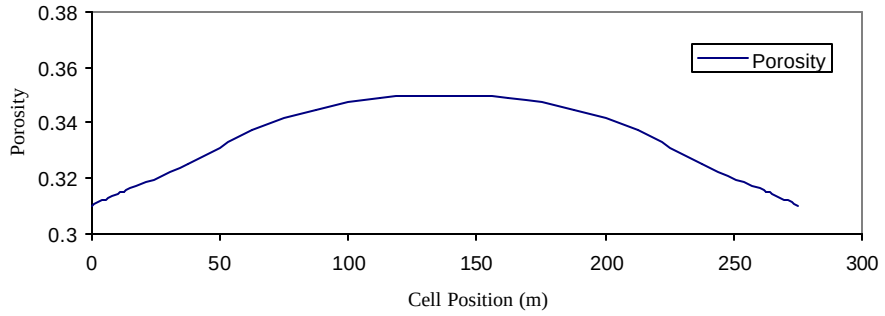

Fig.60 Porosity distribution

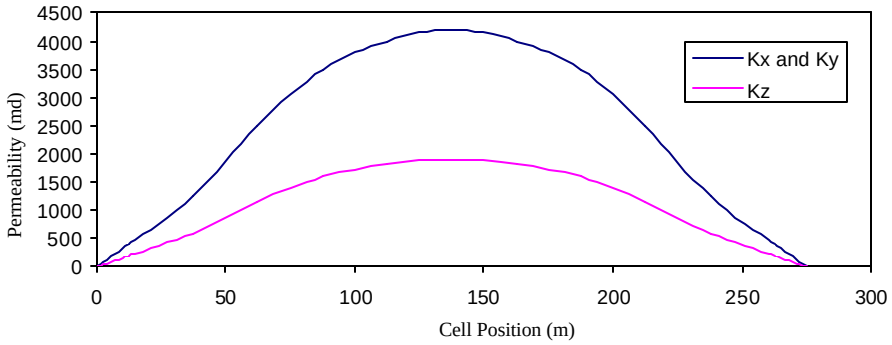

Fig.61 Permeability distribution

In this model, porosity varies from 0.31 – 0.35, permeability decreases from 4,200 md to 0 md. According to their rock properties the model has been divided into three different regions, for different region, different capillary pressure function and relative permeability has been set, the region distribution is as seen in Fig.62. The corresponding functions are the same as described in Chapter 6.

Oil and water properties have been set as the same as those in reservoir Ng2[1].

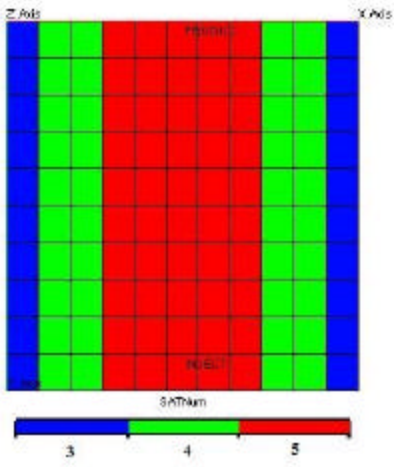

Fig.62 Region Number

The depth for zero capillary pressure has been set at 1,380 m. The original oil saturation distribution for five cell layers is as seen in Fig.63. The oil saturation decreases from the middle to the edge area, and from up to down.

Two wells, one as producer and the other as injector, both lie in the middle of river channel. The production rate and injecting rate have all been set equal to 100 m^3/Day.

Black Oil mode with polymer flooding option in ECLIPSE have been used, and all simulation runs have been set by using fully implicit method. All the simulation processes have been completely convergent.

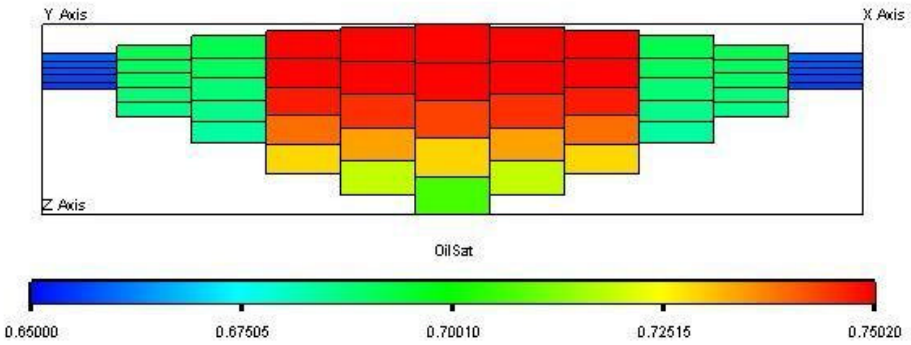

Fig. 63 Original Oil Saturation Distribution Profile

8.1.2 Water Flooding Simulation Result

Simulation results show that the production situation of such a river channel reservoir is the same as that of reservoir $Ng2^1$. It proves that the simulation results for the practical reservoir are theoretically reasonable. At the beginning of production, there is already some part of water. Only after a few months the water cut reaches more than 90%. Most of the oil reserve can be only produced at high water cut stage (Fig.64 and Fig.65). With water flooding, the oil recovery only reaches about 24.77% (Fig.66). Most of oil is residual underground.

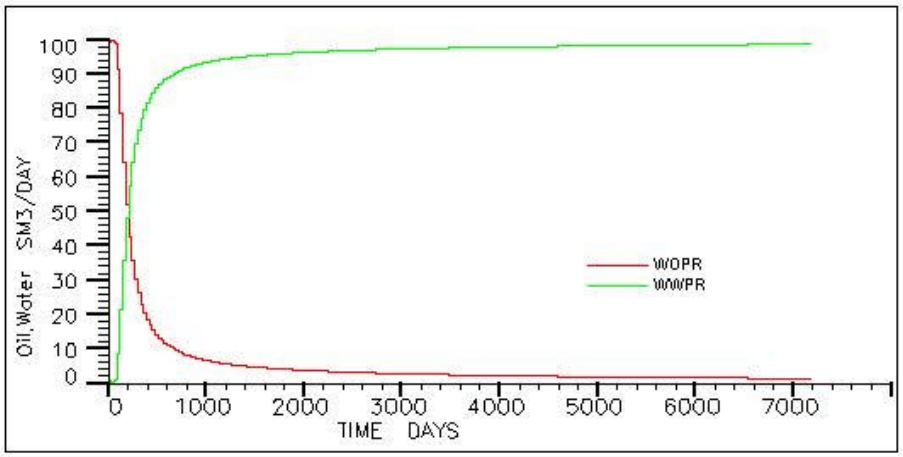

Fig.64 Water and oil Production rate

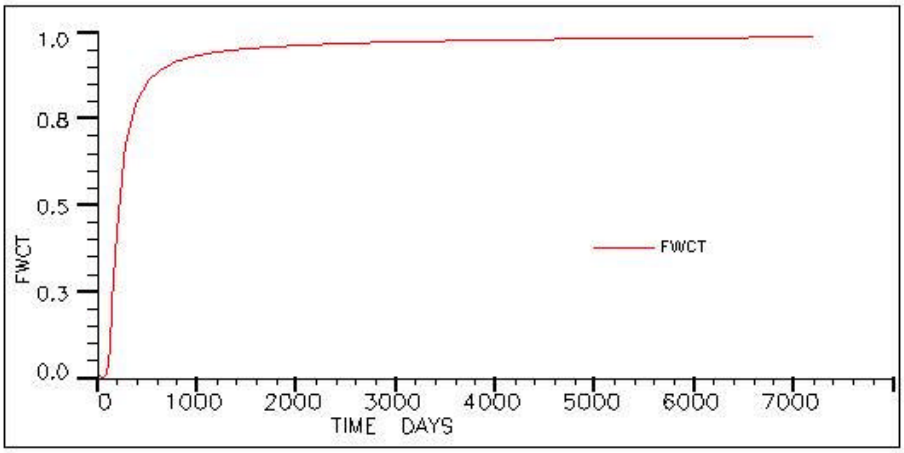

Fig.65 Water cut with water flooding

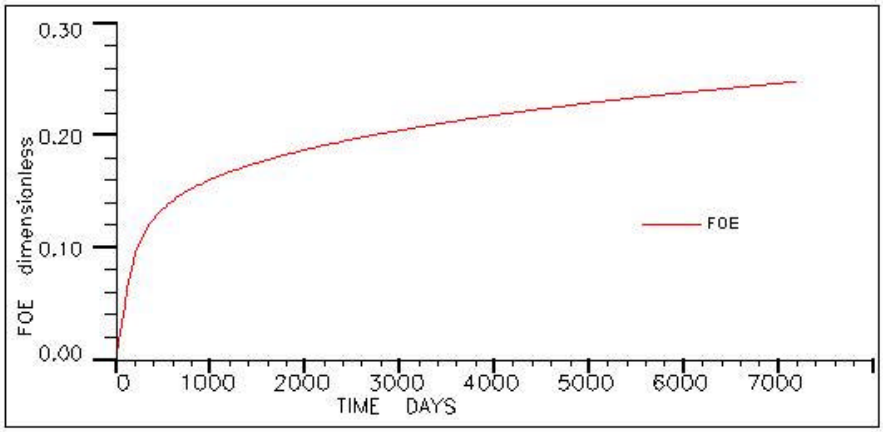

Fig.66 Oil recovery with water flooding

From Fig.67, it is seen that oil saturation in the above layers and in the edging area is still very high. Water flows quickly from the injecting well to the producing well mainly through the middle area of the river channel due to the serious permeability heterogeneity. Water flooding is not efficient for the above layers.

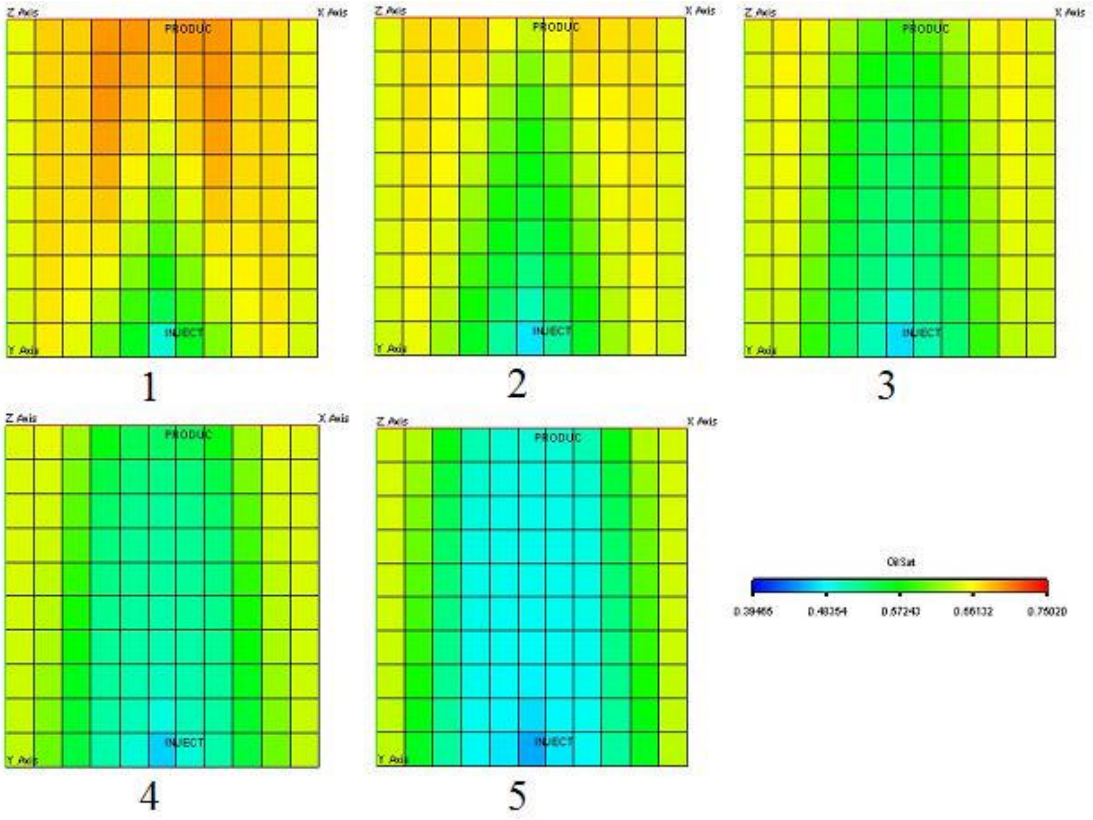

Fig.67 Residual oil saturation distribution after water flooding

8.1.3 Data System Specification for Polymer Flooding

8.1.3.1 Viscosity of Polymer Solution

Three polymer products have been tested in Labor. Fig.68 shows that polymer is sensible to temperature. With the same polymer concentration 1.5 kg/m^3, and water from producing well with salinity 5,727 mg/L, the viscosity of all three polymers has decreased as temperature being increased from 50°C to 90°C.

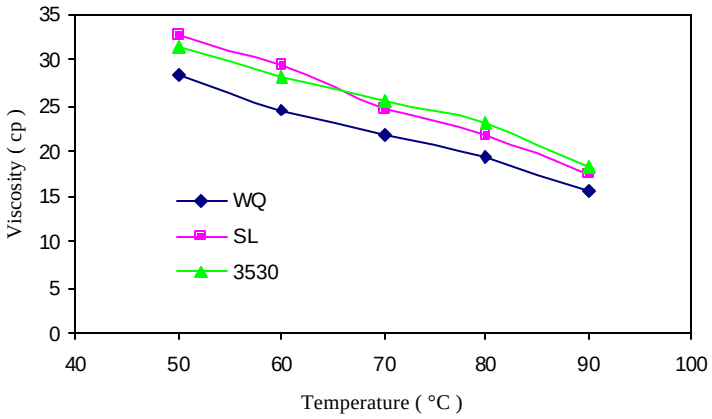

Fig. 68 Relation between viscosity of polymer solution and temperature

Since in the real reservoir the temperature is stabile at about 65°C, a set of labor tests has also been made with water from wells in this area with salinity 4822 mg/L under temperature 65°C. Labor results show that all three polymer products have obvious viscosity-increasing capability (Fig.69). Polymer 3530 and SL are a little better than polymer WQ.

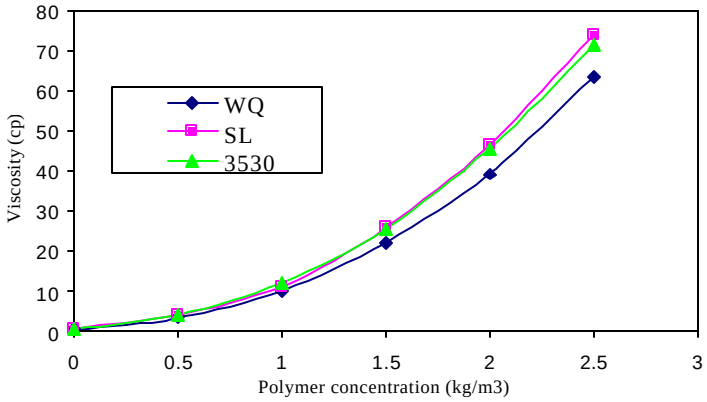

Fig.69 Relation between viscosity and concentration

Data for Polymer SL has been selected for simulation. As required by ECLIPSE, the polymer solution viscosity function is given as a set of multipliers to water viscosity (Fig.70). When concentration of polymer solution is zero, the multiplier is 1; the corresponding viscosity is 0.46 cp, equal to viscosity of pure water.

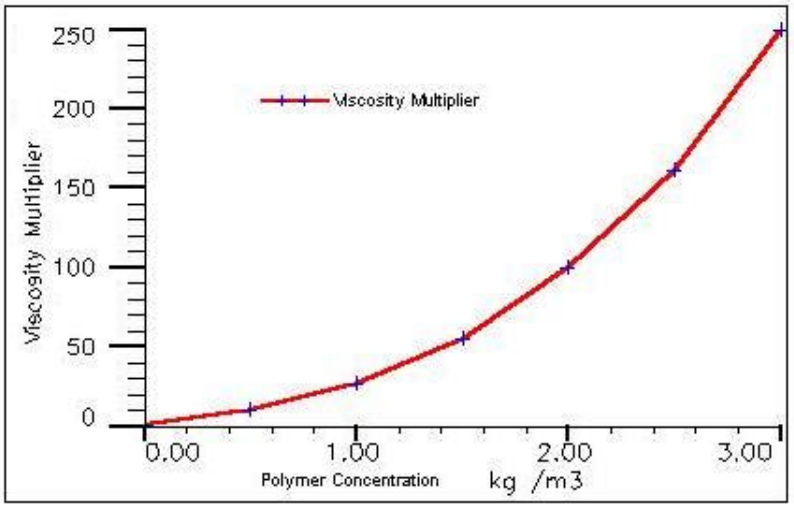

Fig.70 Polymer solution's viscosity function for polymer flooding simulation

8.1.3.2 Polymer Shear Thinning

Polymer solution is not Newtonian fluid, when it flows, its viscosity will be changed, and higher flowing velocity leads to lower viscosity. In ECLIPSE it is defined with a shear-thinning factor. At static state, the viscosity is described as above in the last section. With increasing flowing velocity, the factor decreases from one to a special value, when the velocity is especially high, the polymer molecular structure will be broken down and polymer solution will lose its viscosity increasing capability. Fig. 71 is the shear thinning function for simulation. Since there is no labor data for polymer SL, this function is cited from literature [15]. (a) is with logarithmical horizontal coordinate; (b) is with arithmetical coordinate.

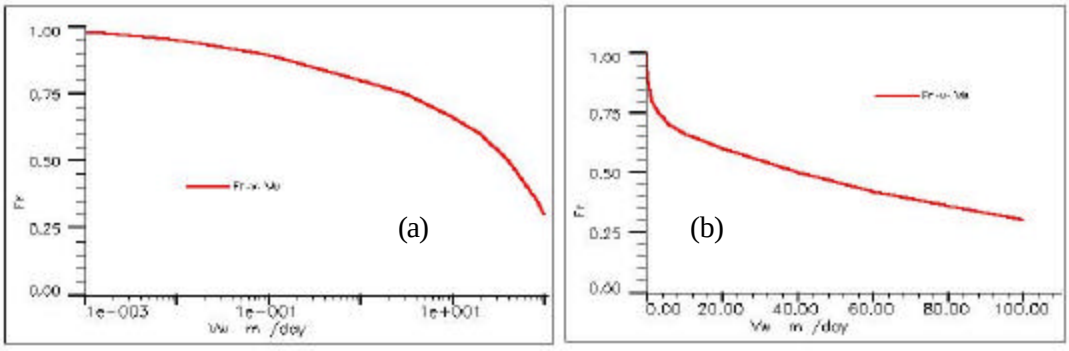

Fig. 71 Shear thinning factor for polymer solution

Since in the practical polymer flooding, the flow velocity can be controlled under the critical value, shear-thinning effect has been assumed reversible.

8.1.4 Polymer Adsorption Effect

As described in chapter 2, polymer retention, due to adsorption, varies with polymer type, molecular weight, rock property, brine salinity, brine hardness, flow rate, and temperature.

Field-measured values of retention range from 7 to 150 ug polymer/ cm^3 of bulk volume. [15]

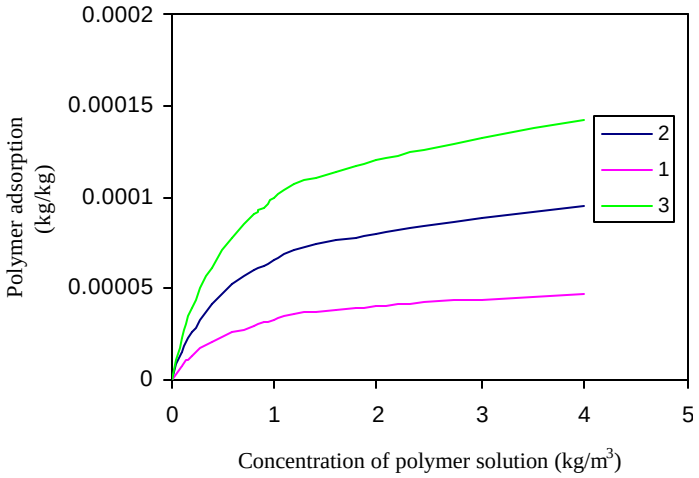

Fig.72 Polymer Adsorption Functions

Because of lack of labor test data of adsorption, in this simulation three different adsorption functions has been assumed. For function 1, the maximum adsorption is 50 ug/(g rock); for function 2, the maximum is 100 ug/(g rock); for function 3, it is 150 ug/(g rock) (Fig.72).

Three run processes have been done with different adsorption functions in Fig.72; polymer slug size has been set the same as 0.455 PV (reservoir pore volume); polymer concentration is 1.0 kg/m^3. Polymer has been injected from 2,560 day to 3,800 day, the oil and water production rate are as seen in Fig.73. With higher adsorption, the enhanced oil recovery will be decreased (Fig.74).

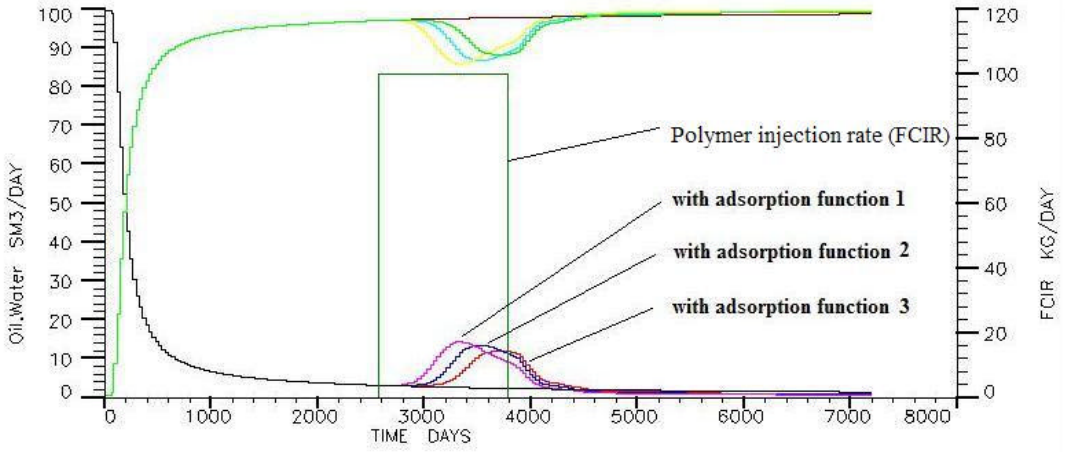

Fig.73 Oil and water production rate with different polymer adsorption function

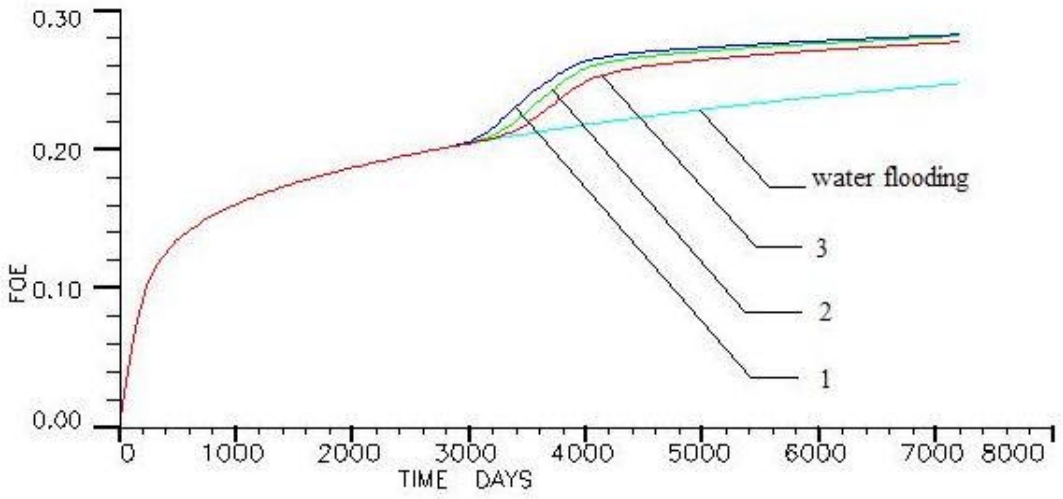

Fig.74 Oil recovery under polymer flooding with different polymer adsorption functions

Polymer retention leads to loss of polymer from solution, which causes the mobility control effect to be lost. If the polymer slug is small, and concentration of injected polymer solution is also low, retention may lead to polymer flooding fail. From these three run processes, it can be seen that with larger polymer injection size, the adsorption effects can be covered. Difference of oil recovery between run 1 and run 2 has been decreased as time passed by.

Result from reference [25] proves that higher permeability leads to lower adsorption. Rock permeability from river channel is even higher than 4,000 md; the adsorption should not be higher than 50 ug/g. From the above figures it can be seen, even with more adsorption, the polymer flooding can still get a favorable enhanced oil recovery. The later described processes have been simulated with adsorption function 2.

8.1.5 Polymer Concentration Effects

The main purpose of polymer flooding is to control the water viscosity by adding polymer into injected water so as to lower the water mobility, especially for high permeability river channel reservoir. Water relative permeability decreasing, which results from polymer adsorption, is not so obvious as that in low permeability rock. The most benefit of polymer flooding is from the viscosity increasing of water phase, which improves the water-driving efficiency.

Higher polymer concentration leads to higher viscosity. Fig.75, Table 7 and Fig.76 show simulation results with different concentrations of injecting polymer solution. Three runs have the same injected polymer slug size: 0.455 PV. They prove that the higher the polymer concentration is, the more oil can be recovered.

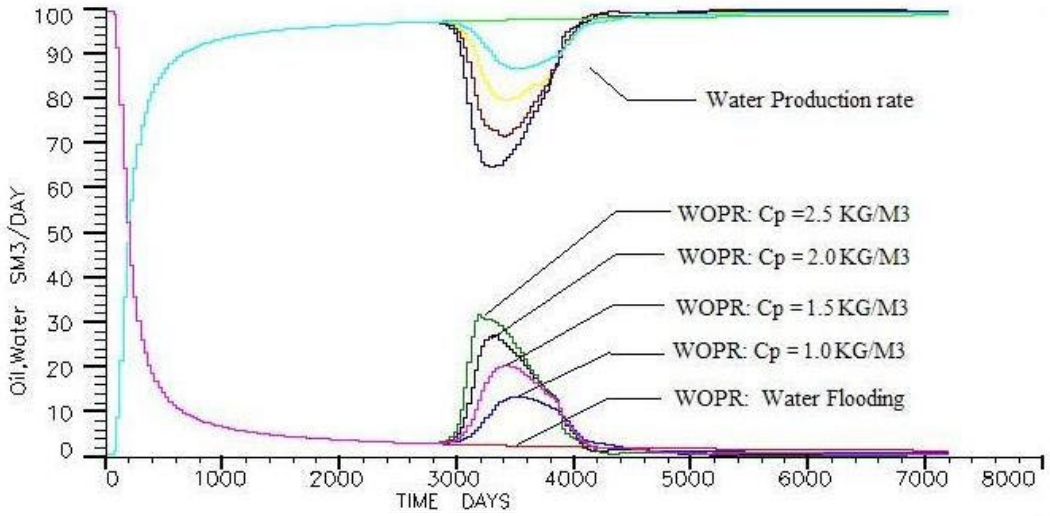

Fig.75 Oil and water production rate with different polymer concentration

Table 7 Oil Recoveries with Different Polymer Concentration

Polymer Concentration (kg/m^3)	0	1	1.5	2	2.5
Final Oil recovery	0.2477	0.2817	0.2998	0.3150	0.3273

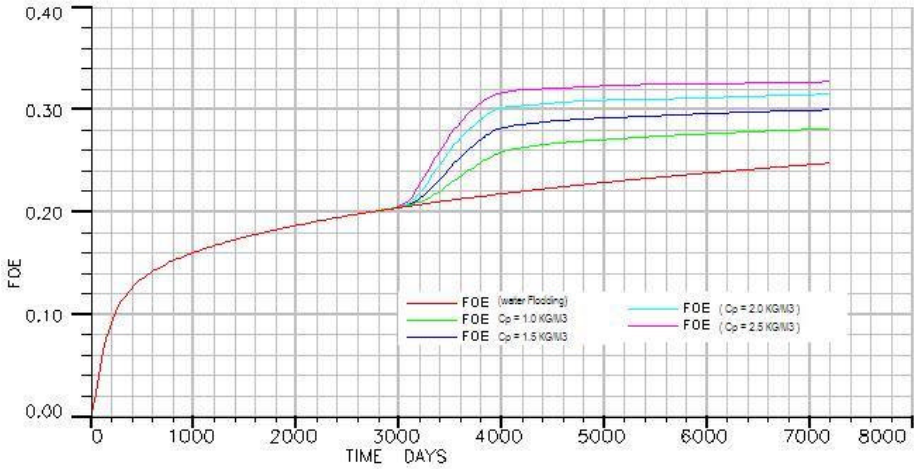

Fig.76 Oil recovery with different polymer concentration

Practically, concentration of polymer solution can not be increased without upper limit. With polymer concentration increasing, the viscosity will be highly increased, as a result, the injecting pressure will correspondingly increase if the injection rate is kept stabile. If the pressure is too high, the reservoir rock will be fractured. For practical field polymer flooding, the concentration rarely exceed 2 kg/m^3. In this reservoir 1.5 kg/m^3 has been selected for further simulation. The feasible method is to increase the polymer slug size with possible polymer concentration.

8.1.6 PolymerSlug Size

Polymer concentration is set as 1.5 kg/m^3, with polymer adsorption function 2, a few runs have been done for different polymer injection slug size. Simulation results are shown in Fig.77, Fig.78 and Table 8.

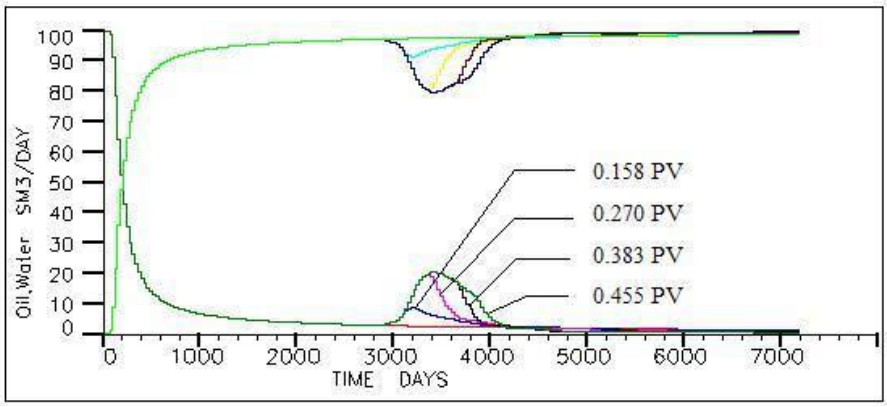

Fig.77 Oil and water production rate with different polymer injection slug size

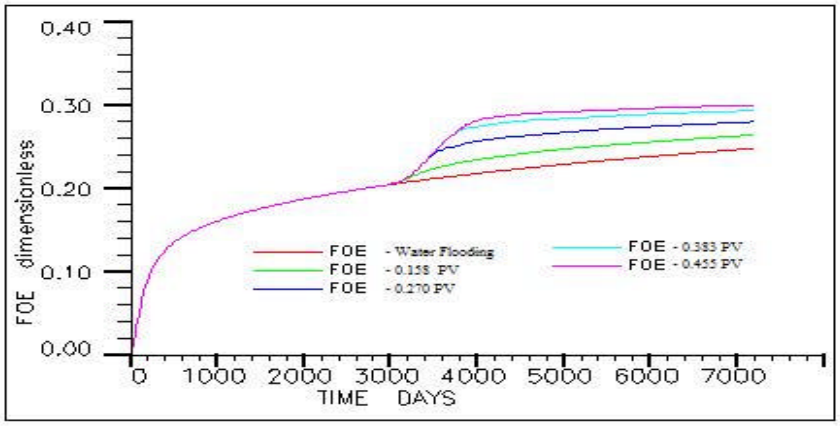

Fig.78 Oil recovery with different polymer slug size

Table 8 Oil Recoveries with different polymer slug size

Polymer slug size (PV)	0	0.158	0.270	0.384	0.455
Final Oil recovery	0.2477	0.264	0.280	0.293	0.300

By increasing polymer slug siz,e more and more oil can be recovered. When 0.455 PV polymer solution is injected, the enhanced oil recovery is more than 5%. In practical field application, the slug size depends on oil price. The enhanced oil recovery is not linearly increasing with polymer consumption enlarging.

8.1.7 Comparison between Water Flooding and Polymer Flooding

The residual oil saturation distribution after polymer flooding with injection slug size 0.384 PV has been selected to compare with which after water flooding (Fig. 79). It shows that oil saturation has been apparently decreased, especially in the upper three layers. Polymer solution has taken obvious effect on improving volumetric driving efficiency.

In the simulation process, in order to simplify the problem, the injection and production specification have been set unchangeable. In field application, through changing the production rate of different producing wells, the oil can be more recovered in the edging area.

Another problem, which should also be mentioned, is that adsorption has been conservatively enlarged. With practical lower adsorption, polymer flooding should be more favorable.

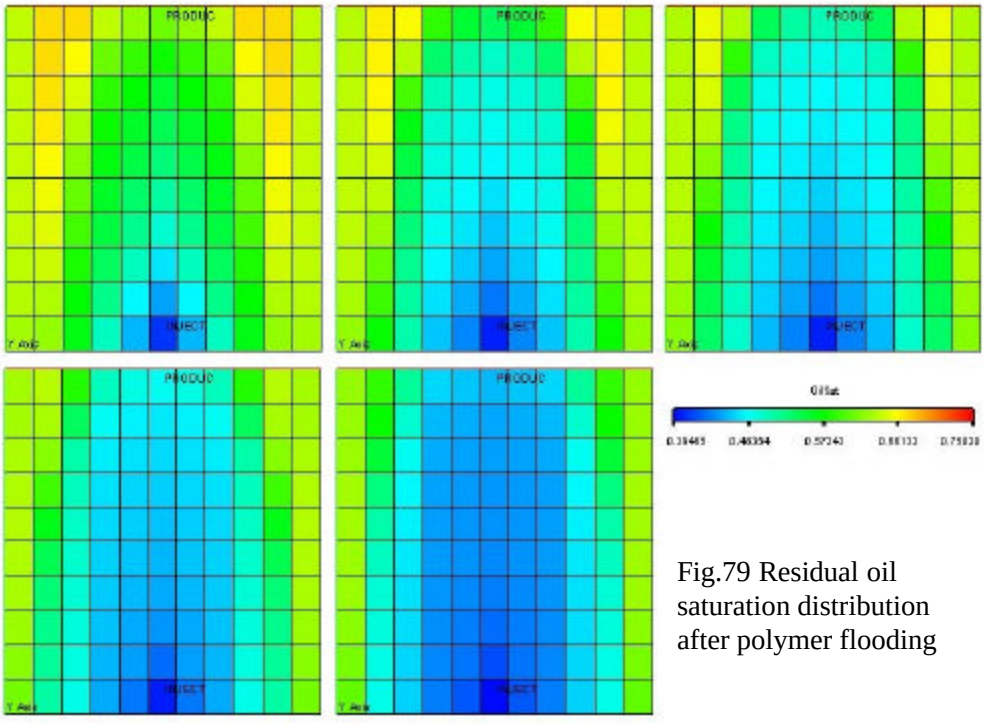

Fig.79 Residual oil saturation distribution after polymer flooding

8.2 Polymer Flooding Simulation in Reservoir $Ng2^1$

Simulation results from the above theoretical river channel reservoir have proved that enhancing oil recovery in such heavy oil reservoir is possible with polymer flooding. Aiming to improve oil recovery in reservoir $Ng2^1$, polymer flooding is also adopted based on the former situation from water flooding. In the following sections the simulation results of polymer flooding are discussed and compared with prediction under normal water flooding.

8.2.1 Polymer Flooding Specification

Viscosity function of polymer solution and polymer shear thinning function have been set the same as seen in Fig.70 and Fig.71. Adsorption function 2 in Fig.72 is selected for practical usage in reservoir $Ng2^1$. Inaccessible pore volume has been set at 0.2 – 0.23, less than irreducible water saturation. The reduction factor has been set at 1.4 –1.5 for maximum adsorption, since the effect on high permeability rock is very limited.

Based on the discussion about polymer concentration selection on theoretical river channel reservoir in last section, 1.5 kg/m^3 polymer solution is selected for the practical reservoir; And
polymer solution is injected from the 5,160th day; different injecting slug size of polymer solution has been tested.

From the 5,160th day the injection rate for the whole reservoir has been set as 930 m^3/day.

Well –59 is set shut off, Well -8-8 and –11-10 are changed into injecting wells from the 5,160th day to complete the injection and production well pattern. Polymer injecting wells and oil producing wells and their injection or production rate are set as seen in Table 9.

All injecting wells inject polymer solution of the same concentration during the same period. The polymer production rate of production wells will also be simulated.

Table 9 Well specification

Well	Type	Injection or production rate (m^3/day)
L7	INJ	80
-56	INJ	220
-66	INJ	100
-42	INJ	50
-68	INJ	100
-8-8	INJ	200
-13-13	INJ	100
-11-10	INJ	80
-54	PROD	140
-11-11	PROD	160
-67	PROD	140
-13-14	PROD	80
-16-13	PROD	80
-69	PROD	80
-10-12	PROD	30
-11-12	PROD	20
-12-12	PROD	40
-60	PROD	160
-59	Shut	
-19-x13	Shut	

8.2.2 Selection of Polymer Slug Size

Polymer flooding with different slug size has been simulated for the practical reservoir. Results are as seen in Fig.80 – Fig.82 and Table 10.

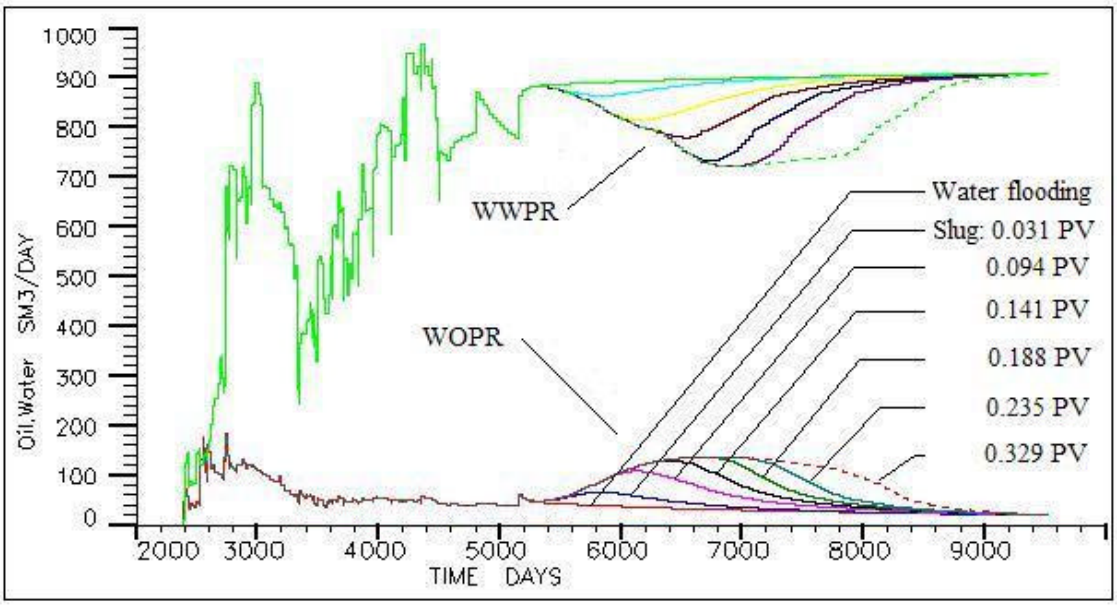

Fig.80 Field oil and water production rate with different polymer slug size

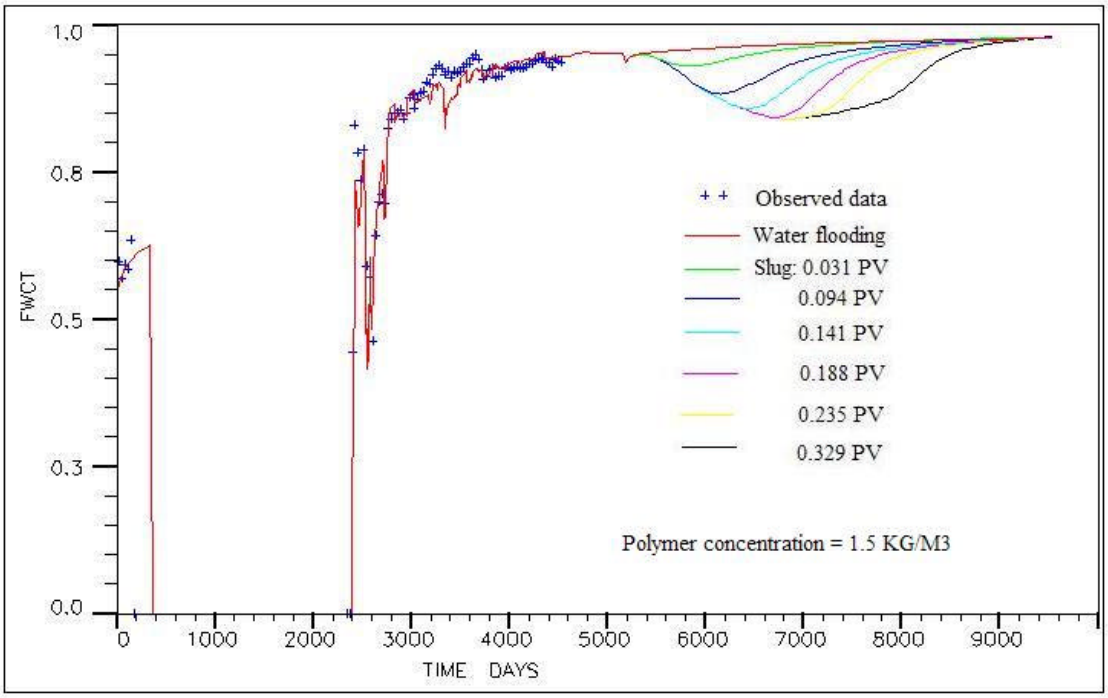

Fig.81 Field water cut with different polymer slug size

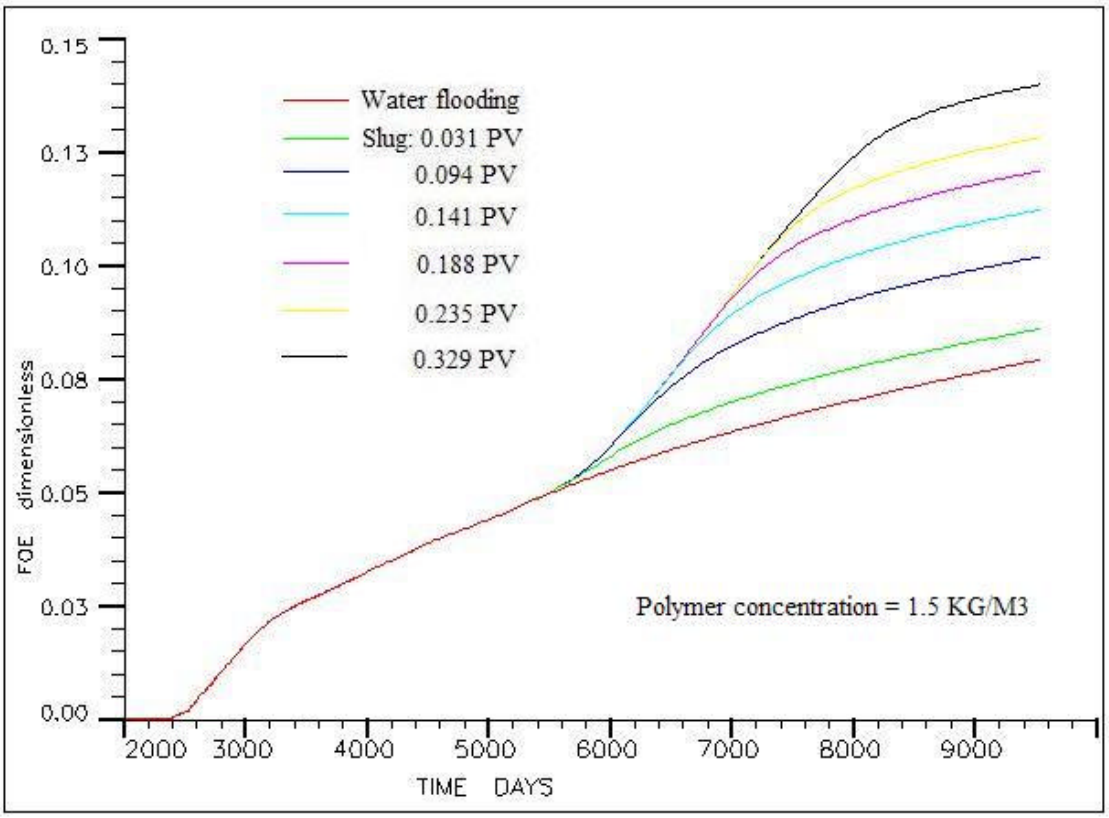

Fig.82 Reservoir Oil recovery with different polymer slug size

When polymer slug size is very small, there is almost no enhanced oil; most of polymer has been adsorbed on the pore surface of the rock when flowing from injection well to production well, as a result, polymer solution loses its capacity. With polymer slug increasing, polymer flooding becomes more and more efficient. The oil production rate can be improved, and the final oil recovery can be obviously enhanced.

With 0.235 PV of polymer solution being injected, the oil peak production rate even reaches 137.2 m^3/day, three times more than that before polymer flooding, which is only 40.6 m^3/day. Water cut decreases from 95% to 84%, then increases again. Polymer flooding takes effect from 5,400 day to 8,400 day. Till the end of polymer flooding, oil production can accumulate to 503349 m^3, 192225 m^3 more than that only with water flooding. The final oil recovery reaches 12.8%, of which, 4.8% comes from polymer flooding.

With greater polymer slug size, 0.329 PV, though the oil peak production rate does not increase, but the effective polymer flooding time-dimension can be elongated, as a result, more oil can be recovered. Cumulative oil production can be enlarged to 549156 m^3; the final oil recovery to 14%, of which, 6.1% is enhanced oil recovery.

Table 10 Simulation result with different polymer slug size

Slug Size (PV)	Polymer Injection Time (day)	Polymer Consumption (ton)	Cumulative Oil Production (m^3)	Enhanced Oil (m^3)	Oil Recovery	Improved Oil Recovery
0		0	311,124	0	0.079	0
0.031	5,160-5,400	334.8	337,853	26,729	0.086	0.007
0.094	5,160-5,880	1,004.4	400,125	89,001	0.102	0.023
0.141	5,160-6,240	1,506.6	440,676	129,552	0.112	0.033
0.188	5,160-6,600	2,008.8	474,320	163,196	0.121	0.042
0.235	5,160-6,960	2,511	503,349	192,225	0.128	0.049
0.329	5,160-7,680	3,515.4	549,156	238,032	0.140	0.061

Only from the simulation results it can be concluded that the more polymer is injected, the higher the enhanced oil recovery can be got. But in practical field polymer flooding, economical interest should certainly be taken into account; polymer slug size can not be enlarged without upper limitation.

Fig.83 shows the relation between polymer consumption and enhanced oil. With polymer consumption increasing, the amount of enhanced oil per ton of polymer will increase to one peak value and then decrease again.

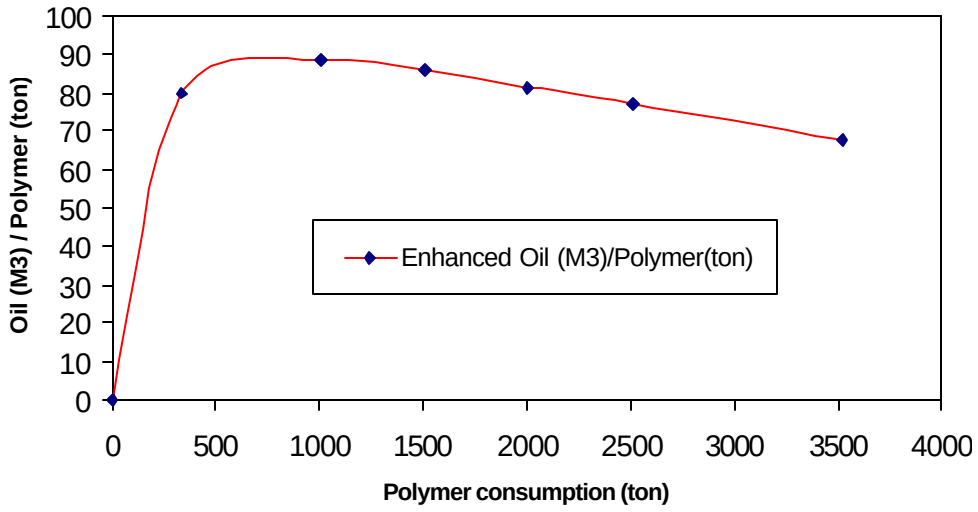

Fig.83 Enhanced oil per ton polymer consumption

With polymer consumption of 334.8 ton, one ton of polymer can recover about 79.8 m^3 of enhanced oil. When polymer consumption reaches 620 tons, polymer gets its greatest efficiency, with about 90 m^3 per ton of polymer. Then its efficiency begins to decrease. But it does not mean that this value of polymer consumption is most favorable, since with 620 ton polymer, the cumulative enhanced oil is only 55800 m^3.

In order to get the greatest absolute profits, more polymer should be used. Some of the internal reports have provided a standard that one ton of such polymer should enhance at lest 70 tons of oil. Based on this critical value, polymer slug size of 0.235 PV has been selected as the most economically favorable one. Each ton of polymer recovers about 76.8 m^3 of enhanced oil.

8.2.3 Description of Polymer Flooding Process

During polymer flooding, viscosity of water is greatly enlarged, water mobility is obviously lowered; as a result, at the front of polymer slug an oil bank is accumulated. With time going, polymer slug flows towards producing wells, before which, the oil bank flows to producing wells earlier, and the oil production rate gradually increases to peak value. Shortly after that the polymer concentration peak value is also reached, then the oil production rate decreases more quickly to the lowest value, and the whole polymer flooding process tends to finish (Fig.84).

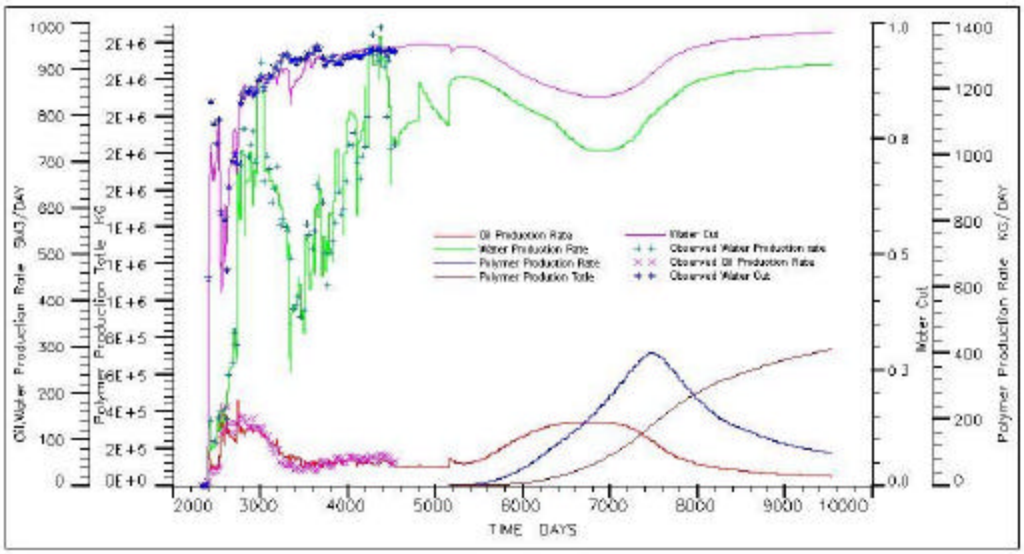

Fig.84 Polymer flooding process for the whole reservoir

With 0.235 PV polymer slug (2,511 tons of polymer), to the end of polymer flooding process only about 739.9 tons of polymer will be produced from producing wells, the others will be adsorbed in reservoir rock underground.

Because of polymer adsorption, the polymer slug is deformed from one rectangle for injection well to a time depending distribution function for production well. The same situation can be seen in Fig.85-Fig.87 for different producing wells.

First of all, from these three example wells, it can be seen that all their oil production rates have been increased. It indicates that polymer flooding for this reservoir will be very successful.

For polymer flooding in such heavy oil river channel reservoir, there are two most special difficulties: (1) serious permeability heterogeneity, (2) high water cut stage due to unfavorable oil-water mobility ratio. These have also been reflected in the above figures. Due to the permeability heterogeneity, polymer solution flows quickly through the middle of the river channel, breaks through shortly after the beginning of polymer injection and reaches production well. For all wells, simulation results of polymer production rate have proved this phenomenon. At high water cut stage, the water saturation underground is already relatively high, when polymer solution comes, its concentration will be lowered by adsorption and as well as by the existing water, as a result, it loses some of its viscosity, this is also one important reason for high flowing velocity.

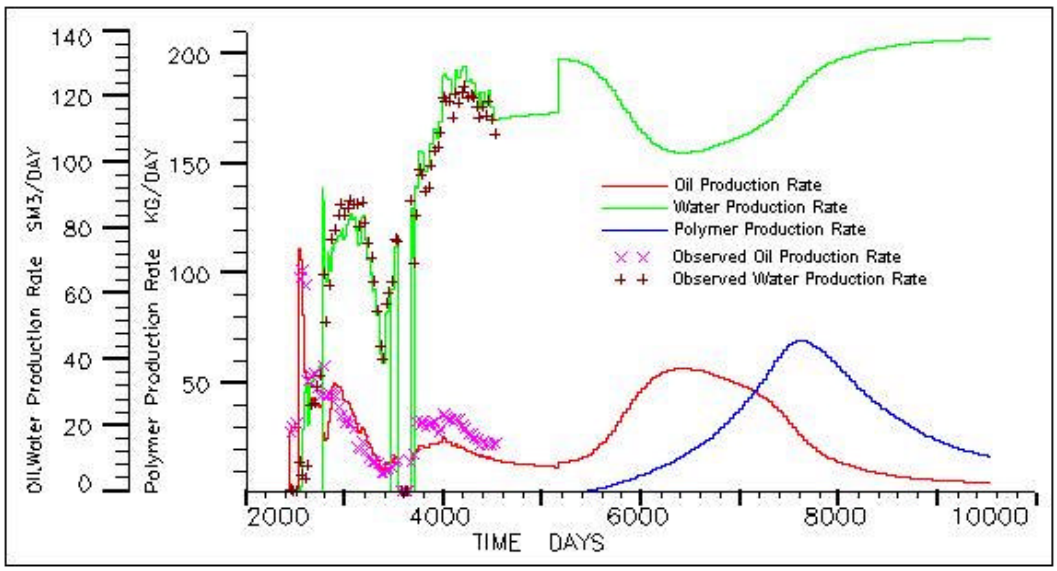

Fig.85 Oil, water and polymer production rate of well-54

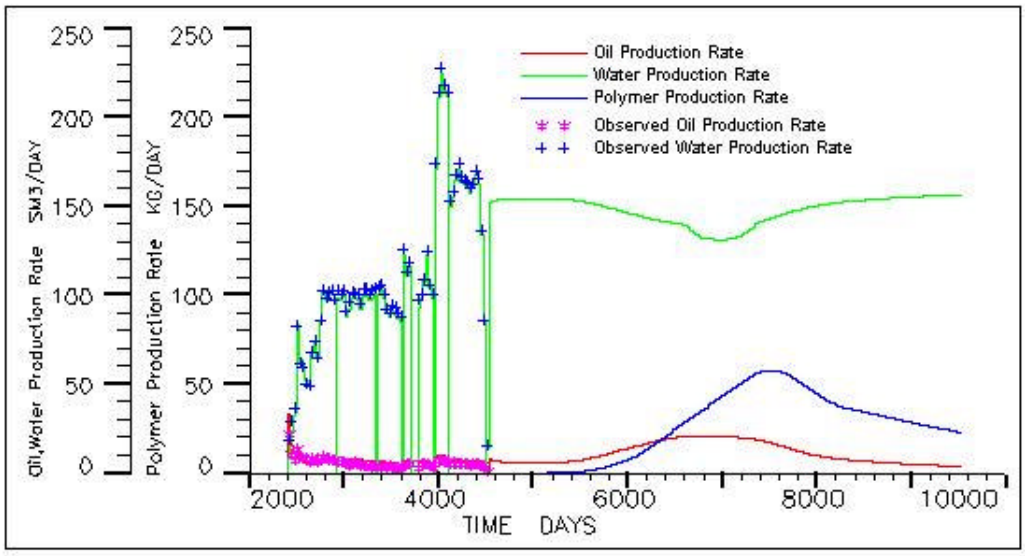

Fig.86 Oil, water and polymer production rate of well -60

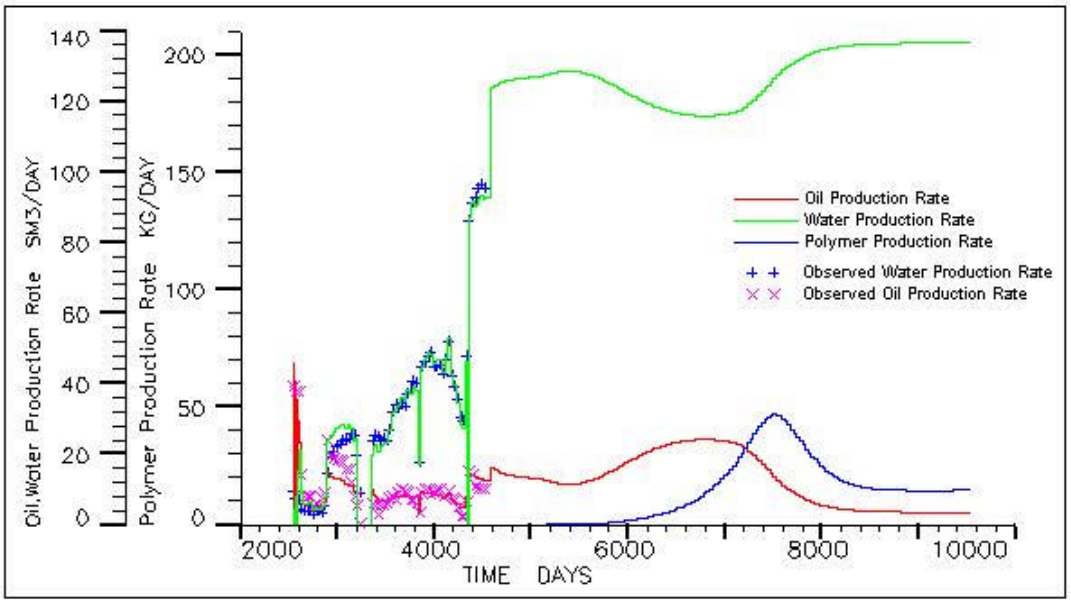

Fig.87 Oil, water and polymer production rate of well -67

In such situation, success can be got only with large polymer slug size. Simulation results from theoretical river model and practical reservoir both support this conclusion.

In the above three figures, another interesting phenomenon arises, that is, the time point of highest polymer production rate is almost the same as that of the quickest oil production decreasing. If a reasonable function models can be selected for polymer production rate and oil production rate (or water cut), they can be bund together by this special time point. For one, at this time point, the first order derivative is equal to zero, and for the other the second order derivative is zero. These function models will be of great importance for the prediction of future production situation. Because the functions can be constructed with earlier observed data, they can be used for prediction. As this idea is not the main object for this dissertation, it will be completed later after this work.

8.2.4 Residual Oil Saturation Distribution after Polymer Flooding

Compared with the oil saturation distribution before polymer flooding, the residual oil saturation has greatly decreased after polymer flooding.

Before polymer flooding, the oil saturation in the upper 5 cell layers has been still very high; only in small area around the wells, the saturation has been decreased by normal water flooding. After polymer flooding, in most area, especially in the middle of river channel where oil reserve can be controlled by injecting wells and producing wells, oil saturation has been decreased to dead oil saturation.

In the under-layered three layers, variation of oil saturation is not so distinct, because the original oil saturation is already near to dead oil saturation. As polymer flooding can not decrease the dead oil saturation, most of oil in these three cell layers can not be recoverable.

In west edging area at left side of river channel, since no wells have been drilled, the oil reserve here could also not be put into development. Since other sand layers in this area seldom contain oil, only for this thin layer to drill more wells it seems not economical.

In the northern area, there is one great part of reserve of this reservoir, but no wells have been drilled. Since this area is already offshore, our company has rented much greater area in this region to a foreign company from America, in the near future, we will still have no right to drill well there.

Above mentioned three area or layers are also the reasons of low final oil recovery. In fact, if only developable reserve being taken onto account, the final oil recovery is about 34%. And improved oil recovery from polymer flooding is more than 12%. For such a complicated heavy oil river channel reservoir, to reach such a recovery is already acceptable.

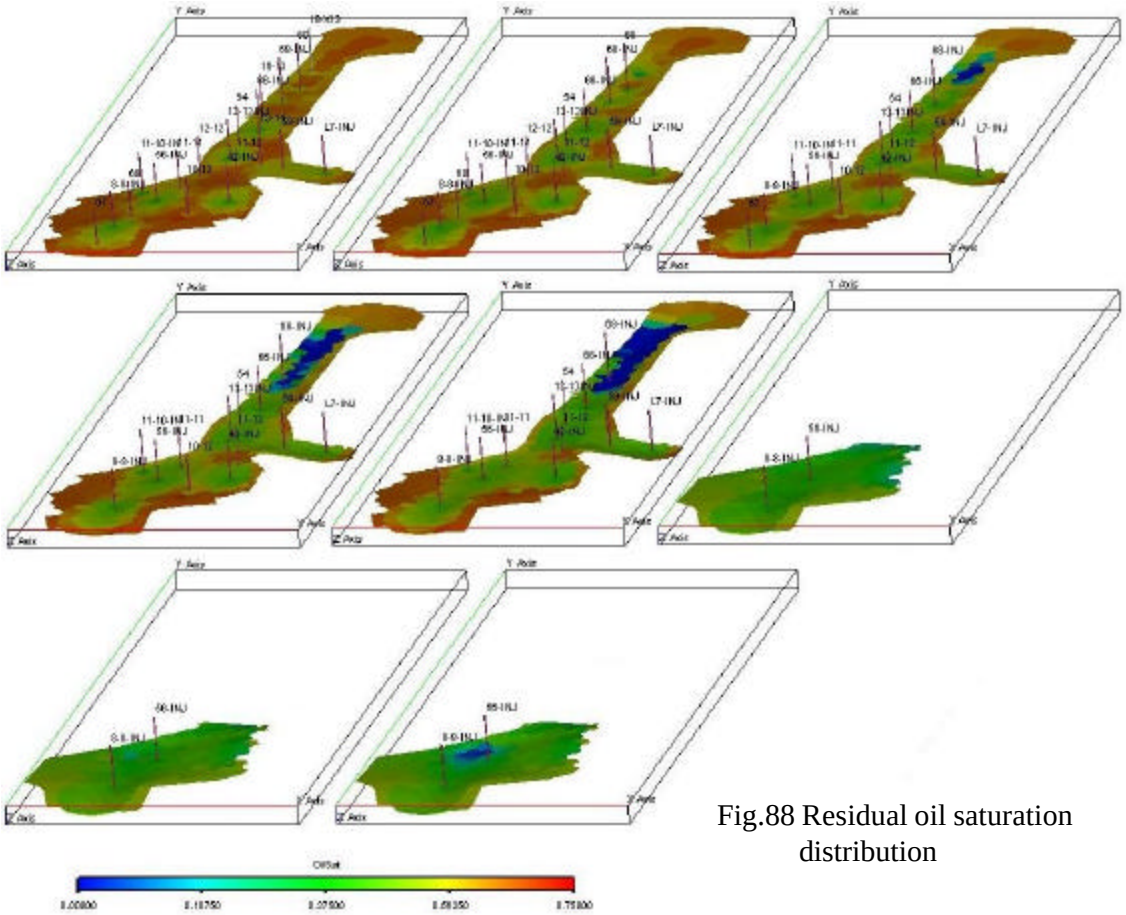

Fig.88 Residual oil saturation distribution

9 Conclusions And Proposals

9.1 Conclusions

(1) To meet China's energy demanding, oil production rate should be increased or at least be kept stabile. Since most of the oil fields have reached their high water cut stage, different improving oil recovery (IOR) methods will be gradually adopted for practical use in the near future.

(2) Z106 is one of the oil fields in Shengli Oilfields Area, which has been developed with water flooding since 1988. Because of the unfavorable oil-water mobility ratio and reservoir heterogeneity, comprehensive water cut reached more than 90% shortly after the beginning of its development. Especially for reservoir $Ng2^1$, the sand rock is sediment from river channel; the permeability heterogeneity and heavy oil properties together lead to extremely poor water flooding efficiency. In order to improve the oil recovery, IOR methods are needed urgently. Considering all practical situations for this reservoir and the present technique level, polymer-flooding method is selected as an IOR test with numerical simulation.

(3) With polymer flooding, polymer transport process must be simulated.

The main property of polymer solution is its capability of enlarging water viscosity, through which, controlling the mobility of water phase and improving the driving efficiency. During polymer flooding simulation, inaccessible pore volume, polymer shear thinning effect, polymer adsorption, and relative reduction factors have been taken into account for construction mathematical model.

All simulations have been done with black oil model with polymer option in ECLIPSE.

(4) Comprehensively using geological data, geophysical data and production data to re-understand the reservoir. Sand layer $Ng2^1$ should be seperated into three disconnected areas. The south-north river channel is one reservoir with its own oil-water system. The reservoir contains two sand layers, which are sediment from river channels of different geological time. In the southern area, they are connected together. Due to the different original water dynamic condition, the two layers have different rock properties, especially different permeability and capillary pressure. The history matching result has proved that this understanding is correct.

(5) Because of the high oil – water viscosity ratio and permeability heterogeneity of river channel sedimentary sandstone, simulation results have shown that with water flooding the final oil recovery for whole reservoir can only reach 7.9%, most of the oil has been produced at high water cut stage, and the oil recovering velocity is very low.

(6) For polymer flooding, polymer adsorption, polymer concentration and polymer slug size have great effects on its efficiency.

With lower polymer adsorption, polymer flooding will be more efficient. This effect will be diminished with polymer slug size increasing.

With a same polymer slug size, the higher the concentration of polymer solution is, the higher enhanced oil recovery polymer flooding has. But in order to keep a high enough injection rate of polymer solution and avoid fracturing reservoir rock, only a reasonable polymer concentration can be applied.

(7) Since in Shengli Oilfields Area there are still many such heavy oil reservoirs, polymer flooding will be of great importance as a tertiary IOR method in this area in the near future.

9.2 Proposals

(1) For numerical reservoir simulation, the most difficult problem is history matching. The difficulty mainly comes from the uncertainty of two sets of parameters: permeability and relative permeability.

Permeability is an average of capability of allowing fluids to flow through the pore channel. Since of the complexity of pore structure, permeability may vary within a great range. More fully understanding of the geological regularity of factors, which affect permeability, should be taken into account.

(2) For polymer flooding, the variation of relative permeability reasoned from polymer adsorption, viscosity increasing of polymer solution, etc. has been simplified by multiplying a coefficient. In practice, the shape of relative permeability function should be varied corresponding to the variation of polymer concentration. More attention should be given to this studying area, since it is also significant to other chemical IOR method. This problem is also parallel to the problem with relative permeability mentioned above.

(3) Clay mineral of rock is always an important factor that affects permeability. It surely plays a great role in polymer adsorption and hence affects the permeability and the relative permeability. Till now there is no satisfactory related publishing, either.

Nomenclature

Symbol	Definition	Units
A	flow area between two cells	m^2
B_o	oil formation volume factor	fraction, unitless
B_w	water formation volume factor	fraction, unitless
C	compressibility	1/Bar
$\overline{C}$	the effective saturation for the injected polymer solution within the total queous phase in the cell.	fraction, unitless
C_a	polymer adsorption	kg/kg
C_p	Polymer concentration	kg/m^3
C_{pi}	Polymer concentration of injected water or produced water through well	kg/m^3
$\hat{D}$	Diffusion coefficient	m^2/Day
ERROR	the relative error of calculated result from simulation model	unitless.
f_{Obs}	observed data (Pressure, water cut or production rate of water or oil)	
f_c	calculated data (Pressure, water cut or production rate of water or oil)	
g	acceleration of gravity	m/s^2
H	depth	m
k	permeability,	md
K_{xx} and K_{yy}	horizontal permeability	md
K_{zz}	vertical permeability	md
K_r	relative permeability	fraction, unitless
$K_{i,go}$	equilibrium coefficient for i component between gas and oil phases	unitless
$K_{i,gw}$	equilibrium coefficient for i component between gas and water phases	unitless
M	shear thinning multiplier	unitless
$\vec{n}$	the outward direction vector of surface of i control volume	
P	viscosity multiplier	unitless
P	Pressure	Bar
dp/dL	pressure gradient	Bar/m
P_c	Capillary pressure	Bar
q	injection rate or production rate per unit	

	of volume through well	m^3/m^3 Day
$q_{m,j}$	mass flow rate of j phase per unit of volume of rock through well	kg/m3day
$\tilde{q}_{v,j}$	volume flow rate of j phase per unit of volume of rock through well	kg/m3day
Q_w, Q_o	injection rate or production rate of water or oil through well	m^3/Day
R_a	area equivalent radius of the grid block in which the well is completed.	m
R_s	solution gas-oil ratio	m^3/m^3
R_k	relative permeability reduction factor	fraction, unitless
R_w	well bore radius	m
RRF	residual resistance factor	fraction, unitless
S	saturation	fraction, unitless
S_j	saturation of j phase	fraction, unitless
S_{IPV}	inaccessible pore volume	fraction, unitless
S_w^*	saturation occupied by polymer solution	fraction, unitless
T	time of production	days
Δt_n	time step	days
T	temperature	°C
T_r	Transmissibility	$cp \cdot m^3 / Day / Bar$
V_p or V	pore volume	m^3
V_b	bulk volume	m^3
V_i	bulk volume of i control volume	m^3
$Z_{i,j}$	mass fraction of i component in j phase	fraction, unitless

Geek Symbol	Definition	Units
$\dot{g}$	shear rate	1/s
m	viscosity of flowing fluid	cp
m_j	viscosity of j phase,	cp
Φ	fluid potential	bar
f	porosity	fraction, unitless
r_j	density of j phase	kg/m^3

μ_m	viscosity of fully mixed polymer solution	cp
$\mu_{w,eff}$	the effective viscosity of water phase	cp
v	apparent fluid flowing velocity,	m/s
w	Todd-Longstaff mixing parameter	fraction, unitless

Subscript

c	polymer
f	fluid
m	of mass unit
o, w, g	oil, water and gas
r	rock
v	of volume unit

Superscript

n-1, n, n+1	time step number

Reference

[1] Data from Statistics of Import and Export by China's government.

[2] United States Energy Information Administration, "China: An Energy Sector Overview," International Energy Outlook 1999 (IEO99), Washington, DC: Government Printing Office, April 1999.

[3] Web-site of Shengli Oil Field, www.slof.com.

[4] Okandan E., Heavy crude oil recovery, Martinus Nijhoff Publishers, V-VII, 1984.

[5] Sullivan, B.R.: "Jurisdictional Agency Certification of Tertiary Oil Recovery Projects Under the Windfall Profit Tax- The Texas Approach", SPE 9771, 1981.

[6] Green DW, Willhite GP, Enhanced Oil Recovery, Henry L. Doherty Memorial Fund of AIME, Society of Petroleum Engineers, Richardson, Texas,1998.

[7] H. Cholet, Well Production Practical Handbook, Editions Technip, Paris, 2000.

[8] David J. Pye, Improved Secondary Recovery by Control of Water Mobility, Journal of Petroleum technology, August 1964.

[9] Riley B. Needhaam, Peter H. Doe, Polymer flooding review, Journal of Petroleum Technology, December 1987.

[10] Binghai Wang and Kai Qian, Geological Research and Exploration Practice in the Shengli Petroleum Province, The Petroleum University Press, 1992.

[11] J. Bear, Dynamics of Fluids in Porous Media, Dover Publications, Inc., New York, 1972.

[12] Gian Luigi Chierici, Principles of Petroleum Reservoir Engineering, Volume 2, Springer-Verlag, 1995: Page 123-229.

[13] Dakuang Han, Qinlei Chen and Cunzhang Yan, Fundamental of reservoir numerical simulation, Petroleum Industry Press, 1993.

[14] Aziz, Khalid, Petroleum reservoir simulation, Elsevier Science Publishers LTD,1979.

[15] Larry W. Lake, Enhanced Oil Recovery, Prentice Hall, 1989.

[16] Shupe, R.D., Chemical Stability of Polyacrylamide Polymers, Journal of Petroleum Technology, August 1981 (33).

[17] Flory, Paul J., Principles of Polymer Chemistry, Ithaca, New York, Cornell University Press, 1953.

[18] Rapier Dawson and Ronald B. Lantz, Inaccessible Pore Volume in Polymer Flooding, Trans. AIME, Vol.253, 1972.

[19] Eclipse Manuals 2002A.

[20] Szabo, M.T., Some Aspects of Polymer Retention in Porous Media Using a C^{14}-Tagged Polyacrylamide, Trans., AIME, Vol. 259, 1975.

[21] Szabo, M.T., Laboratory Investigations of Factors Influencing Polymer Flood Performance, Trans., AIME, Vol. 259, 1975.

[22] J.G. Dominguez and G.P. Willhite, Retention and flow characteristics of polymer solutions in porous media, SPE Journal, April, 1977.

[23] G.J. Hirasaki and G.A. Pope, Analysis of factors influencing mobility and adsorption in the flow of polymer solution through porous media, SPE Journal, August 1974.
[24] A. Zaitoun and N. Kohler, The role of adsorption in polymer propagation through reservoir rock, SPE 16274, 1987.
[25] Saul Vela, D.W. Peaceman and E.I. Sandvik, Evaluation of polymer flooding in a layered reservoir with crossflow, retention, and degradation, SPE Journal, April 1976.
[26] F.N. Schneider and W.W. Owen, Steady-state measurement of relative permeability for polymer oil systems, SPE 9408, 1980.
[27] F.H.L. Wang, Effect of wettability alteration on water/oil relative permeability, dispersion and flowable saturation in porous media, SPE Reservoir Engineering, May 1988.
[28] A. Zaitoun and N. Kohler, Two-phase flow through porous media: Effects of an adsorbed polymer layer, SPE 18085, 1988.
[29] M. A. Barrufet and L. Ali, Modification of relative permeability curves by polymer adsorption, SPE 27015, 1994.
[30] P. Barreau, H. Bertin, D. Lasseux, Ph. Glénat and A. Zaitoun, Water control in producing wells: Influence of an adsorbed polymer layer on relative permeabilities and capillary pressure, SPE Reservoir Engineering, November 1997.
[31] A. Zaitoun and H. Bertin, Two-phase flow property modifications by polymer adsorption, SPE 39631, 1998.
[32] P. Barreau, D. Lasseux, H. Bertin, Ph. Glénat and A. Zaitoun, Polymer adsorption effect on relative permeability and capillary pressure: Investigation of a pore scale scenario, SPE 37303, 1997.
[33] C.G. Zheng, B.L. Gall, H.W. Gao, A.E.Miller and R.S. Bryant, Effects of polymer adsorption and flow behaviour on two-phase flow in porous media, SPE 64270, June 2000.
[34] Ph. Elmkies, H. Bertin, D. Lasseux, M. Murray and A. Zaitoun, Further investigations on two-phase flow property modification by polymers: Wettability effects, SPE 64986, 2001.
[35] L. Ali and M. A. Barrufet, Using centrifuge data to investigate the effects of polymer treatment on relative permeability, Journal of Petroleum Science and Engineering 29 (2001) 1-16.
[36] P.L. Bondor, G.J. Hirasaki and M.J. Tham, Mathematical simulation of polymer flooding in complex reservoirs, SPE Journal, October 1972.
[37] F. Häfner, D. Sames and H.D. Voigt, Wärme- und Stofftransport: mathematische Methoden, Springer-Verlag, 1992.
[38] G.E. Slater and S.M. Farouq-Ali, Simulator of oil recovery by polymer flooding, The Journal of Canadian Petroleum, October-December 1970.
[39] P. Forsyth, A control volume finite element method for local mesh refinement, SPE 18415, 1989.
[40] Z. E. Heinemann, C. W. Brand, Margit Munka and Y.M. Chen, Modelling reservoir geometry with irregular grids, SPE 18412, 1989.

[41] L. S. Fung, A. D. Hiebert and L. Nghiem, Reservoir simulation with a control volume finite element method, SPE 21224, 1991.

[42] C. L. Palagi and K. Aziz, Use of Voronoi Grids in Reservoir Simulation, SPE 22889, 1991.

[43] Deyuan Li and Guangnan Chen, Finite difference method of parabolic partial differential equation, Science Press, 1998, ISBN 7-03-004669-2.

[44] Jinfu Chen and Zhi Guan, Numerical method of partial differential equation, Qinghua University Press, 1987.

[45] R.H. Mcneal, An asymmetrical finite difference network, Quart. Appl. Math. (1953) 11.

[46] Detailed reservoir description of Z106 Oilfield, Final report, 1999.

[47] Holger Kulke, Regional Petroleum Geology of the World: Part I Europe and Asia, Gebrüder Borntraeger – Berlin – Stuttgart, 1994.

[48] Saadi Manseur, Djebbar Tiab, Ali Berkat and Tao Zhu, Horizontal and vertical permeability determination in clean and shaly reservoirs, SPE 76773, May 2002.

[49] Mehdi Honarpour, Leonard Koederitz and A. Herbert Harvey, Relative permeability of petroleum reservoirs, CRC Press, 1990.

[50] Zeng Wenchong, An important theoretical problem of hydrocarbon reservoir evaluation, Petroleum Exploration and Development, 2(34), 1982.

[51] Calvin C. Mattax and Robert L. Dalton, Reservoir simulation, SPE Monograph series, Richardson, TX, 1990.

[52] Howard B. Bradley, Petroleum Engineering Handbook, Society of Petroleum Engineers, Richardson, TX, U.S.A., 1992.

[53] Bi Yanpeng et al. Detailed Reservoir description and residual oil distribution research in east area of Gudao Oil field, Internal researching report, 1998.

[54] Collection of achievements for reservoir simulation techniques in practice, Petroleum Industry Press, 1996.

[55] John R. Fanchi, Principles of applied reservoir simulation, Gulf Publishing Company, Houston, TX, 1997.

[56] R. B. Needham and P. H. Doe, Polymer flooding review, Journal of Petroleum Technology, December 1987.

[57] R.L Jewett and G.F. Schurz, Polymer flooding – A current appraisal, Journal of Petroleum Technology, June 1970.

[58] H.L. Chang, Polymer flooding technology – Yesterday, today and tomorrow, Journal of Petroleum Technology, August 1978.

[59] Mahendra Pratap, R.P. Roy, R.K. Gupta ad Daljeet Singh, Field Implementation of Polymer EOR Technique – A Successful Experiment in India, SPE 38872, 1997.

[60] B.K. Maitin, Performance Analysis of several Polyacrylamide Floods in North German Oil Fields, SPE/DOE 24118, 1992.

[61] D.M. Wang, Y.X. Hao, E. Delamaide, Z.G. Ye, S. Ha and X.C. Jiang, Results of two polymer flooding pilots in the central area of Daqing Oilfield, SPE 26401, 1993.

[62] T.L. Chen, Z.Y. Song, Y. Fan C.Z. Hu, Q. Ling and J.X. Tang, A pilot test of polymer flooding in an evaluated-temperature reservoir, SPE Reservoir Evaluation & Engineering, February 1998.
[63] Homayoun Hodaie and A.S. Bagci, Polymer-augmented water flooding in a reservoir with a bottomwater zone, SPE 25633, April 1993.
[64] Ezeddin Shirif, Mobility control by polymers under bottom-water conditions, Experimental Approach, SPE 64506, October 2000.
[65] B.L. Knight and J.S. Rhudy, Recovery of high-viscosity crudes by polymer flooding, The Journal of Canadian Petroleum Technology, October-December, 1977.
[66] Khalid Aziz, Reservoir Simulations Grids: Opportunities and Problems, SPE 25233, presented at the 12th SPE Symposium on Reservoir Simulation held in New Orleans, USA, February 28- March 3, 1993.
[67] Oreskes, N., K. Shrader-Frechette, and K. Belitz: Verification, Validations, and Conformation of Numerical Models in the Earth Sciences, Science, pp.641-646, Feb. 4, 1994.
[68] Toronyi, R.M. and N.G. Saleri: Engineering Control in Reservoir Simulation, SPE 17937, Proceedings of 1988 Society of Petroleum Engineers Fall Conference, Oct. 2-5, 1988.
[69] Honarpour M., Koederitz L. and Harvey A. H., Relative Permeability of Petroleum Reservoirs, CRC Press, 1986.